From single-drug pharmacokinetics and pharmacodynamics to multi-drug interaction modeling: using population-based modeling to increase accuracy of anesthetic drug titration

Hannivoort, Laura Naomi

From single-drug pharmacokinetics and pharmacodynamics to multi-drug interaction modeling: using population-based modeling to increase accuracy of anesthetic drug titration

"Surfing the wave"

Laura Naomi Hannivoort


university of groningen

Layout: L.N. Hannivoort
Cover photo: © 2009 L.N. Hannivoort
Wave Rock, Hyden, Western Australia

Printed by: Gildeprint - Enschede
ISBN: 978-94-034-0704-3 (printed version)
978-94-034-0703-6 (electronic version)

Financial support for the publication of this thesis by the following organisations is greatly appreciated:

- Het Fonds Klinische en Experimentele Anesthesiologie

rijksuniversiteit groningen

From single-drug pharmacokinetics and pharmacodynamics to multi-drug interaction modeling: using population-based modeling to increase accuracy of anesthetic drug titration

"Surfing the wave"

Proefschrift

ter verkrijging van de graad van doctor aan de
Rijksuniversiteit Groningen
op gezag van de
rector magnificus prof. dr. E. Sterken
en volgens besluit van het College voor Promoties.

De openbare verdediging zal plaatsvinden op

dinsdag, 26 juni 2018 om 11:00 uur

door

Laura Naomi Hannivoort

geboren op 6 september 1984
te Enschede

Promotores
Prof. dr. M.M.R.F. Struys
Prof. dr. A.R. Absalom

Copromotores
Dr. H.E.M. Vereecke
Dr. P. Colin

Beoordelingscommissie
Prof. dr. K. Meissner
Prof. dr. A. Dahan
Prof. dr. D.J. Touw

Paranimfen
Rebekka Hannivoort
Carlijn Hofstra-Wiersema

Table of Contents

Chapter 1: Introduction and aims of the thesis

General introduction

Several factors have helped significantly to make anesthesia as safe as it is today: an improving knowledge of pharmacology and better methods of drug titration, technology (monitoring and safeguarding of vital functions, delivery systems of anesthetic drugs and monitoring of drug effect) and a better recognition of the role of, and how to reduce the influence of human factors (errors, communication, crew resource management training) with lessons learned from the aviation industry. Mainly the first two have ensured that mortality from anesthesia has decreased from 1:2250 in patients in good condition and 1:360 in patients in poor condition in the early 1950s[1] to as low as 1:250,000 in healthy patients and about 1:1800 in patients in very poor condition in 1999.[2] In more recent years, human factors have played a greater role, but the first two are still important and progress can still be made in anesthetic pharmacology and technology.

This thesis attempts to contribute to advances in knowledge and technology in anesthetic pharmacology, by investigating the following topics:

- the development of improved pharmacokinetic and pharmacodynamic models for single drugs,
- the development of drug interaction models that describe the combined effects of multiple drugs and the performance of several commonly used surrogate parameters of anesthetic effect,
- the development of a new parameter of anesthetic potency based on the interaction models, which can be used in clinical practice to guide anesthesia in an intuitive manner.

In the next paragraphs, detailed background information is provided to highlight the gaps in knowledge that need to be explored further and to present the aims of this thesis within this field.

Pharmacokinetics (PK)

Pharmacokinetics describe the time-course of the plasma concentration of the drug, or 'what the body does to the drug'. Absorption, distribution, metabolism and elimination are all processes that play a part in how much of the drug circulates in the bloodstream, resulting in the plasma concentration of a drug. This is a dynamic process, where the concentration changes continuously, depending on the aforementioned processes, as well as continuation or cessation of drug administration.

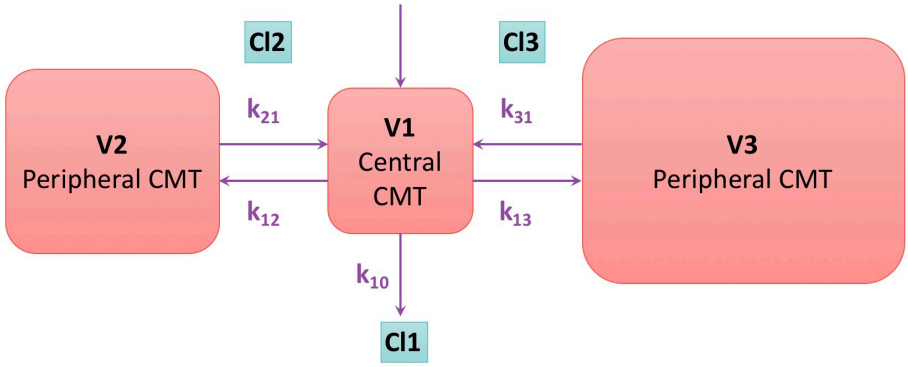

Figure 1. Three-compartment pharmacokinetic model with a central compartment and two peripheral compartments. V1-3 = volume of the respective compartments (CMT); Cl1-3 = clearance to and from the respective compartments, k_{ij} = equilibration rate constant from compartment i to compartment j.

PK modeling is often used to quantify the pharmacokinetics of a drug. There are several methods for PK modeling, one of the most often used methods being population-based compartmental PK modeling. With this method, one or multiple compartments, each with a certain volume and a certain distribution clearance, are used to evaluate the plasma concentration of the drug at a certain point in time. A single-compartment model has only one compartment of a certain volume, in which the drug is administered into, and the drug is also cleared out of the compartment (by elimination and/or metabolism). Often this compartment roughly resembles the vascular compartment, i.e. the bloodstream. Multiple-compartment models also describe the distribution of a drug out of the bloodstream (central compartment 1), into one or more peripheral compartments, for which equilibration rate constants (k) describe the movement of drug into and out of the peripheral compartments, as well as a clearance out of the central (vascular) compartment (again, by elimination and/or metabolism). The often-used three compartment model comprises of a central compartment and two peripheral compartments: one compartment with a relatively low volume and high equilibration rate, which roughly resembles well-perfused tissues in which the drug can rapidly distribute into and out of, and a compartment with a high volume and low equilibration rate. This compartment roughly resembles poorly perfused tissues which the drug slowly distributes into, but when saturated also keeps distributing back into the bloodstream for a long time after drug administration is terminated. Figure 1 shows an example of a three-compartment PK model, with a central compartment and two peripheral compartments with certain volumes and equilibration rate constants between compartments. Figure 2 shows the time-concentration relationship as described by a three-compartment model following a bolus dose into the central

compartment, also depicting the movement of drug in and out of the compartments at different time points in the process, in the form of communicating vessels. One must keep in mind though, that these compartments are mathematical in nature, and are not strictly analogous with any physiological compartment. Compartmental pharmacokinetics allow for the use of relatively simple mathematics to describe the time-concentration relationship, without the immense complexity of human physiology and pharmacology, and they manage to do so with clinically acceptable accuracy.[3]

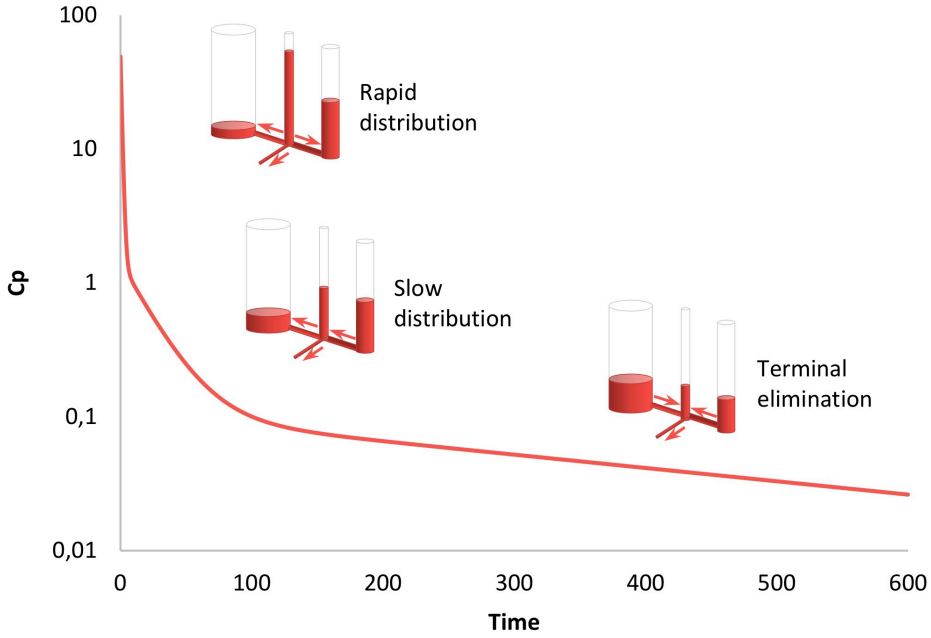

Figure 2. Plasma concentration vs. time, depicting the different pharmacokinetic phases (distribution and elimination) after a bolus dose of a certain drug. Cp = plasma concentration.

Pharmacodynamics (PD)

Pharmacodynamics describe 'what the drug does to the body', or more accurately, the relation between the concentration at the site of drug effect and the actual effect. To enable pharmacodynamics analysis, one needs to be able to measure the effect. This can be both desired effects and unwanted side-effects. For anesthetic drugs, the desired effect may for instance be adequate anesthesia, and side-effects may be hemodynamic in nature, such as on blood pressure (hypo- or hypertension), heart rate (bradycardia) or cardiac output, or delayed recovery from anesthesia. These effects are not always easy to quantify, as the actual effect cannot always be measured, and surrogate measurements are often used. "Adequacy of anesthesia" in itself cannot be measured, and is actually a combined effect of hypnosis, analgesia (or rather: balance between nociception and antinociception) and immobility. A dichotomous measurement can be

used to determine adequacy of anesthesia, such as a motor response to skin incision, or an increase in heart rate and blood pressure in response to a painful stimulus, sweating or pupillary dilatation. During surgery, the anesthesiologist will seek to prevent these responses, and therefore needs a parameter that can predict whether a patient will or will not tolerate a painful stimulus such as skin incision. Electroencephalograph (EEG) derived monitors are often used, which measure to a certain extent the hypnotic component of anesthesia by measuring the drug-induced changes in the electrical activity of the brain. Monitoring systems that attempt to measure the balance between nociception and antinociception are under development, but it remains to be seen how these monitors perform.

Even the effects that we consider to be hemodynamic side effects (such as low blood pressure) are often only surrogates of true side effects (i.e. organ/tissue damage), and although there is little doubt that intraoperative hypotension plays a role in development of perioperative tissue damage (myocardial ischemia, kidney injury, ischemic stroke etc.), there is no consensus to what 'intraoperative hypotension' is and at what level it is actually harmful, as many different definitions exist in the medical literature.[4]

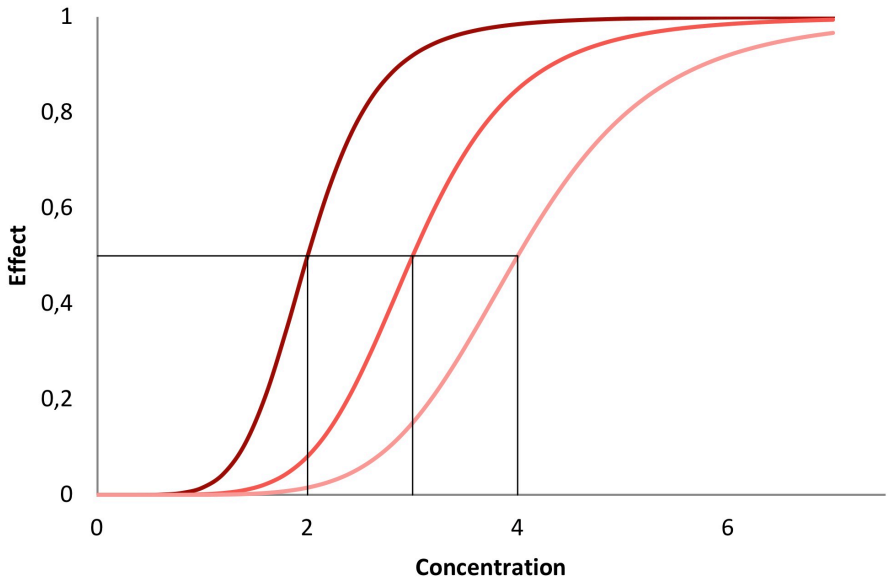

Figure 3. Sigmoidal E_{max} curve, with three different values for C_{50} (2, 3 and 4, respectively).

In short, there is as of yet no accurate method to assess whether a patient is under adequate anesthesia, without over- or underdosing. Therefore, surrogate measurements will have to suffice, and that is what is currently available for the assessment of pharmacodynamic effects, as is the case in this thesis. Pharmacodynamics

are often referred to as the dose-response relationship, but a more accurate term would be the concentration-effect relationship, as 'dose' implies that pharmacokinetic processes are included in the pharmacodynamic descriptions, while these are separate processes. Pharmacodynamics may appear to be linear at clinically applied concentrations for some drugs, in which case a concentration-effect curve would be a straight line, but more often, the relationship is non-linear, and can be described by a sigmoidal E_{max} curve, or Hill equation:

$$\text{Effect} = E_0 + (E_{max} - E_0)\frac{C^{\gamma}}{{C_{50}}^{\gamma} + C^{\gamma}} \quad (1)$$

where E_0 is the effect at baseline, E_{max} is the maximum effect, C is the concentration, C_{50} is the concentration associated with 50% maximum effect and γ describes the steepness of the concentration-effect curve (also called the Hill coefficient). Figure 3 shows an example of a sigmoidal E_{max} curve.

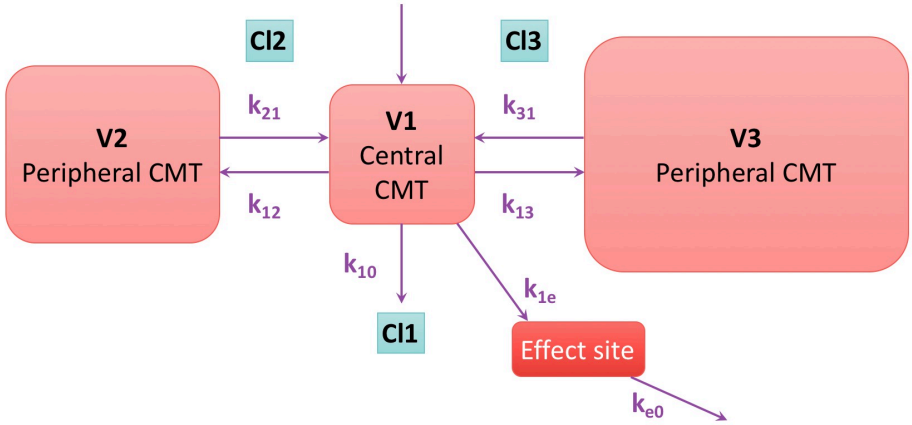

Figure 4. Three-compartment model with the addition of an effect site compartment with negligible volume, which makes k_{1e} small and inconsequential, with k_{e0} being the primary determinant of the concentration in the effect site. V1-3 = volume of the respective compartments (CMT); CL1-3 = clearance to and from the respective compartments, k_{ij} = equilibration rate constant between compartment i to compartment j.

Pharmacokinetics/pharmacodynamics (PKPD)

Pharmacodynamic effects, or their surrogates, can be linked to pharmacokinetic models. Ideally, the drug concentration at the site of effect would be measured. However, this is impossible in most situations, as the site of drug effect is usually inaccessible (for instance, in the brain, or more accurately, at receptor level). The concentration at the site of drug effect and its time course are therefore estimated from the data. Often this is done by 'attaching' a so-called effect-site compartment to the compartmental PK

model. This effect-site compartment has negligible volume, and an elimination rate constant k_{e0}, which ultimately describes the lag that occurs between the rise or decline in plasma concentration and the increase or decrease in effect. Figure 4 shows the previously shown three-compartment model with the addition of an effect-site compartment. Figure 5 shows the lag that can occur between plasma concentration and effect, and it is this lag or hysteresis (Figure 6) that the PKPD model attempts to explain, also called 'collapsing the (hysteresis) loop'. Again, these models are purely mathematical in nature, and the addition of an effect-site compartment with negligible volume is not in itself translatable to an anatomical structure, but allows for modeling of the lag between the rise in plasma concentration and effect.

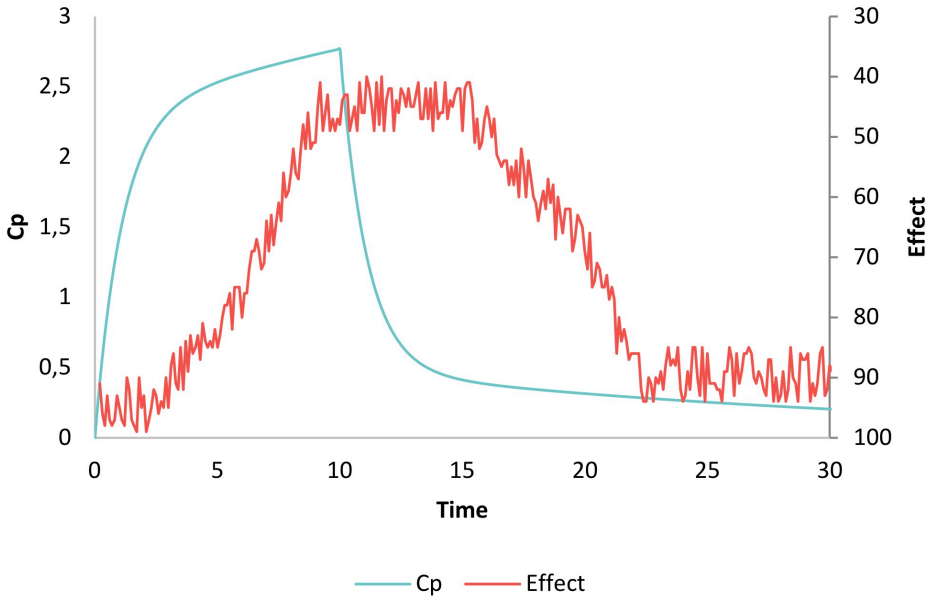

Figure 5. Plasma concentration during and after a 10-minute infusion, and corresponding lag in measured effect (for instance, EEG-derived indices). Cp = plasma concentration.

As PKPD models are used to describe and predict the time course of the drug concentration and effect, they can be used to calculate dosing schemes for use in clinical practice, i.e. a bolus dose and adjusting maintenance rates over time to account for the distribution of the drug into the peripheral tissues, instead of a bolus dose and maintaining the same infusion rate throughout the procedure. Limitations are that the calculation of these bolus doses and infusion rates should not be too complicated, usually based on patient weight. Additional covariates make the calculations more difficult and prone to error. Computers nowadays are also capable of calculating and displaying the concentration time course on the basis of manual drug delivery (bolus

and infusion rates), and the user can adjust infusion rates to target a certain plasma or effect-site concentration. PKPD models can also be implemented in target-controlled infusion (TCI) pumps, which allow the user to target a certain plasma (PK) or effect-site (PKPD) concentration for a certain drug, and the TCI pump will automatically adjust the infusion rate to maintain a stable concentration (in plasma or the effect site). Also, when targeting effect-site concentrations, the TCI-pump calculates the loading dose required to reach the targeted effect-site concentration the fastest, which requires an 'overshoot' of the plasma concentration to drive the drug into the effect site, without overshooting the effect-site concentration. This cannot be done accurately without the use of PKPD models, and dosing by hand commonly results in a large overshoot in both plasma and effect-site concentrations. The use of TCI-pumps reduces the risk of overdosing in the initial loading dose, and also reduces the risk of overdosing as time progresses, or underdosing when the infusion rate is lowered too far or too soon in an attempt to prevent overdosing.

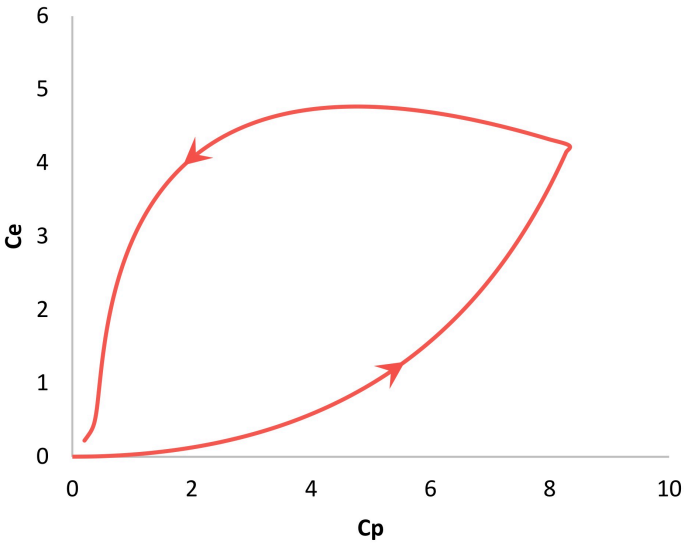

Figure 6. Hysteresis between plasma and effect-site concentrations. Arrows indicate which part of the loop occurs during increasing or decreasing plasma concentrations, respectively. Cp = plasma concentration; Ce = effect-site concentration.

Model development studies

Setting up a study for the purpose of developing PKPD models requires consideration of several aspects, as the model is only as good as the data it is derived from. First, one must consider the study population: healthy volunteers or patients. The major advantage of the former is the absence of co-morbidities and chronic co-medication, as well as the use of other anesthetic drugs such as opioids and muscle relaxants, and

allows for good base models for investigating drug interactions and interaction modeling. A disadvantage is that models developed from healthy volunteers may be less accurate when extrapolated to patient populations. Second, one must decide whether to use arterial or venous blood samples for concentration measurements. Arterial sampling provides a more accurate approximation to the concentration which is delivered to the target organ, whereas venous samples convey more information on the uptake of drug in tissues distal to the sampling site (for instance, the forearm), which is usually not the site of interest, and this may pose problems for the accuracy of the model.[5] Arterial line placement is however associated with more serious complications than venous line placement (dissection or thrombosis of the artery), even though these complications are very rare in healthy volunteer populations. A third consideration is the dosing of the drug in question. For this, a thorough understanding of the drug is necessary, including what is already known about the drug's pharmacokinetics and –dynamics, and if possible, even simulating beforehand to determine the best dosing scheme and/or blood sampling schedule. In some cases, PK and/or PKPD models may already be in existence, but lack accuracy, reducing its use in clinical practice and future research. These models require optimization, but these models may still be used for drug dosing during optimization studies.[6]

Not only is drug dosing important, but the time of sampling also plays a great role in how accurate a model is. Considering the drug for which the concentration vs. time graph is shown in Figure 2: if one were to only take samples from 10 minutes after the bolus onwards, and stop sampling after an hour, the measured concentrations would all be in a somewhat straight line (the 'slow distribution' phase in Figure 2). This would suggest that a one-compartment model would best describe the data, resulting in the conclusion that the drug follows one-compartment pharmacokinetics (and therefore this would not be the slow distribution phase, as there is no distribution, only the terminal elimination phase). Though it does indeed describe the data well, the data does not describe the actual pharmacokinetics well, due to poor sampling. Therefore, when modeling PKPD, one must make sure to take samples early enough in the drug administration to be able to capture the rapid distribution, but also late enough to be able to capture the terminal elimination phase. Clinical trial simulations, based on existing knowledge about the pharmacokinetics of a drug, may help in determining the best sampling scheme for a PK or PKPD study, thereby determining the optimal experimental design.

Dexmedetomidine

As mentioned, the development of PKPD models requires a thorough understanding of the drugs in question. One of the drugs that is investigated extensively in this thesis is dexmedetomidine. Dexmedetomidine is a selective α2-adrenoceptor agonist, with

sedative, analgesic and anxiolytic effects. It is more selective than its closest relative, clonidine.[7] Although α1-adrenoceptor activation antagonizes the α2 sedative effects, this is markedly less so for dexmedetomidine than for clonidine.[8] An interesting property of α2-adrenoceptor agonists is that subjects remain rousable even at relatively high concentrations.[9] This makes it an interesting drug for the use in situations where sedation is desired, but some amount of interaction with the patient is required. This may for instance be in sedation in Intensive Care Units (ICU), in procedural sedation, or for awake craniotomies, where the patient is required to perform certain tasks to ensure no vital parts of the brain are damaged.[10] Also, the respiratory drive is largely maintained in dexmedetomidine sedation.[11, 12]

Whereas most anesthetic drugs tend to induce hypotension, α2-adrenoceptor agonists like dexmedetomidine have a biphasic effect on blood pressure. This is due to the fact that dexmedetomidine influences α2-adrenoceptors both in the central nervous system and in the vascular wall. At low concentrations, dexmedetomidine activates mainly presynaptic α2-adrenoceptors in the central nervous system and α2-adrenoceptors in the vascular endothelial cells. This results in vasodilation and lowering of the heart rate.[13, 14] At higher concentrations, α2-adrenoceptors in the vascular smooth muscle are activated, resulting in vasoconstriction and hypertension (and a further decrease in heart rate).[15, 16]

Several PK models exist for dexmedetomidine, like the Dyck model.[17] This model is fairly accurate at lower concentrations, but underestimates concentrations in the higher ranges.[12] One of the goals of this thesis was therefore to develop an optimized dexmedetomidine PK model (Chapter 2). Whereas several PK models are in existence, no PKPD models exist for dexmedetomidine. A second goal was therefore to explore both the sedative (Chapter 3) and the hemodynamic (Chapter 4) effects of dexmedetomidine, and develop PKPD models for both types of effect, increasing the probability of rapidly titrating dexmedetomidine to the desired effect within the limits posed by the hemodynamic side effects.

Interactions

Another issue that makes titrating a general anesthetic more difficult, is not just the complexity of the pharmacokinetics and –dynamics of individual drugs, but also the interaction between drugs. A general anesthetic is rarely administered through one drug only, often two or more drugs are combined to achieve anesthesia, with at least a hypnotic and an analgesic drug. Examples of the hypnotic drugs are the volatile anesthetics such as sevoflurane, and the intravenous drug propofol. Examples of the analgesics are the opioids, such as morphine, fentanyl, or the rapidly acting remifentanil.

It would be too simple to say these drugs only have an effect on either sedation or analgesia, as combining them may very well influence the total effect of both sedation and analgesia beyond what would be expected by simply 'adding up' the effects.

Interactions can be both on a pharmacokinetic and pharmacodynamic level. On a pharmacokinetic level, certain drugs may influence the absorption of other drugs, the volume of distribution, or (hepatic) metabolism of a drug, increasing or decreasing the plasma concentration of either the drug itself or perhaps its active metabolites. Pharmacokinetic interactions will eventually influence pharmacodynamics, as an increase or decrease in drug concentration or that of active metabolites, increases or decreases the availability of the active component to be distributed to the site of drug effect.

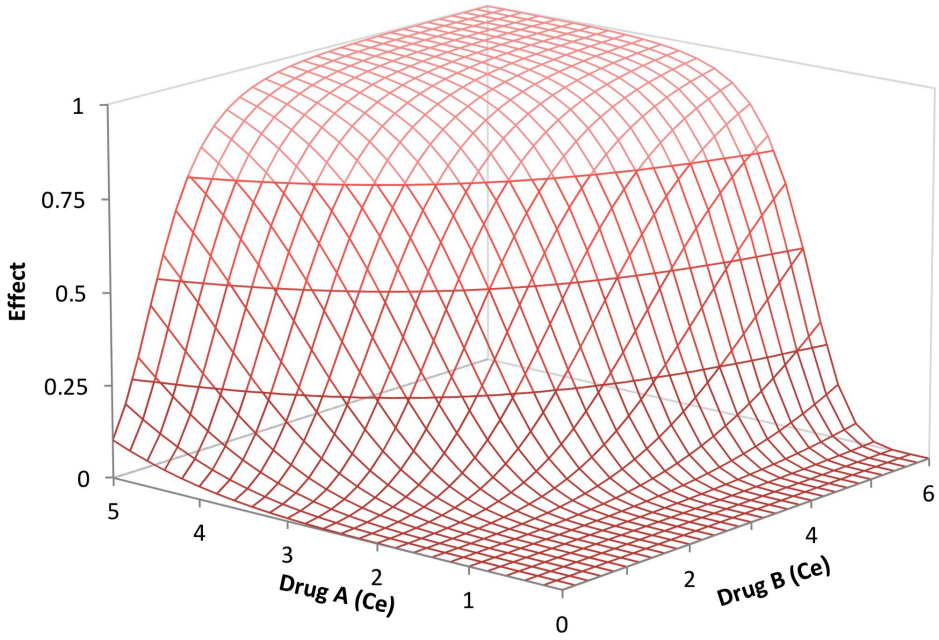

Figure 7. Three-dimensional response surface model of the interaction between two drugs, and the effect. Ce = effect-site concentration.

Pharmacodynamic interactions take place at the site of drug effect. Interactions can be described as being additive, synergistic (supra-additive) or antagonistic (infra-additive). Often, the manner of interaction is not clearly elucidated, and may comprise of competitive binding at the receptor level or identical pathways (often additive interaction), or different actions at separate receptor types or different pathways (often synergism or antagonism). Most drug interaction studies only quantify the magnitude of the interaction in a limited fashion, and sometimes only on a pharmacokinetic level, or

only for a dose or concentration corresponding with 50% of maximum effect (D50 or C50, respectively).

However, anesthetic drugs can have profound pharmacodynamic interactions, and the presence of these interactions is used in daily practice, for instance by using the synergism between opioids and hypnotic drugs to be able to limit the amount of both drugs given to achieve adequate anesthesia. In addition, 50% of maximum effect is unacceptable if the desired effect is for instance probability of tolerance of a painful stimulus; a 95% probability or higher would be desirable in clinical practice.

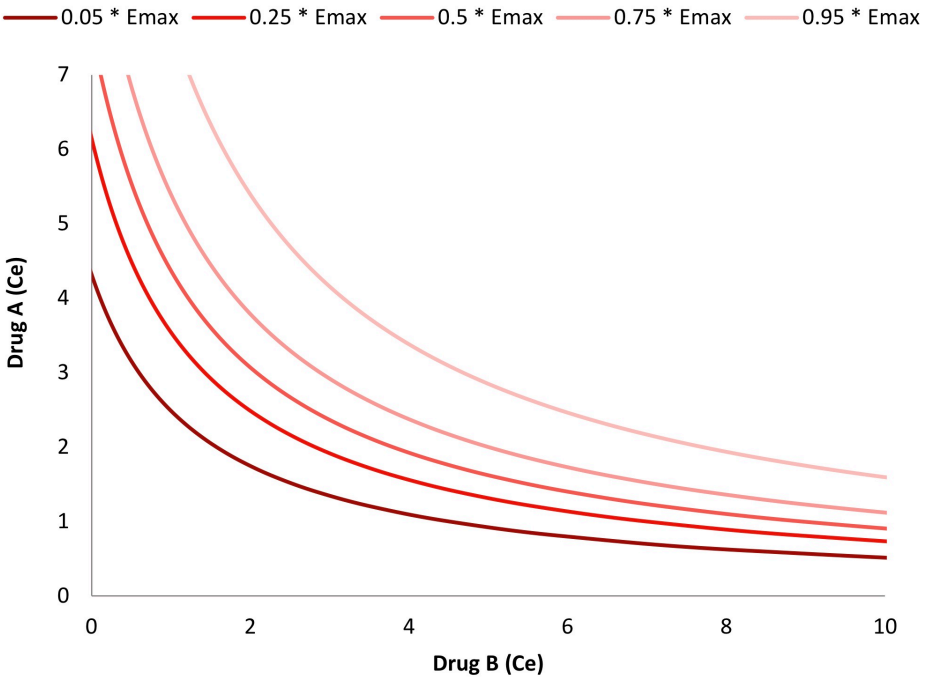

Figure 8. Five isoboles of the response surface model in Figure 6, corresponding with 5%, 25%, 50%, 75% and 95% of maximum effect, respectively. Emax = maximum effect, Ce = effect-site concentration.

Rather than only investigating the interaction at the level of 50% maximum effect, response surface modeling explores the full spectrum of effects, from (near) 0 to (near) maximum effect, at a range of combinations of the two drugs. An example of response surface modeling is shown in Figure 7. The effect can be both a continuous measurement such as an EEG-derived hypnotic monitor, and a dichotomous measurement such as probability of tolerance of a stimulus. Another way to visualize two-drug interactions is through the use of isoboles, which are two-dimensional representations of a slice of the response surface model. Figure 8 shows five isoboles

derived from the response surface model in Figure 7, corresponding with 5%, 25%, 50%, 75% and 95% of maximum effect.

Interactions can be described using various models. The term U is often used in interaction modeling, and can be seen as the combined potency of the drugs that are used, normalized to their respective C50s. In short, U can be seen as the concentration of a new, virtual drug, with the characteristics of the drugs that are investigated. U can be used to describe a certain probability of effect P (for dichotomous endpoints):

$$P = \frac{U^{\gamma}}{1 + U^{\gamma}} \quad (2)$$

where γ is the slope parameter, or steepness of the concentration-effect relationship. This is actually a sigmoid Emax equation (Eq. 1) with $E_0 = 0$ and $E_{max} = 1$. Heyse et al.[18] describes the different interaction models in detail in their appendix. A more simplified explanation will be presented here, describing only models relevant to this thesis. The simplest interaction model is the additive model:

$$U = U_A + U_B \quad (3)$$

where U_A is the normalized concentration of drug A ($C_A/C50_A$) and U_B is the normalized concentration of drug B ($C_B/C50_B$). Equation 3 is a form of the Greco model (Eq. 4), which has the addition of an interaction parameter α. If α = 0, the interaction is additive, and is the same as Eq. 3. If α > 0, the interaction is synergistic and if α < 0, the interaction is infra-additive.

$$U = U_A + U_B + \alpha \times U_A \times U_B \quad (4)$$

The third model is the reduced Greco model, which assumes α in Eq. 4 to be equal to 1, and removes the additive component of drug B:

$$U = U_A \times (1 + U_B) \quad (5)$$

In this model, the C50 of drug B is the concentration that apparently reduces the C50 of drug A by 50%, and assumes drug B had no effect on its own (if $U_A = 0$, $U = 0$).

Bouillon introduced the Hierarchical model[19], which is more complex than the Greco and reduced Greco models. It was developed with the clinical effects of opioids and hypnotics in mind. The idea is that a stimulus with a certain (preopioid) intensity is administered to a patient. The preopioid intensity is attenuated by the opioid. The attenuated (postopioid) stimulus is then affected by the hypnotic, which determines whether the patient ultimately responds to the stimulus or not (Figure 9).

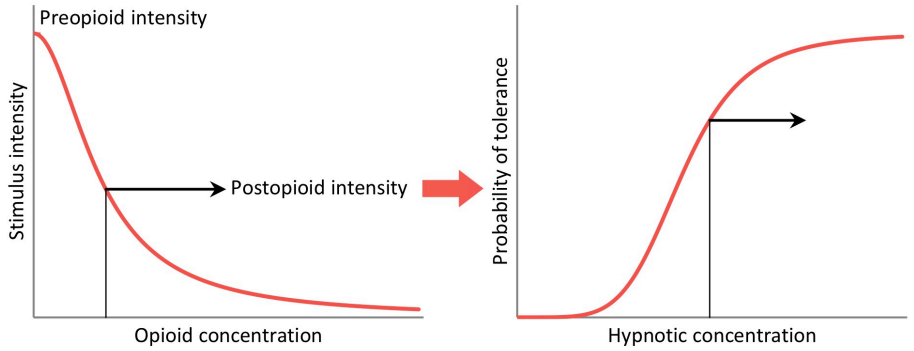

Figure 9. The Hierarchical model. The stimulus with a preopioid intensity undergoes attenuation by the opioid. This attenuation (the postopioid intensity) determines in part the shape of the concentration-effect curve of the hypnotic drug. The hypnotic concentration then determines the probability of tolerance of the stimulus.

In the original model, the probability of tolerance to a stimulus is described as:

$$P = \frac{{C_H}^{\gamma}}{(C50_H \times postopioid\ )^{\gamma} + {C_H}^{\gamma}} \tag{6}$$

$$postopioid\ = preopioid \times \left(1 - \frac{{C_O}^{\gamma_O}}{(C50_O \times preopioid\ )^{\gamma_O} + {C_O}^{\gamma_O}}\right) \tag{7}$$

where *postopioid* is the stimulus intensity after attenuation by the opioid, *preopioid* is the stimulus intensity in absence of the opioid, C_H is the concentration of the hypnotic, C_O is the concentration of the opioid, $C50_H$ is the concentration of the hypnotic resulting in 50% of maximum effect, $C50_O$ is the concentration of the opioid resulting in 50% of maximum effect, γ is the slope parameter for the probability of tolerance, and γ_O is the slope parameter for the opioid vs. stimulus intensity relationship.

If $U = U_H$ / *postopioid*, then this model can be described as such:

$$U = \frac{U_H}{preopioid} \times \left(1 + \left(\frac{U_O}{preopioid}\right)^{\gamma_O}\right) \tag{8}$$

where U_H is the normalized concentration of the hypnotic ($C_H/C50_H$) and U_O is the normalized concentration of the opioid ($C_O/C50_O$).

This model is considered to be overparameterized, because several parameters (preopioid intensity and the C50s for both hypnotic and opioid) cannot be estimated

independently. For studies with only a single stimulus, intensity can be set to 1 to solve this problem. The model can then be simplified to:

$$U = U_H \times (1 + U_O{}^{\gamma_O}) \quad (9)$$

This model is in fact similar to the reduced Greco model in Eq. 5, with the addition of a slope factor γ_O for the opioid effect (drug B in Eq. 5). In case of multiple stimuli, solving the problem of overparameterization can be done in several ways, but the reader is referred to the appendix of the sevoflurane-remifentanil interaction study by Heyse et al.[18] for further explanation, as this thesis does not investigate multiple stimuli in interaction studies.

In clinical practice, as is the case with the basics of pharmacokinetics and pharmacodynamics, the way most anesthesiologists use this knowledge is arbitrary and based on rough dosing schemes and mainly experience. Interaction modeling may increase the accuracy of drug dosing even in the presence of multiple drugs,[20] limiting the risks of under- and overdosing and as such, undesired effects such as awareness or pain sensation on the one hand, and hemodynamic instability or delayed recovery on the other. Three studies have been done to extensively quantify the interactions between propofol and remifentanil (Bouillon et al.[19]), propofol and sevoflurane (Schumacher et al.[21]) and sevoflurane and remifentanil (Heyse et al.[18]), on tolerance of noxious and non-noxious stimuli. Bouillon and Schumacher also modeled the interaction on continuous measurements, such as the bispectral index and other hypnotic monitors. All three studies used response surface modeling to visualize the interaction between the two drugs. Chapter 5 expands on the sevoflurane-remifentanil interaction by exploring the combined effect on not only hypnotic monitors, as Bouillon and Schumacher did previously, but also on marketed 'analgesic' monitors, and the effect that noxious stimulation has on these continuous measurements, also using response surface modeling.

In anesthetic practice, it is not uncommon to use more than two drugs. For instance, anesthesia may be induced by using an intravenous drug such as propofol, combined with an opioid, and as soon as the airway is secured, anesthesia can be maintained using volatile anesthetics such as sevoflurane, with the addition of an opioid. Thus, to be able to maintain a stable anesthesia with three drugs with differing methods of administration (propofol and perhaps the opioid in bolus doses, sevoflurane at a certain continuous rate, with the opioid in bolus doses or continuous infusion), not only is a good understanding of the interactions necessary, but also some way to visualize or even help titrate the drugs. This is where triple interaction modeling comes into play. Chapter 6 explores the interaction between sevoflurane, propofol and remifentanil, on

tolerance of laryngoscopy – a noxious stimulus – by combining the data from the three previously mentioned studies by Bouillon[19] (propofol-remifentanil), Schumacher[21] (propofol-sevoflurane) and Heyse[18] (sevoflurane-remifentanil). These three studies were all performed in a similar manner, with reproducible drug administration, very similar trial designs and similar, clinically relevant endpoints (in particular: tolerance of laryngoscopy). The trial design used was a modification of the crisscross trial design as described by Short et al.[22] In this design, study subjects receive one of the tested drugs at a stable concentration, while the second drug is titrated stepwise, where measurements are done after ample time for equilibration (12-15 minutes) to ensure pseudo-steady state conditions. Due to the similar design and similar endpoints, these studies can be combined to model a triple interaction. These (two or three drug) interaction models can be visualized on advanced monitors such as the SmartPilot View (Drägerwerk, Lubeck, Germany) or the Navigator (GE Healthcare, Chicago, IL, USA).

Apart from aid through visualization, Chapter 6 also focusses on the Noxious Stimulation Response Index (NSRI), which has previously been described by Luginbühl et al. for the propofol-remifentanil interaction. The NSRI has been expanded in Chapter 6 to include the triple interaction model. The NSRI is a transformation of the probability of tolerance of laryngoscopy, scaled from 100 (no drug effect) to 0 (profound drug effect). This index allows for better quantification of the interaction drug effect, as an NSRI of 20 by the use of any two-drug combination between sevoflurane, propofol and remifentanil, or the three drugs together, all correspond with a probability of 90% that the patient will tolerate laryngoscopy.

Aims of this thesis

The aim of this thesis is to explore several strategies in quantifying the pharmacology of anesthetic drugs in order to enable more accurate titration of individual drugs or multidrug combinations.

- The very basis on which all other models rely, is an adequate pharmacokinetic model. For dexmedetomidine, an optimized PK model was developed.
- The next step is to incorporate pharmacodynamics to create a PKPD model. The previously developed dexmedetomidine PK model was expanded to include a PD component based on the desired sedative effects.
- In a unique way, for the same drug, a PD model was developed on the hemodynamic side effects of dexmedetomidine, again using the previously developed PK model as a basis. This may increase the safety of

dexmedetomidine administration by titrating to desired sedative levels while maintaining a safe hemodynamic profile.

- The next step is pharmacodynamic interaction modeling, where two drugs are delivered to stable effect site concentrations, and the interactive effect between these two drugs can be investigated. In an expansion of an existing interaction model for sevoflurane-remifentanil for tolerance of different stimuli, additional modeling was performed to investigate the interaction between these two drugs on hypnotic and analgesic monitor measurements.
- A step above and beyond two-drug interaction modeling is multiple drug interaction modeling. A first great step has been made by investigating the interaction between sevoflurane, propofol and remifentanil, and by expanding the NRSI to include this triple interaction.

References

1. Beecher HK, Todd DP: A study of the deaths associated with anesthesia and surgery: based on a study of 599, 548 anesthesias in ten institutions 1948-1952, inclusive. Ann Surg 1954; 140: 2-35

2. Lienhart A, Auroy Y, Péquignot F, Benhamou D, Warszawski J, Bovet M, Jougla E: Survey of anesthesia-related mortality in France. Anesthesiology 2006; 105: 1087-97

3. Masui K, Upton RN, Doufas AG, Coetzee JF, Kazama T, Mortier EP, Struys MM: The performance of compartmental and physiologically based recirculatory pharmacokinetic models for propofol: a comparison using bolus, continuous, and target-controlled infusion data. Anesth Analg 2010; 111: 368-79

4. Bijker JB, van Klei WA, Kappen TH, van Wolfswinkel L, Moons KGM, Kalkman CJ: Incidence of intraoperative hypotension as a function of the chosen definition: literature definitions applied to a retrospective cohort using automated data collection. Anesthesiology 2007; 107: 213-20

5. Persson J, Hasselstrom J, Maurset A, Oye I, Svensson JO, Almqvist O, Scheinin H, Gustafsson LL, Almqvist O: Pharmacokinetics and non-analgesic effects of S- and R-ketamines in healthy volunteers with normal and reduced metabolic capacity. Eur J Clin Pharmacol 2002; 57: 869-75

6. Shafer SL, Varvel JR, Aziz N, Scott JC: Pharmacokinetics of fentanyl administered by computer-controlled infusion pump. Anesthesiology 1990; 73: 1091-102

7. Virtanen R, Savola JM, Saano V, Nyman L: Characterization of the selectivity, specificity and potency of medetomidine as an alpha 2-adrenoceptor agonist. Eur J Pharmacol 1988; 150: 9-14

8. Guo TZ, Tinklenberg J, Oliker R, Maze M: Central alpha 1-adrenoceptor stimulation functionally antagonizes the hypnotic response to dexmedetomidine, an alpha 2-adrenoceptor agonist. Anesthesiology 1991; 75: 252-6

9. Hall JE, Uhrich TD, Barney JA, Arain SR, Ebert TJ: Sedative, amnestic, and analgesic properties of small-dose dexmedetomidine infusions. Anesth Analg 2000; 90: 699-705

10. Lobo FA, Wagemakers M, Absalom AR: Anaesthesia for awake craniotomy. British journal of anaesthesia 2016; 116: 740-4

11. Belleville JP, Ward DS, Bloor BC, Maze M: Effects of intravenous dexmedetomidine in humans. I. Sedation, ventilation, and metabolic rate. Anesthesiology 1992; 77: 1125-33

12. Hsu YW, Cortinez LI, Robertson KM, Keifer JC, Sum-Ping ST, Moretti EW, Young CC, Wright DR, Macleod DB, Somma J: Dexmedetomidine pharmacodynamics: Part I: Crossover comparison of the respiratory effects of dexmedetomidine and remifentanil in healthy volunteers. Anesthesiology 2004; 101: 1066-76

13. Talke P, Lobo E, Brown R: Systemically administered alpha2-agonist-induced peripheral vasoconstriction in humans. Anesthesiology 2003; 99: 65-70

14. Figueroa XF, Poblete MI, Boric MP, Mendizábal VE, Adler-Graschinsky E, Huidobro-Toro JP: Clonidine-induced nitric oxide-dependent vasorelaxation mediated by endothelial alpha(2)-adrenoceptor activation. Br J Pharmacol 2001; 134: 957-68

15. Snapir A, Posti J, Kentala E, Koskenvuo J, Sundell J, Tuunanen H, Hakala K, Scheinin H, Knuuti J, Scheinin M: Effects of low and high plasma concentrations of dexmedetomidine on myocardial perfusion and cardiac function in healthy male subjects. Anesthesiology 2006; 105: 70

16. Ebert TJ, Hall JE, Barney JA, Uhrich TD, Colinco MD: The effects of increasing plasma concentrations of dexmedetomidine in humans. Anesthesiology 2000; 93: 382-94

17. Dyck JB, Maze M, Haack C, Azarnoff DL, Vuorilehto L, Shafer SL: Computer-controlled infusion of intravenous dexmedetomidine hydrochloride in adult human volunteers. Anesthesiology 1993; 78: 821-8

18. Heyse B, Proost JH, Schumacher PM, Bouillon TW, Vereecke HE, Eleveld DJ, Luginbuhl M, Struys MM: Sevoflurane remifentanil interaction: comparison of different response surface models. Anesthesiology 2012; 116: 311-23

19. Bouillon TW, Bruhn J, Radulescu L, Andresen C, Shafer TJ, Cohane C, Shafer SL: Pharmacodynamic interaction between propofol and remifentanil regarding hypnosis, tolerance of laryngoscopy, bispectral index, and electroencephalographic approximate entropy. Anesthesiology 2004; 100: 1353-72

20. Struys MM, De Smet T, Mortier EP: Simulated drug administration: an emerging tool for teaching clinical pharmacology during anesthesiology training. Clin Pharmacol Ther 2008; 84: 170-4

21. Schumacher PM, Dossche J, Mortier EP, Luginbuehl M, Bouillon TW, Struys MM: Response surface modeling of the interaction between propofol and sevoflurane. Anesthesiology 2009; 111: 790-804

22. Short TG, Ho TY, Minto CF, Schnider TW, Shafer SL: Efficient trial design for eliciting a pharmacokinetic-pharmacodynamic model-based response surface describing the interaction between two intravenous anesthetic drugs. Anesthesiology 2002; 96: 400-8

Chapter 2: Development of an optimized pharmacokinetic model of dexmedetomidine using target-controlled infusion in healthy volunteers

Modified from *Anesthesiology 2015; 123:357-67*

Laura N. Hannivoort, Douglas J. Eleveld, Johannes H. Proost, Koen M. E. M. Reyntjens, Anthony R. Absalom, Hugo E. M. Vereecke, Michel M. R. F. Struys

Abstract

Background: Several pharmacokinetic models are available for dexmedetomidine, but these have been shown to underestimate plasma concentrations. Most were developed with data from patients during the postoperative phase and/or in intensive care, making them susceptible to errors due to drug interactions. The aim of this study is to improve on existing models using data from healthy volunteers.

Methods: After local ethics committee approval, the authors recruited 18 volunteers, who received a dexmedetomidine target-controlled infusion with increasing target concentrations: 1, 2, 3, 4, 6, and 8 ng/ml, repeated in two sessions, at least 1 week apart. Each level was maintained for 30 min. If one of the predefined safety criteria was breached, the infusion was terminated and the recovery period began. Arterial blood samples were collected at preset times, and NONMEM (Icon plc, Ireland) was used for model development.

Results: The age, weight, and body mass index ranges of the 18 volunteers (9 male and 9 female) were 20 to 70 yr, 51 to 110 kg, and 20.6 to 29.3 kg/m^2, respectively. A three-compartment allometric model was developed, with the following estimated parameters for an individual of 70 kg: V1 = 1.78 l, V2 = 30.3 l, V3 = 52.0 l, CL = 0.686 l/min, Q2 = 2.98 l/min, and Q3 = 0.602 l/min. The predictive performance as calculated by the median absolute performance error and median performance error was better than that of existing models.

Conclusions: Using target-controlled infusion in healthy volunteers, the pharmacokinetics of dexmedetomidine were best described by a three-compartment allometric model. Apart from weight, no other covariates were identified.

Introduction

Dexmedetomidine is an α2-adrenoceptor agonist with sedative, analgesic, and anxiolytic properties. Patients receiving low doses of dexmedetomidine remain rousable despite otherwise appearing to be deeply asleep. This makes it a useful drug for conscious sedation, specific surgical procedures such as awake craniotomies, and sedation in intensive care units (ICUs). In experimental settings, dexmedetomidine is used in the context of "opioid-reducing anesthesia" techniques[1] and to attenuate perioperative inflammatory responses.[2] To compensate for the rather slow pharmacokinetic profile of the drug, which results in increasing plasma concentrations over time with fixed-rate infusions, target-controlled infusion (TCI) using an accurate pharmacokinetic model is likely to be helpful in managing and titrating sedation by maintaining stable and predictable plasma concentrations.

Few dexmedetomidine pharmacokinetic models have been developed with data from healthy volunteers. The Dyck model combines pharmacokinetic data derived from the studies of plasma concentrations after a bolus dose[3] with data acquired during and after a computer-controlled infusion.[4] However, this is a very preliminary model, with height as the only covariate, and the model has been shown to be inaccurate at higher target concentrations.[5] The Dutta model is derived from the data from a healthy population, using computer-controlled infusion with an unpublished model.[6] Venous blood samples were used, although this is likely not an accurate measurement of drug delivery to target organs in non-steady-state conditions, and may have influenced the accuracy of the parameters of the Dutta model. Most of the existing pharmacokinetic models for dexmedetomidine were obtained from trials involving postoperative and/or ICU patients, using either computer-controlled infusion with an unpublished model[7] or continuous infusion.[8-10] This approach is sensitive to the influence of confounding drugs such as subtherapeutic levels of anesthetic drugs, additional sedation or analgesia, and other medications. The resulting pharmacokinetic models are thus less applicable to single drug pharmacokinetic modeling. Of the available "ICU" models, the Talke model[7] is often used, but similar to the Dyck model, it also has been shown to underestimate plasma concentration at higher target concentrations of dexmedetomidine.[11] Shafer *et al*.[12] suggested that using TCI administration during model development may provide more appropriate parameters for use in subsequent TCI. Only the Dyck, Dutta, and Talke models used TCI administration (Dutta and Talke used unpublished models) for model development.

For these reasons, we believe that some improvement is desirable for pharmacokinetic models of dexmedetomidine. The aim of this study is to develop a pharmacokinetic

model for dexmedetomidine, using TCI administration in healthy volunteers, using data from a population with a wide range of ages and weights and a wide range of drug concentrations.

Materials and Methods

The study was approved by the local Medical Ethics Review Committee (University Medical Center Groningen, Groningen, The Netherlands; Medical Ethics Review Committee number: 2012/400) and was registered in the ClinicalTrials.gov database (NCT01879865). Written informed consent was obtained from 18 healthy volunteers, who were recruited and screened by QPS (a contract research organization based in Groningen, The Netherlands). Subjects were stratified according to age and sex (6 subjects, 3 male and 3 female, for each age group: 18 to 34 yr, 35 to 54 yr, and 55 to 72 yr). Inclusion criteria were American Society of Anesthesiologists physical status I, absence of any medical history of significance, and absence of chronic use of medication (oral contraceptives excluded), alcohol, drugs, or tobacco. Exclusion criteria were known intolerance to dexmedetomidine and body mass index (BMI) less than 18 kg/m^2 or greater than 30 kg/m^2. Women who were pregnant or nursing were also excluded. Subjects were instructed not to use medication or drugs in the 2 weeks before the study days, not to drink coffee or alcohol or smoke tobacco in the 2 days before each study day, and to fast from 6 h before the start of the study. To study the intraindividual variability of pharmacokinetic estimations more effectively, the volunteers were enrolled in two separate sessions, at least 1 week and at most 3 weeks apart. We hypothesized that there may be a difference between the first and second sessions due to currently unknown but identifiable causes such as the variation in level of anxiety or adrenergic tone between sessions.

Monitoring

An 18- or 20-gauge IV cannula was placed in a vein on the subject's nondominant arm or hand. A 20-gauge arterial cannula was placed in the radial artery of the same arm under local anesthesia (lidocaine 1%), using the Seldinger technique, and used for continuous arterial blood pressure monitoring and blood sampling. Standard anesthetic monitoring was performed using a Philips MP50 monitor (Philips Healthcare, The Netherlands). Noninvasive blood pressure was measured and recorded at 5-min intervals on the arm opposite the IV and arterial line. All subjects maintained spontaneous ventilation, with a nasal cannula (O2/CO2 Nasal Filterline®; Covidien, USA) for oxygen delivery as needed, from 0 to 4 l/min. Capnography was monitored by means of side-stream sampling through the nasal cannula (Microstream® carbon dioxide extension; Philips Healthcare).

All monitored parameters were captured by a computer running RUGLOOP II software (Demed, Belgium). RUGLOOP II also controlled the syringe pump (Orchestra® Module DPS; Orchestra® Base A; Fresenius Kabi, Germany) for dexmedetomidine administration.

Drug Infusion

Dexmedetomidine was delivered through TCI using the Dyck model.[4] Computer simulations with the Dyck model were performed during study design to determine optimal infusion scheme and sampling times. Various sampling schedules were tested with 10 to 15 samples per patient. In each simulated sampling schedule, samples were included before each increase in target concentration and before the start of the recovery period. For each schedule, 1,000 sets of 20 patients were simulated, taking into account log-normally distributed interindividual variability of 40% and proportional residual variability of 20%. Each dataset was analyzed with NONMEM 7.2 (Icon plc, Ireland) (as described in the section Modeling) assuming log-normally distributed interindividual variability, and its performance was evaluated by calculating the root-mean-squared-error (RMSE, in percentage) of the estimated population values for V1, CL, and the maximum value of all parameters (V1, V2, V3, CL, Q2, and Q3) as measures of the precision of the estimated model parameters. The sampling times were varied until the lowest RMSE values were obtained. These simulations revealed that for more accurate determination of the central volume V1, a short initial infusion was necessary, followed by the first TCI period starting at 10 min, with sampling times at 2 min and before the first TCI period. With 13 sampling points (excluding blank), the optimal sampling scheme (as described in the section Arterial Blood Sampling and Dexmedetomidine Analysis) resulted in RMSEs of 23% (V1), 19% (CL), and a maximum of RMSE 36%.

The initial drug infusion was given at 6 µg kg^{-1} h^{-1} for 20 s. To ensure accurate infusion history for the TCI system, this infusion was controlled by the TCI steering algorithm (TCI target set to 1 ng/ml for 20 s, then returned to 0). After 10 min, TCI was restarted with stepwise increasing targets of 1, 2, 3, 4, 6, and 8 ng/ml. Each target was maintained for 30 min.

Because dexmedetomidine bolus doses can induce hypertension and reflex bradycardia, the infusion rate of dexmedetomidine was limited to 6 µg kg^{-1} h^{-1} for the first four steps using a limiting infusion rate algorithm as part of the TCI control system. For 6 and 8 ng/ml, the maximum infusion rate was increased to 10 µg kg^{-1} h^{-1} to facilitate reaching the target within a reasonable time.

The following criteria were used to ensure the safety of the subjects:

- 30% increase from baseline mean arterial blood pressure for more than 5 min;
- 30% decrease from baseline mean arterial blood pressure for more than 5 min;
- Heart rate less than 40 beats/min for more than 5 min;

- Changes in cardiac conduction or cardiac rhythm;
- Inability to maintain a patent airway and/or a decrease of oxygen saturation (Spo2) less than 93% despite the use of simple airway maneuvers and/ or supplementation of up to 4 l/min O2 *via* nasal cannula;
- Modified Observer's Assessment of Alertness/Sedation score of 0 (no response to painful stimulus), as assessed before each increase in target concentration.[13]

If any of these criteria were met, or if the last TCI step was completed, dexmedetomidine infusion was halted, and the recovery period started, which lasted 5 h.

Arterial Blood Sampling and Dexmedetomidine Analysis

We performed simulations using the Dyck model to determine optimal sampling times for optimal model parameter estimations. Arterial blood samples were taken at baseline, 2 min after the initial 20-s infusion, before each increase in target concentration (at 10 min and every 30 min thereafter), before the start of the recovery period, and at 2, 5, 10, 20, 60, 120, and 300 min in the recovery period. EDTA tubes (4 ml) were used for blood sample collection. Each sample was stored on ice and centrifuged within 30 min after obtaining the sample. The obtained plasma samples were stored at −80°C until the study was finished.

The samples were analyzed by contract research organization QPS, using reverse-phase high-performance liquid chromatography triple quadrupole mass spectrometry. Ten microgram of deionized water and 10 µg of internal standard working solution (10 ng/ml of medetomidine-$^{13}C,d_3$ [Toronto Research Chemicals, Canada] in deionized water) were added to 100 µl of plasma sample (thawed at room temperature). Protein precipitation was induced by the addition of 300 µl of MeOH (methanol HiPer- Solv Chromanorm gradient grade for high-performance liquid chromatography [Merck, Germany]) and brief vortexing. The samples were centrifuged at 14,000 rpm for 5 min, and the supernatant was transferred to clean 10-ml glass tubes. The solvent was evaporated to dryness in a Turbovap LV evaporator (Zymark; Biotage, Sweden) at 45°C under a gentle stream of nitrogen. The sample residue was redissolved in deionized water:formic acid (100:0.1 v/v):acetonitrile (80:20 v/v) and briefly vortexed. All liquid chromatography-mass spectrometry analysis was conducted on an API 4000 triple quadrupole mass spectrometer (AB SCIEX, Canada) equipped with a type 1100 liquid chromatograph (Agilent, USA) comprising a thermostatted well plate autosampler, a thermostatted column compartment, and a binary pump. Liquid chromatography was done with an xBridge C18 column (3.5 µm, 2.1 × 50 mm; Waters, The Netherlands) and using an AJO-04286 guard column (Phenomenex, The Netherlands). The autosampler temperature was +4°C, and an injection volume of 10 µl was used. A binary gradient separation at a

flow rate of 500 µl/min was used with solvents A (deionized water:formic acid 100:0.1 v/v) and B (acetonitrile), as follows: 0.00 to 0.20 min 80:20 A:B v/v; 1.00 to 2.00 min 20:80 A:B v/v; 2.10 to 5.00 min 80:20 A:B v/v. The column was kept at 40°C. Tandem mass spectrometry was done by using positive ion turbo ionspray in multiple reaction monitoring mode and using the transitions *m/z* 201.2 → 95.1 for dexmedetomidine and *m/z* 205.2 → 99.0 for medetomidine-$^{13}C,d_3$. The spray voltage was 3,000 V, and the probe temperature was 150°C. Other parameters were optimized: collision energy 27 eV, declustering potential 56.0 V, and collision cell exit potential 6.0 V. Nitrogen was used as the collision gas. "Zero air" from a local unit was used for curtain gas, ion source gasses 1 and 2 at 35, 50, and 80 psig, respectively. Quantification range limits for this method were 0.020 to 20 ng/ml.

Modeling

The time course of dexmedetomidine plasma concentration was modeled using a three-compartment mammillary pharmacokinetic model with volumes V1, V2, and V3, elimination clearance CL, and intercompartmental clearances Q2 and Q3. The *a priori* model assumed allometric scaling where volumes scale linearly and clearances scale to the ¾ power exponent of the body size descriptor, which was total body weight. Model parameters were estimated relative to a reference subject, a 35-yr-old, 70-kg, and 170-cm individual. Population parameters were assumed to be log-normally distributed and a proportional error model was used for residual error.

During model development, examination of *post hoc* variability was used to guide testing of parameter–covariate relations. Models were compared on the basis of Akaike information criteria (AIC) and performance error as described by Varvel *et al*.[14] using median performance error (MDPE) and median absolute performance error (MDAPE). The performance error was calculated as:

$$PE = \frac{Cp_{observed} - Cp_{predicted}}{Cp_{predicted}} \times 100\%$$

where *Cp* is dexmedetomidine plasma concentration. We estimated model predictive performance for out-of-sample observations, that is, samples not within the estimation data set using repeated two-fold cross-validation. This involves random partitioning of the observations into two equal (number of individuals) sets: D1 and D2. Model parameters were estimated using D1 and the resulting model was used to predict D2. The process is repeated exchanging D1 and D2. To reduce Monte-Carlo variability due to random partitioning, cross-validation was repeated 10 times, each with different random partitions of D1 and D2. All of the out-of-sample predictions were collected, and MDPE and MDAPE were calculated.

During model building, we required a decrease in AIC of at least 9.2 when adding parameters, corresponding to a relative likelihood (Akaike weight) of greater than 0.99 for the modified model, while removing model parameters required a decrease in AIC. In addition, we required model modifications to decrease MDAPE for the out-of-sample predictions. CIs for population parameters were described using likelihood profiles. We compared the predictive performance of the final model with models by Dyck,[4] Dutta,[6] Talke,[7] Lin,[8] Venn,[9] and Välitalo.[10]

Results

Forty-three volunteers were screened by QPS. Of these, 26 passed the screening and 18 volunteers were selected to participate, divided into the age-sex–stratified groups. Two subjects (1 male, group: 35 to 54 yr; 1 female, group: 18 to 34 yr) withdrew after the first session, resulting in 34 completed sessions. The age range was 20 to 70 yr, weight range was 51 to 110 kg, and BMI range was 20.6 to 29.3 kg/m^2. Of the two subjects who had withdrawn after the first session, one reported a hematoma after arterial line placement; the other withdrew due to a headache the night after the first session.

For each step in the infusion stage, the number of completed sessions is as follows (of a total of 34 sessions): 1 ng/ml: 34 sessions; 2 ng/ml: 32 sessions; 3 ng/ml: 19 sessions; 4 ng/ml: 12 sessions; 6 ng/ml: 4 sessions; and 8 ng/ml: 1 session. The reasons for stopping the dexmedetomidine infusions were reaching 8 ng/ml in one session, an Observer's Assessment of Alertness/Sedation score of 0 in 22 sessions, bradycardia in 6 sessions (4 volunteers), hypertension in 2 sessions (2 volunteers), and airway obstruction requiring continuous manual airway maneuvers (jaw thrust, chin lift) in 3 sessions (2 volunteers). None of the volunteers required any medical intervention at the time of stopping the dexmedetomidine infusion.

Table 1. Dexmedetomidine Model Parameters

$V1(l) = 1.78 \times (WT/70) \times e^{\eta 1} \times e^{\eta 2}$		Variance	CV (%)
$V2(l) = 30.3 \times (WT/70)$	η1 (IIV)	0.0356	19.0
$V3(l) = 52.0 \times (WT/70) \times e^{\eta 3}$	η2 (IOV)	0.273	56.0
$CL(l/min) = 0.686 \times (WT/70)^{0.75} \times e^{\eta 4}$	η3 (IIV)	0.0635	25.6
$Q2(l/min) = 2.98 \times (V2/30.3)^{0.75}$	η4 (IIV)	0.0276	16.7
$Q3(l/min) = 0.602 \times (V3/52.0)^{0.75}$			

ηi are normally distributed random variables with a mean of 0 and variances as shown in the table
CL = elimination clearance; CV = coefficient of variation; Q2-Q3 = intercompartmental clearances between compartment 1 and 2 or 3, respectively; V1-V3 = volume of corresponding compartments; WT = subject weight; IIV = interindividual variation; IOV = interoccasion variation

Side effects of dexmedetomidine infusions included obstructive apnea in eight subjects (55 to 72 yr age group, as well as two subjects in the 35 to 54 yr age group) requiring some degree of manual airway maneuvers, but no airway devices of any kind were necessary. Five subjects experienced symptomatic orthostatic hypotension, mostly after the end of the study, when they started mobilizing. Slow mobilization and fluid

administration (IV or orally) were in most cases sufficient to counter this; however, two subjects required atropine 0.5 mg administration for sustained bradycardia after orthostatic hypotension, and one subject received 5 mg ephedrine to counter the hypotension. Two subjects experienced nausea, one subject also with vomiting. One received only ondansetron 4 mg in one session and the other subject received dexamethasone 5 mg and ondansetron 4 mg in both sessions. These events are likely associated with the hypotensive events. A headache during the following night or day was reported by two subjects.

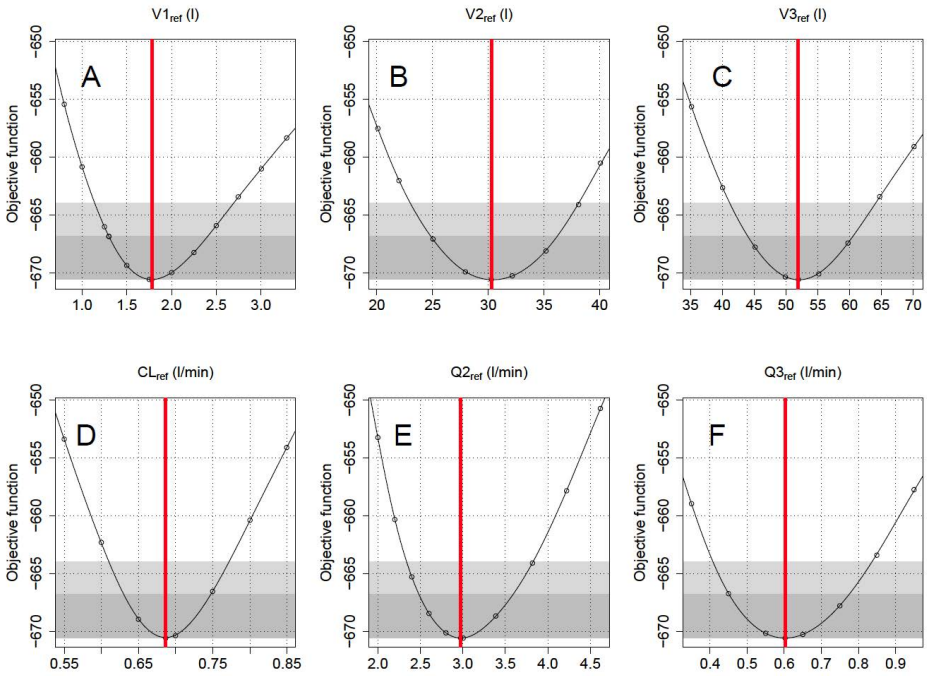

Figure 1. (A–F) Likelihood profiles show changes in objective function value when fixing model parameters at particular values. The red line is the parameter estimate in the final model. The parameter interval where the likelihood profile is shaded dark gray corresponds to the 95% CI (change in objective function <3.84), and the light gray region corresponds to the 99% CI (change in objective function <6.63).

CL = elimination clearance; Q2–Q3 = intercompartmental clearances between compartment 1 and 2 or 3, respectively; V1–V3 = volume of corresponding compartments.

In total, 408 arterial plasma samples were obtained. One sample result was reported as being lower than, but close to, the lower limit of quantification (0.019 ng/ml) and was treated as a normal observation. Twenty-nine other samples were below the

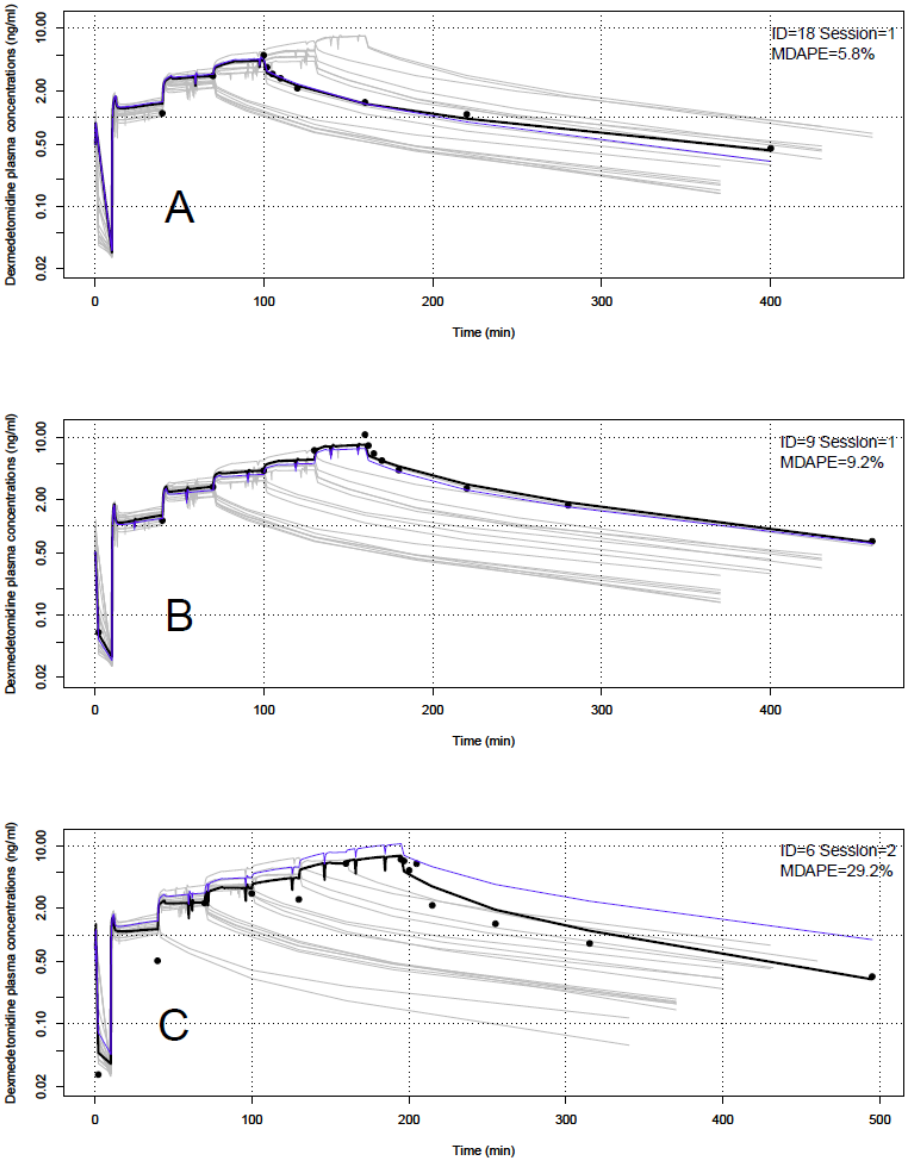

Figure 2. Observations and predictions for individuals and sessions with the best (A), median (B), and worst (C) median absolute performance error (MDAPE). Filled circles are measured plasma concentrations, the black line is the individual post hoc prediction, gray lines are individual post hoc predictions for other individuals in the same session, and the blue line is the population prediction. ID = volunteer identification number.

lower limit of quantification. These samples were excluded from analysis. In all, 379 samples were used for analysis. When estimating the *a priori* model, we found that the population variability estimates for Q2 and Q3 were very small and these were fixed

to 0. Using compartmental allometry, as described by Eleveld *et al.*,[15] for Q2 and Q3 lead to a small improvement in model performance (ΔAIC = −6.70; ΔMDAPE [out-of-sample] = −0.23). Also, fixing the population variability of *V2* to 0 led to an improved model (ΔAIC = −1.49; ΔMDAPE [out-of-sample] = −0.05). Covariate search using a two-compartment model did not achieve the same level of performance as the three-compartment model. No other parameter–covariate relations were found to improve the model, neither did using estimated fat-free-mass[16] as body size descriptor. Considering systematic differences in model parameters between the first and second session did not lead to

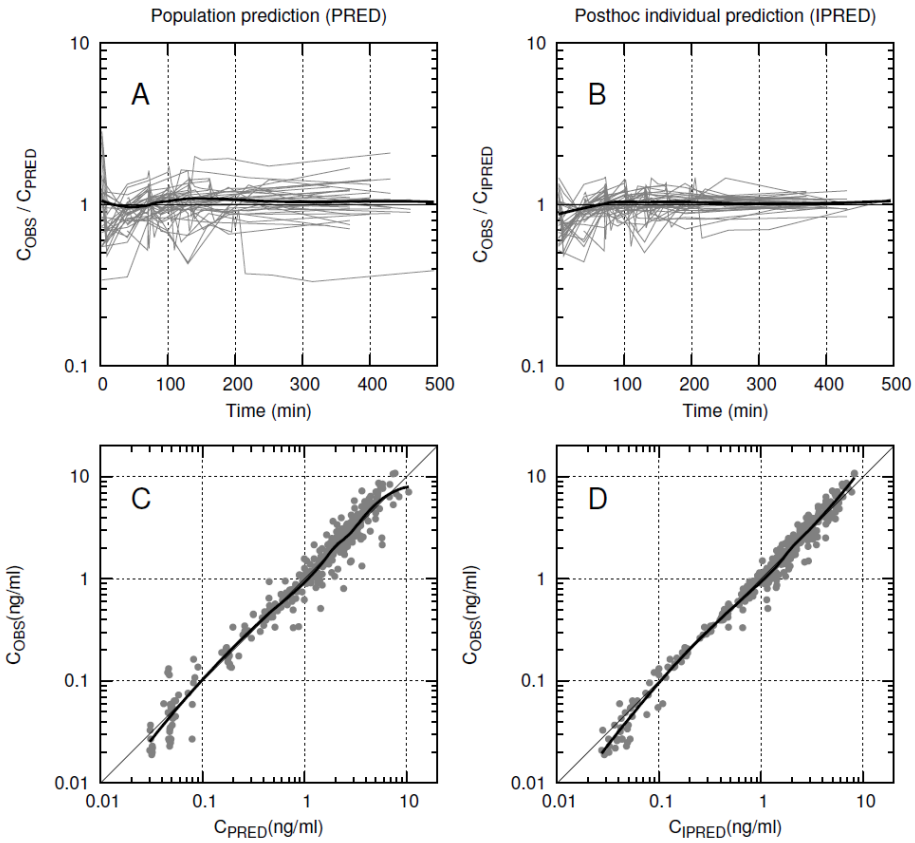

Figure 3. (A) Population-observed/-predicted plasma dexmedetomidine concentrations versus time. (B) Post hoc individual-observed/-predicted plasma dexmedetomidine concentrations versus time. (C) Population-observed versus population-predicted plasma dexmedetomidine concentrations. (D) Post hoc individual-observed versus individual-predicted plasma dexmedetomidine concentrations. The black lines are Loess smoothers.

C_{IPRED} = post hoc individual-predicted plasma concentration; C_{OBS} = observed (measured) plasma concentration; C_{PRED} = population-predicted plasma concentration.

an improved model. Adding interoccasion variance to V1, but not to other parameters, improved model fit (ΔAIC = −14.52; ΔMDAPE [out-of-sample] = −0.41). The equations of the final model are shown in table 1.

The likelihood profiles (fig. 1) show the parameter CIs for the estimated parameters and suggest that there were no problems with parameter identification. Figure 2 shows the best, median, and worst fits of our model. Population and *post hoc* predictions *versus* time and observed dexmedetomidine concentrations are shown in figure 3.

Discussion

Using TCI administration with a preliminary model in healthy volunteers, the pharmacokinetics of dexmedetomidine were best described by a three-compartmental model with allometric scaling of weight to the volumes and elimination clearance, along with compartmental allometric scaling of the intercompartmental distributions. No other covariates were identified.

We used data from healthy volunteers for our pharmacokinetic study, as volunteer studies provide some unique possibilities. A major advantage is the absence of adjuvant medication. In a patient population, dexmedetomidine will almost always be coadministered with other drugs, including anesthetic and analgesic drugs, as clinical indications for dexmedetomidine are limited to procedures in the operating room, postanesthesia care unit, and ICU. In our study, we used escape medication in 4 of 34 sessions (11.8%)—2 sessions (same volunteer): atropine 0.5 mg IV, dexamethasone 5 mg IV, and ondansetron 4 mg IV; 1 session: ephedrine 5 mg IV; and 1 session: ondansetron 4 mg IV. All of these were given in the recovery period, most of these (all atropine and ephedrine doses) between 2 and 3.5 h into the recovery period. If there is a pharmacokinetic interaction between any of these drugs and dexmedetomidine, the influence will have been mostly limited to the last plasma sample.

Selecting healthy volunteers also provided us with the opportunity to use a stratified population, with a larger age range. A wide BMI inclusion range gave us a wider range of weights to assess the influence of weight on dexmedetomidine pharmacokinetics. None of the existing models were able to include weight as a covariate, and two models (Dyck and Lin) included height as the only covariate (for CL). Another feature of our model is the use of compartmental allometric scaling,[15] which assumes that intercompartmental clearances, Q2 and Q3, are better scaled to the volumes of their respective compartments, V2 and V3, than with weight. Eleveld *et al*.[15] recently showed significant differences in the pharmacokinetics of propofol in volunteers and patients. It is as of yet unknown whether there is a systematic difference between patients and volunteers for the pharmacokinetics of dexmedetomidine, and whether volunteer models can be extrapolated to patient populations. However, our current investigation does play an important role in making a comparative study possible, by providing a pharmacokinetic model based on volunteers for future comparisons.

In our study, we studied each volunteer twice. This enabled us to determine whether there is interoccasion variability in dexmedetomidine pharmacokinetics. Both sessions were similar in drug dosing scheme and sampling times. It is reasonable to expect

subjects to be more anxious or have a higher adrenergic tone during the first session, when they do not know what to expect, compared with the second session. This may cause changes in hemodynamic factors that might influence the pharmacokinetic estimations. Although we found that adding interoccasion variance to V1 had a significant effect on our model performance, we did not find any significant systematic influence of session order on the model parameters, which suggests that variations in stress level that occur systematically between the first and second session probably have only little effect on the pharmacokinetics of dexmedetomidine. Interestingly, for V1, interoccasion variance was greater than interindividual variance, indicating that there are factors changing (nonsystematically) between sessions that have a greater effect on V1 than the differences between individuals. As of yet, we can only guess at what these factors are.

During experiment design, we determined the optimal sampling times, that is, when the pharmacokinetic model parameters could be estimated most precisely, using the Dyck model. These simulations revealed that our step-up method, while appropriate for determining V2, V3, and clearances, allowed poorer determination of the central compartment volume. Therefore, we included a 20-s initial infusion before starting the step-up TCI scheme, which would give us more information on V1. The use of a limited infusion rate likely also eliminated, at least in part, potential issues concerning front-end kinetics, as there is no assumption that a bolus dose is distributed instantaneously throughout the vascular system. Avram and Krejcie[17] suggested that three-compartment modeling of drugs given by infusion instead of bolus injection may still estimate front-end kinetics with reasonable accuracy.

Table 2. Parameters of the Final Model and Dexmedetomidine Models in the Literature[4, 6-10], for a 35-yr-old Person with a Height of 170 cm and Weight of 70 kg

	Final Model	Dyck	Dutta	Talke	Lin	Venn	Välitalo
V1 (l)	1.78	7.99	13	16.6	63.4	44.1	104
V2 (l)	30.3	13.8	55	85.5	41.3	104.5	-
V3 (l)	52.0	187	-	-	284.3	-	-
CL (l/min)	0.686	0.4177	0.55	0.751	0.694	0.82	0.65
Q2 (l/min)	2.98	2.26	0.833	1.37	2.43	2.255	-
Q3 (l/min)	0.602	1.99	-	-	0.086	-	-

CL = elimination clearance; Q2-Q3 = intercompartmental clearances between compartment 1 and 2 or 3, respectively; V1-V3 = volume of corresponding compartments

In several articles referenced by Avram and Krejcie, smaller central compartment volumes have been found with continuous infusions than with bolus injections. In our study, V1 was 1.78 l (for an individual of 70 kg), which is smaller than V1 for other models (table 2) thereby modeling the high peak concentrations observed after a fast infusion. Another possible explanation for the smaller V1 is the effect of the direct vasoconstrictive effect of dexmedetomidine, resulting in a decreased central compartment. Because of our early sampling, this effect may have been more pronounced in the model than for studies with delayed sampling.

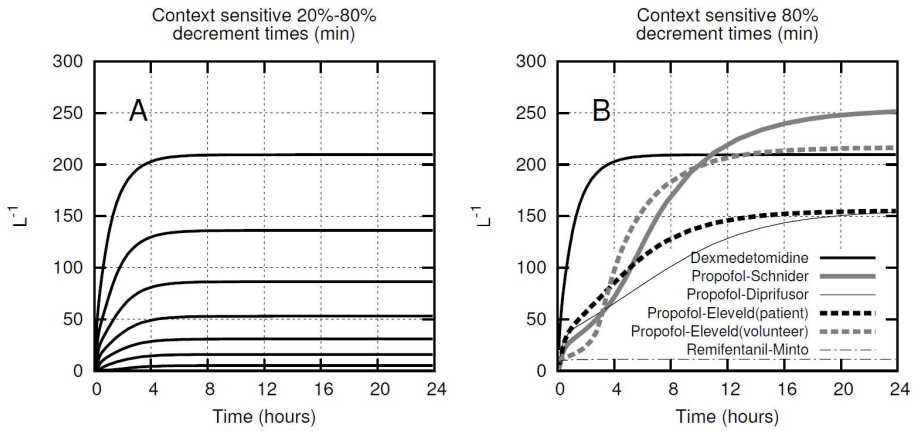

Figure 4. (A) Context-sensitive 20 (lower line), 30, 40, 50, 60, 70, and 80% (upper line) decrement times for dexmedetomidine. (B) Context-sensitive 80% decrement times for dexmedetomidine, propofol (Diprifusor,[18] Schnider,[19] and Eleveld[15] models), and remifentanil (Minto[20] model).

The context-sensitive decrement times (fig. 4) of dexmedetomidine plasma concentrations show that the shapes of the graphs are similar for the 20 to 80% decrement times. For infusions shorter than approximately 10 h, the 80% decrement time for dexmedetomidine is longer than those associated with propofol. However, for infusions longer than approximately 12 h, the 80% decrement times for propofol increase substantially, reaching similar values to dexmedetomidine.

Our model has a low bias and high accuracy (table 3, MDPE and MDAPE, respectively), also in cross-validation (out-of-sample). Figure 3 confirms this, as only in the highest concentrations (sparse data), the precision decreases and bias increases. Figure 5 shows the population predictions *versus* time and observed concentrations for previously published dexmedetomidine pharmacokinetic models,[4, 6-10] showing poorer fits for all models compared with our final model.

Table 3. MDPE and MDAPE for the Final Model and Models from the Literature

	MDPE (%)	MDAPE (%)
Final model		
In-sample	0.6	14.4
Out-of-sample	0.7	15.7
Dyck	20.7	38.6
Dutta	-26.7	27.7
Talke	4.9	21.0
Lin	22.6	33.7
Venn	23.3	29.6
Välitalo	-0.6	36.1

Out-of-sample MD(A)PE was obtained from repeated two-fold cross-validation. MDAPE = median absolute performance error; MDPE = median performance error

Also, as seen in the C_{obs}/C_{pred} *versus* time graphs in figures 3 and 5, our model predicts initial concentrations more accurately than the existing models, indicating that the accuracy concerning front-end kinetics is acceptable.

Comparison of the final model with the previously published models revealed a lower MDAPE for the new model, both in-sample and with out-of-sample cross-validation (table 3). The bias of our model, as estimated with MDPE, was low. Figure 5 and table 3 also show that both "healthy volunteer" models, Dyck (fig. 5, A and G) and Dutta (fig. 5, B and H), are biased and imprecise, with high MDPE and MDAPE. The Dyck model underestimates the plasma concentrations in the higher concentration ranges, which is likely due to a larger volume of distribution, combined with a higher intercompartmental clearance for the third compartment Q3 (table 2). Underestimation of the Dyck model was previously demonstrated by Hsu *et al*.[5] and our study confirms this. The Dutta model overestimates plasma concentrations, with the greatest overestimation in the first 50 min of infusion. This may be explained by the relatively low volume of distribution and low intercompartmental clearance. Whether this can be explained by the site of sampling (venous instead of arterial) is unclear. In a study by Persson *et al*.[21] with ketamine, "venous models" have higher compartment volumes and intercompartmental clearance than "arterial models."

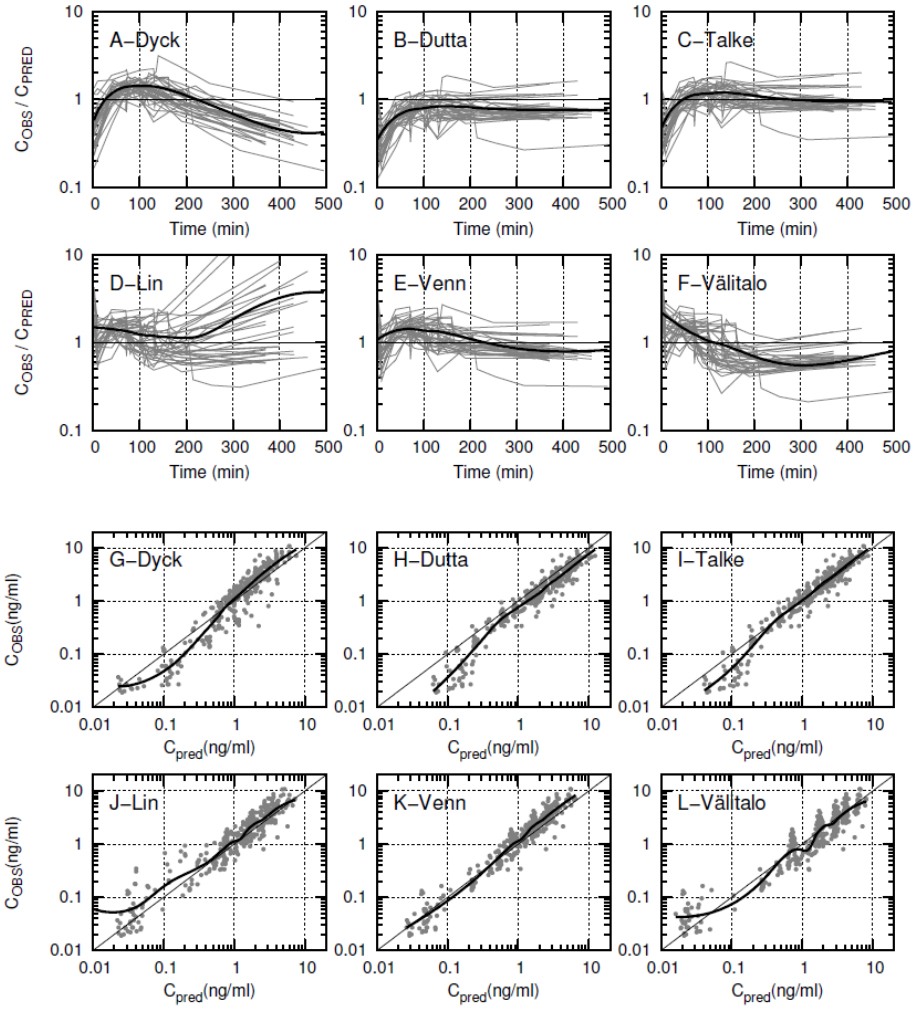

Figure 5. (A–F) Observed/predicted plasma dexmedetomidine concentrations versus time for existing pharmacokinetic models. (G–L) Observed versus predicted plasma dexmedetomidine concentrations for existing pharmacokinetic models. The black lines are Loess smoothers.
C_{OBS} = observed (measured) plasma concentration; C_{PRED} = population-predicted plasma concentration.

The Talke model performs quite well compared with the other models. The MDPE and MDAPE are only slightly higher than that of our model. The C_{obs}/C_{pred} *versus* time graph for the Talke model shows that initial infusion results in overestimation, whereas later in the period (at higher concentrations), the Talke model underestimates the plasma concentration, which confirms the findings by Snapir *et al*.[11] During the last hours of the recovery phase, predictions seem to be quite accurate. The Lin model is very inaccurate

and biased, and the volumes of all three compartments are very high in this model. One needs to keep in mind that this model was developed from data of Chinese patients, whereas other models were most likely developed from Caucasian data. It has been suggested that ethnicity may have an important influence on drug pharmacokinetics, especially if the drug is highly protein bound or undergoes hepatic metabolism.[22] Because dexmedetomidine is highly bound to plasma albumin (94%) and α1-glycoprotein and is metabolized extensively by the liver, this influence may very well be significant between Caucasians and Chinese subjects, as also stated by Lin *et al*.[8] The Venn model also has a high MDPE and MDAPE. As with the Dyck model, this is likely due to a higher volume of distribution as well as intercompartmental clearance. The C_{obs} *versus* C_{pred} graph for the Välitalo model (fig. 5L) shows a large spread, but the most illustrative is the C_{obs}/C_{pred} *versus* time graph (fig. 5F), which shows that there is a large underestimation in the beginning and a large overestimation in the recovery phase. This is not surprising because the Välitalo is a one-compartment model and therefore does not describe drug distribution to peripheral compartments. The large (central) compartment results in initially low plasma concentration predictions, whereas the absence of peripheral distribution results in relatively high late-phase predictions. The bias as calculated by the MDPE is very low for this model, as the overestimations and underestimations cancel each other out.

In conclusion, we developed a three-compartmental pharmacokinetic model for dexmedetomidine, derived from data from healthy male and female volunteers for a wide range in age and weight. The model is also reasonably accurate in the early-phase front-end kinetics, while maintaining the simplicity of a standard three-compartment model for easier use in TCI. Before implementation, this model should be validated prospectively to assess the performance in a patient population.

References

1. Ziemann-Gimmel, Goldfarb, Koppman, Marema: Opioid-free total intravenous anaesthesia reduces postoperative nausea and vomiting in bariatric surgery beyond triple prophylaxis. British Journal of Anaesthesia 2014; 112: 906-11

2. Ueki M, Kawasaki T, Habe K, Hamada K, Kawasaki C, Sata T: The effects of dexmedetomidine on inflammatory mediators after cardiopulmonary bypass. Anaesthesia 2014; 69: 693–700

3. Dyck JB, Maze M, Haack C, Vuorilehto L, Shafer SL: The pharmacokinetics and hemodynamic effects of intravenous and intramuscular dexmedetomidine hydrochloride in adult human volunteers. Anesthesiology 1993; 78: 813-20

4. Dyck JB, Maze M, Haack C, Azarnoff DL, Vuorilehto L, Shafer SL: Computer-controlled infusion of intravenous dexmedetomidine hydrochloride in adult human volunteers. Anesthesiology 1993; 78: 821-8

5. Hsu YW, Cortinez LI, Robertson KM, Keifer JC, Sum-Ping ST, Moretti EW, Young CC, Wright DR, Macleod DB, Somma J: Dexmedetomidine pharmacodynamics: Part I: Crossover comparison of the respiratory effects of dexmedetomidine and remifentanil in healthy volunteers. Anesthesiology 2004; 101: 1066-76

6. Dutta S, Lal R, Karol MD, Cohen T, Ebert T: Influence of cardiac output on dexmedetomidine pharmacokinetics. J Pharm Sci 2000; 89: 519-27

7. Talke P, Richardson CA, Scheinin M, Fisher DM: Postoperative pharmacokinetics and sympatholytic effects of dexmedetomidine. Anesth Analg 1997; 85: 1136-42

8. Lin L, Guo X, Zhang MZ, Qu CJ, Sun Y, Bai J: Pharmacokinetics of dexmedetomidine in Chinese post-surgical intensive care unit patients. Acta Anaesthesiol Scand 2011; 55: 359-67

9. Venn RM, Karol MD, Grounds RM: Pharmacokinetics of dexmedetomidine infusions for sedation of postoperative patients requiring intensive caret. Br J Anaesth 2002; 88: 669-75

10. Valitalo PA, Ahtola-Satila T, Wighton A, Sarapohja T, Pohjanjousi P, Garratt C: Population pharmacokinetics of dexmedetomidine in critically ill patients. Clin Drug Investig 2013; 33: 579-87

11. Snapir A, Posti J, Kentala E, Koskenvuo J, Sundell J, Tuunanen H, Hakala K, Scheinin H, Knuuti J, Scheinin M: Effects of low and high plasma concentrations of dexmedetomidine on myocardial perfusion and cardiac function in healthy male subjects. Anesthesiology 2006; 105: 70

12. Shafer SL, Varvel JR, Aziz N, Scott JC: Pharmacokinetics of fentanyl administered by computer-controlled infusion pump. Anesthesiology 1990; 73: 1091-102

13. Chernik DA, Gillings D, Laine H, Hendler J, Silver JM, Davidson AB, Schwam EM, Siegel JL: Validity and reliability of the Observer's Assessment of Alertness/Sedation Scale: study with intravenous midazolam. J Clin Psychopharmacol 1990; 10: 244-51

14. Varvel JR, Donoho DL, Shafer SL: Measuring the predictive performance of computer-controlled infusion pumps. J Pharmacokinet Biopharm 1992; 20: 63-94

15. Eleveld DJ, Proost JH, Cortinez LI, Absalom AR, Struys, Michel M R F: A General Purpose Pharmacokinetic Model for Propofol. Anesthesia and Analgesia 2014; 118: 1221-37

16. Anderson BJ, Holford NHG: Mechanism-based concepts of size and maturity in pharmacokinetics. Annu Rev Pharmacol Toxicol 2008; 48: 303-32

17. Avram MJ, Krejcie TC: Using front-end kinetics to optimize target-controlled drug infusions. Anesthesiology 2003; 99: 1078-86

18. Marsh B, White M, Morton N, Kenny GN: Pharmacokinetic model driven infusion of propofol in children. Br J Anaesth 1991; 67: 41-8

19. Schnider TW, Minto CF, Gambus PL, Andresen C, Goodale DB, Shafer SL, Youngs EJ: The influence of method of administration and covariates on the pharmacokinetics of propofol in adult volunteers. Anesthesiology 1998; 88: 1170-82

20. Minto CF, Schnider TW, Egan TD, Youngs E, Lemmens HJ, Gambus PL, Billard V, Hoke JF, Moore KH, Hermann DJ, Muir KT, Mandema JW, Shafer SL: Influence of age and gender on the pharmacokinetics and pharmacodynamics of remifentanil. I. Model development. Anesthesiology 1997; 86: 10-23

21. Persson J, Hasselstrom J, Maurset A, Oye I, Svensson JO, Almqvist O, Scheinin H, Gustafsson LL, Almqvist O: Pharmacokinetics and non-analgesic effects of S- and R-ketamines in healthy volunteers with normal and reduced metabolic capacity. Eur J Clin Pharmacol 2002; 57: 869-75

22. Johnson JA: Influence of race or ethnicity on pharmacokinetics of drugs. Journal of Pharmaceutical Sciences 1997; 86: 1328–1333

Chapter 3: Dexmedetomidine pharmacokinetic-pharmacodynamic modelling in healthy volunteers: 1. Influence of arousal on bispectral index and sedation

Modified from *British Journal of Anaesthesia 2017; 119:200-10*

Pieter Colin, Laura N. Hannivoort, Douglas J. Eleveld, Koen M.E.M. Reyntjens, Anthony R. Absalom, Hugo E.M. Vereecke, Michel M.R.F. Struys

Abstract

Background: Dexmedetomidine, a selective α2-adrenoreceptor agonist, has unique characteristics, such as maintained respiratory drive and production of arousable sedation. We describe the development of a pharmacokinetic-pharmacodynamic model of the sedative properties of dexmedetomidine, taking into account the effect of stimulation on its sedative properties.

Methods: In a two-period, randomized study in 18 healthy volunteers, dexmedetomidine was delivered in a step-up fashion by means of target-controlled infusion using the Dyck model. Volunteers were randomized to a session without background noise and a session with pre-recorded looped operating room background noise. Exploratory pharmacokinetic-pharmacodynamic modelling and covariate analysis were conducted in NONMEM using bispectral index (BIS) monitoring of processed EEG.

Results: We found that both stimulation at the time of Modified Observer's Assessment of Alertness/Sedation (MOAA/S) scale scoring and the presence or absence of ambient noise had an effect on the sedative properties of dexmedetomidine. The stimuli associated with MOAA/S scoring increased the BIS of sedated volunteers because of a transient 170% increase in the effect-site concentration necessary to reach half of the maximal effect. In contrast, volunteers deprived of ambient noise were more resistant to dexmedetomidine and required, on average 32% higher effect-site concentrations for the same effect as subjects who were exposed to background operating room noise.

Conclusions: The new pharmacokinetic-pharmacodynamic models might be used for effect-site rather than plasma concentration target-controlled infusion for dexmedetomidine in clinical practice, thereby allowing tighter control over the desired level of sedation.

Introduction

Dexmedetomidine use in clinical practice is popular because of its unique characteristics as a selective α2-adrenoceptor agonist. It is currently licensed for sedation in intensive care units in Europe and the USA and for procedural sedation in the USA. Moreover, there is frequent off-label use, for instance for procedural sedation (in Europe), sedation during awake fibreoptic intubation, and awake craniotomies. Patients under dexmedetomidine sedation experience little respiratory depression, are more easily roused, and are better able to communicate compared with propofol or midazolam sedation.[1] Also, dexmedetomidine has been investigated as a possible opioid-reducing technique[2] and might attenuate perioperative inflammatory responses.[3]

For sedation in intensive care units, a slow titration to effect, with or without a loading dose, is acceptable, because a fast onset of effect is often not necessary. However, during procedural sedation or in the operating room, a faster onset of effect is often desired. Fast titration to the desired effect with limited or no overshoot, thereby limiting potential side-effects, can be attained using target controlled infusion (TCI). For effect-site TCI, an accurate pharmacokinetic-pharmacodynamic (PKPD) model is necessary. Currently, only pharmacokinetic (PK) models are available for dexmedetomidine; no PKPD models.

We recently published an optimized dexmedetomidine PK model.[4] In this twin paper, we describe the pharmacodynamic effects of dexmedetomidine in healthy volunteers, and model these effects into PKPD models. In this article, we describe and model the sedative effects of dexmedetomidine using our previously published PK model, and using bispectral index (BIS) and the Modified Observer's Assessment of Alertness/Sedation (MOAA/S) as measures of sedative effects. In an accompanying paper,[5] we describe and model the haemodynamic effects of dexmedetomidine.

Methods

Study design

This study was approved by the local medical ethics review committee (METC, University Medical Center Groningen, Groningen, the Netherlands; METC number: 2012/400) and was registered in the ClinicalTrials.gov database (NCT01879865). Written informed consent was obtained from all volunteers. The study conduct was described in detail by Hannivoort and colleagues,[4] who reported on the development of a pharmacokinetic model based on measured dexmedetomidine plasma concentrations collected throughout the study.

In brief, 18 healthy volunteers, nine male and nine female, stratified according to age and sex (18-34, 35-54 and 55-72 yr) received dexmedetomidine i.v. on two separate occasions, at least 1 week and at most 3 weeks apart. Both sessions were identical in protocol, except for the use of acoustic noisecancelling headphones (Bose QuietComfort 15, Framingham, MA, USA), either without background noise or with pre-recorded looped operating room background noise (monitor beeps and alarms, air conditioning noise, talking, equipment noise etc.). In both sessions, the volunteers were instructed to keep their eyes closed throughout the session, and they were stimulated as little as possible apart from at set times for the assessment of depth of sedation. Randomization using sealed envelopes was used to determine the order of the 'background silence' and 'background noise' sessions.

Standard anaesthesia monitoring was applied, with the inclusion of an arterial line for blood pressure monitoring and blood sampling, as described by Hannivoort and colleagues.[4] An initial short infusion, given at 6 µg kg^{-1} h^{-1} for 20 s, was followed by a 10 min recovery period. Thereafter, dexmedetomidine was delivered as a TCI using the Dyck model[6] with stepwise increasing targets of 1, 2, 3, 4, 6, and 8 ng ml^{-1}. Each target was maintained for 30 min. The maximal infusion rate was limited to 6 µg kg^{-1} h^{-1} for the first four steps; for the target of 6 and 8 ng ml^{-1}, the maximal infusion rate was increased to 10 µg kg^{-1} h^{-1} to facilitate attainment of the target within a reasonable time. Volunteers were monitored until 300 min after cessation of the TCI dexmedetomidine infusion. The syringe pump (Orchestra® Module DPS, Orchestra® Base A, Fresenius Kabi, Bad Homburg, Germany) that was used to deliver the dexmedetomidine infusion was controlled by RUGLOOP II software (Demed, Temse, Belgium) programmed with the Dyck model.[6]

Pharmacodynamic measurements

A BIS Vista monitor (Covidien, Boulder, CO, USA) was used to record BIS continuously to study depth of hypnosis. The MOAA/S scale was used to quantify the level of sedation and rousability of the volunteer at the following time points: immediately before the start of dexmedetomidine infusion, 2 min after the start of the initial short infusion, immediately before the start of the TCI infusion, and at the end of each TCI target step. During the recovery period, MOAA/S scores were recorded every 2 min for the first 30 min, and every 10 min thereafter, until the volunteer reached the maximal score on the MOAA/S scale. All monitored parameters were recorded electronically using RUGLOOP II software.

Data handling

The final data set contained BIS measurements at a sampling rate of 1Hz, which, for some subjects, resulted in >30,000 observations per session. To reduce the computational burden, we reduced the number of BIS measurements per subject. We also applied a median filter to reduce the influence of artifacts, outlying data, or both during model development. The width (span) of the median filter was 60 s. Data reduction was performed by retaining the first out of every 50 consecutive median filtered observations.

The data set used for modelling contained a median of 372 (range 115-556) BIS measurements per subject per session, corresponding to a sampling rate of 1 min^{-1}. All unfiltered MOAA/S observations were retained in the data set, with a median of 25 (range 8-40) observations per subject per session.

Population pharmacokinetic-pharmacodynamic modelling

The PKPD modelling was based on individual PK parameter estimates from the dexmedetomidine PK model published previously.[4] The individual predicted PK parameters (V1, V2, V3, CL, Q2 and Q3) derived from this model were fixed for each individual and each session (Hannivoort and colleagues[4]. reported that V1 was different between occasions) during further pharmacodynamic (PD) modelling.

Different structural models were evaluated to test whether hysteresis exists between the individually predicted dexmedetomidine plasma concentrations ($IPRED_{plasma}$) and PD measures. Direct models relating $IPRED_{plasma}$ directly to the PD measure were compared against delay drug effect models, such as an effect compartment model or an indirect response model. Drug effects were described using linear, E_{max} and sigmoid E_{max} models.

Once the base model structure was established, graphical analysis was conducted to identify potential correlations between post hoc predicted PKPD parameters and subject

covariates. Subject covariates considered were as follows: weight, height, BMI, age, sex, and session (background silence vs background noise). These covariates were tested in the model, and the resulting change in goodness-of-fit (GOF) was evaluated. For the continuous covariates (age, height and weight), a linear relationship was assumed, whereas for the categorical covariate (sex), an additional parameter was added to differentiate between males and females. Where appropriate, inclusion of model parameters, covariates, or both was tested at the 5% significance level by comparing the decrease in objective function (OFV) against the critical quantile of the corresponding χ^2 distribution (e.g. a 3.84 decrease in OFV for inclusion or exclusion of a single parameter).

Population pharmacodynamic modelling of the confounding effect of the rousability on BIS

During dexmedetomidine sedation, the stimulation inherent in MOAA/S scoring results in a transient increase (arousal) in BIS. The MOAA/S observations were regarded as a sudden, instantaneous stimulation of the subject, and the perturbation in BIS was modelled as a leftward shift in the effect-site concentration necessary to reach half of the maximal effect (C_{50}). Thus, there are two BIS curves corresponding to a stimulated (aroused) and unstimulated (non-aroused) pharmacodynamic state. The dissipation of arousal (equation 1) was modelled using a single parameter (k_{in}), in conjunction with an indirect response model (IRM). The pharmacodynamic arousal state is used as a linear interpolation between two sigmoid drug effect models (given by equations 2 and 3), as described in equation 4:

$$\frac{dRELAX}{dt} = k_{in} \times \big(1 - A(RELAX)\big) \tag{1}$$

$$BIS_{i,NSTIM} = Baseline\ BIS_i \times \left(1 - \frac{C_e}{C_e + C_{50,i}}\right) \tag{2}$$

$$BIS_{i,STIM} = Baseline\ BIS_i \times \left(1 - \frac{C_e}{C_e + (C_{50,i} * (1 + \Delta C_{50,i}))}\right) \tag{3}$$

$$BIS_i(t) = BIS_{i,NSTIM} \times A(RELAX) + BIS_{i,STIM} \times \big(1 - A(RELAX)\big) \tag{4}$$

In short, an unstimulated subject is in a state of relaxation (i.e. non-aroused), during which the 'amount' in the relaxation-compartment (i.e. A(RELAX)) equals 1. At the moment of stimulation, the compartment is reset, i.e. the 'amount' in this compartment is set to zero, corresponding to a stimulated, aroused state. Thereafter, the state returns to a state of relaxation at a rate of k_{in}. As seen from equation (4), the amount in the relaxation-compartment is used as a linear interpolation between an unstimulated

(equation 2) and a stimulated (equation 3) BIS model. In equations (2) and (3), the dexmedetomidine effect-site concentration (C_e) to achieve half of the maximal decrease in BIS in an unstimulated subject is given by C_{50}, whereas the proportional change in the C_{50} for a stimulated subject is described by ΔC_{50}.

Population pharmacodynamic modelling of categorical MOAA/S observations

Categorical MOAA/S observations were modelled using a model for ordered categorical variables. This model was parameterized such that the parameters estimate cumulative probabilities (e.g. the probability of observing an MOAA/S score ≤ 3) on the logit scale. Inter-individual variability (IIV) and drug effect were implemented on these baseline logits using an exponential and an additive component, respectively. Inclusion of random effects beyond the IIV on the baseline logits was not considered to avoid issues with identifiability of the model parameters. Equation (5) gives an example of the model for the logit of the cumulative probability (Pr) of observing an MOAA/S score ≤ 3.

$$Logit(\Pr[\mathrm{MOAA/S} \leq 3]) = \theta_{LLE0} \times e^{\eta_i} + \theta_{\Delta 01} + \theta_{\Delta 12} + \theta_{\Delta 23} + \frac{E_{max} \times {C_e}^{\gamma}}{{C_{50}}^{\gamma} + {C_e}^{\gamma}} \quad (5)$$

The baseline logit is described by a typical value for the logit to be equal to zero (θ_{LLE0}), including an exponential random effect (η_i) on this logit and additional terms to estimate the difference between successive logits (e.g. $\theta_{\Delta 01}$ estimates the difference between the logit for an MOAA/S score ≤ 1 and the logit of an MOAA/S = 0). The drug acts to increase the baseline logit according to a sigmoid E_{max} model based on the predicted effect-site concentration (C_e). The parameters of this sigmoid E_{max} model describe the maximal change in the logit (E_{max}), the effect-site concentration necessary to reach half of the maximal effect (C_{50}) and the Hill coefficient of the concentration-effect relationship (γ).

The logits were back-transformed to cumulative probabilities using the inverse of the logit transformation. Subsequently, the probabilities for each category were obtained by subtraction from the cumulative probabilities with the probability to observe an MOAA/S score ≤ 5 being 1.

Parameter estimation and model evaluation

The first-order conditional estimation algorithm with interaction (FOCE-I) as implemented in NONMEM® (version 7.3; Icon Development Solutions, Hannover, MD, USA) was used to fit BIS data. For the categorical MOAA/S data, the Laplacian approximation to the likelihood was used. Inter-individual variability and inter-occasion variability (IOV) were modelled using an exponential model. Residual unexplained variability was described using additive or proportional error models, or both.

During model building, the GOF of the different models was compared numerically using the Akaike information criterion (AIC) and the median absolute (population-)prediction error (MdAPE). At each stage, GOF was graphically evaluated by inspecting plots of the individual or population predicted vs observed responses, and plots of the conditionally weighted residuals (CWRES) vs individual predictions and time. As a safeguard to over-parameterization, only models with a condition number of the Fisher information matrix (FIM) < 500 were retained in the model building hierarchy. Finally, models were validated internally using prediction-corrected visual predictive checks (pcVPC) according to Bergstrand and colleagues.[7]

All models were fitted to the data using PsN[8] and Pirana[9] as back- or front-end, or both, to NONMEM®. The numerical and graphical assessment of the GOF and the construction of the pcVPCs were conducted in R® (R Foundation for Statistical Computing, Vienna, Austria).

All simulations were performed in a Microsoft Excel® Macro-Enabled Worksheet (Microsoft Office Professional Plus 2013), which is supplied in the Online Supplementary material. The worksheet depends on the 'PKPD tools for Excel' package developed by T. Schnider and C. Minto, which is available from http://www.pkpdtools.com/excel (last accessed April 18th 2017).

Statistical analysis

All model parameters are reported as typical values with associated relative standard errors (RSE) and 95% confidence intervals (CIs) derived from log-likelihood profiling.[10]

Results

Data

Figure 1 shows the median filtered BIS signal and the observed MOAA/S for four representative subjects from our study during the step-up TCI administration. The dashed lines indicate when a new TCI target was set. Immediately before changing the TCI target, MOAA/S was scored. This figure clearly shows the perturbation in the BIS signal induced by stimulating the subjects at the time of MOAA/S scoring and the subsequent attenuation of the effect of stimulation. The complete time courses of BIS and MOAA/S observations for all subjects used for modelling, are shown in Online Supplementary Figures S1 and S2.

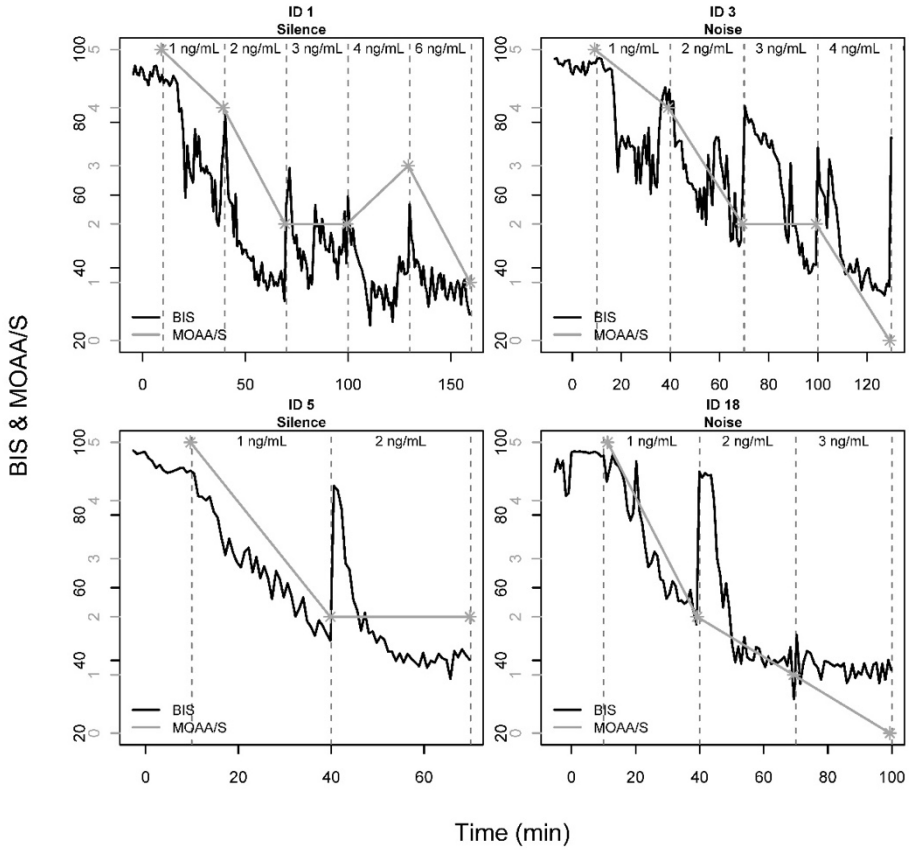

Figure 1. Median filtered BIS values and MOAA/S observations for the step-up TCI administration for four representative subjects. Dashed vertical lines indicate when a new TCI target was set. Immediately before this, MOAA/S was assessed.

BIS = bispectral index; MOAA/S = Modified Observer's Assessment of Alertness/Sedation; TCI = target-controlled infusion.

Model development for BIS

In a first attempt to describe the effect of dexmedetomidine on BIS measurements, a sigmoid E_{max} model was used. Rousability was accounted for according to equations (1)-(4) and the delay between plasma PK and BIS effects was described using an effect compartment model. Modifications to this base structure were evaluated. Firstly, the Hill coefficient (γ) was fixed to 1, resulting in a decrease in the condition number from 1327 to 120; at the same time, the MdAPE decreased from 13.1 to 13.0%. Secondly, a logit transform, as shown in equations (6) and (7), was used to describe the intersubject variability in BIS at baseline. The inclusion of the logit transformation decreased the MdAPE further to 12.8%. Under this transformation, all baseline BIS predictions are restricted between 0 and 100. This significantly improved the pcVPC for the BIS model.

$$Baseline\ BIS_i = 100 \times \left(\frac{e^{(Logit_i)}}{1 + e^{(Logit_i)}} \right) \tag{6}$$

$$Logit_i = \log \left(\frac{(Baseline\ BIS/100)}{1 - (Baseline\ BIS/100)} \right) + \eta_i \tag{7}$$

The significance of the rousability component of the model was evaluated by exclusion of this component, as described by equations (1), (2) and (4), from the final model. The resulting decrease in GOF (ΔAIC = +2358) and simultaneous increase in the MdAPE to 13.5%, underpin the importance of accounting for arousal in the BIS model. Furthermore, a comparison between the parameter estimates for both models revealed a significant shift in k_{e0} (0.120 vs 0.991 min^{-1}), baseline BIS (96.8 vs 89.7), and C_{50} (2.63 vs 4.78 ng ml^{-1}) upon removal of the rousability component. Inclusion of inter-occasion variability on the estimated PKPD parameters did not significantly improve the GOF of the model. Inclusion of age, weight, height, or sex did not result in a significant decrease in the OFV. Therefore, no covariates were included in the final model.

Final model for BIS

The final model parameters are described in Table 1. The likelihood profiles, which were generated to identify potential problems with parameter identification, are shown in Online Supplementary Figure S3. Goodness-of-fit plots, such as post hoc predictions vs observations and CWRES vs time, are shown in Figure 2. Online Supplementary Figure S4 shows the pcVPC. Overall, these figures demonstrate that the presented model adequately describes observed changes in BIS during and after dexmedetomidine administration and that all parameters of the model are estimated with acceptable precision.

Table 1. Final model parameters with associated relative standard errors (RSE, %) derived from log-likelihood profiling.

	Final BIS model		
	Parameter	Estimate (RSE%[b])	IIV[a] (RSE%[b])
θ_1	$Base_{BIS}$[e]	96.8 (1.20)	1.34[d] (56.3)
θ_2	$ke0_{BIS}$ (min^{-1})	0.120 (3.80)	-
θ_3	C_{50} (ng ml^{-1})	2.63 (15.9)	69.5 (40.2)
θ_4	ΔC_{50}[e]	1.71 (18.3)	81.8 (40.8)
θ_5	k_{in} (min^{-1})	0.130 (24.6)	122 (41.1)
	$\sigma_{RUV,Additive}$ [c]	10.6 (1.20)	-
	Final MOAA/S model		
	Parameter	Estimate (RSE%[b])	IIV[a] (RSE%[b])
θ_6	θ_{LLE0}[e]	-10.1 (14.6)	12.5 (37.4)
θ_7	$\theta_{\Delta 01}$[e]	0.394 (14.0)	-
θ_8	$\theta_{\Delta 12}$[e]	1.83 (5.6)	-
θ_9	$\theta_{\Delta 23}$[e]	1.13 (7.7)	-
θ_{10}	$\theta_{\Delta 34}$[e]	1.55 (9.1)	-
θ_{11}	$ke0_{MOAA/S}$ (min^{-1})	0.0428 (17.0)	-
θ_{12}	C_{50} (ng ml^{-1})	0.428 (25.6)	-
θ_{13}	E_{max}[e]	10.4 (13.3)	-
θ_{14}	$\Delta C_{50,noise\ cohort}$[e]	0.316 (35.0)	-

[a] calculated according to: $\sqrt{e^{\omega} - 1} * 100\%$; [b] derived from loglikelihood profiling; [c] expressed as standard deviation; [d] expressed as standard deviation in the logit domain; [e] dimensionless parameter

For the volunteer cohort exposed to ambient operating room noise, the C_{50} is given by C_{50} * (1 - $\Delta C_{50,noise\ cohort}$); ω = estimated variance of the inter-individual variability (IIV); σ = estimated variance of the residual unexplained variability (RUV);

We found that changes in plasma dexmedetomidine concentrations are reflected in BIS, with a half-life of effect-site equilibration of 5.8 min. In unstimulated subjects, half of the maximal effect (~ BIS_{48}) is attained at 2.63 ng ml^{-1}. In the stimulated state, subjects achieve a BIS value of 48, on average, when the dexmedetomidine effect site concentration approaches 7.13 ng ml^{-1}. The post hoc predicted values of C_{50}s and ΔC_{50}s were found to be uncorrelated but highly variable within our study population. Inter-individual variability was estimated to be 69.5% and 81.8% for C_{50} and ΔC_{50}, respectively.

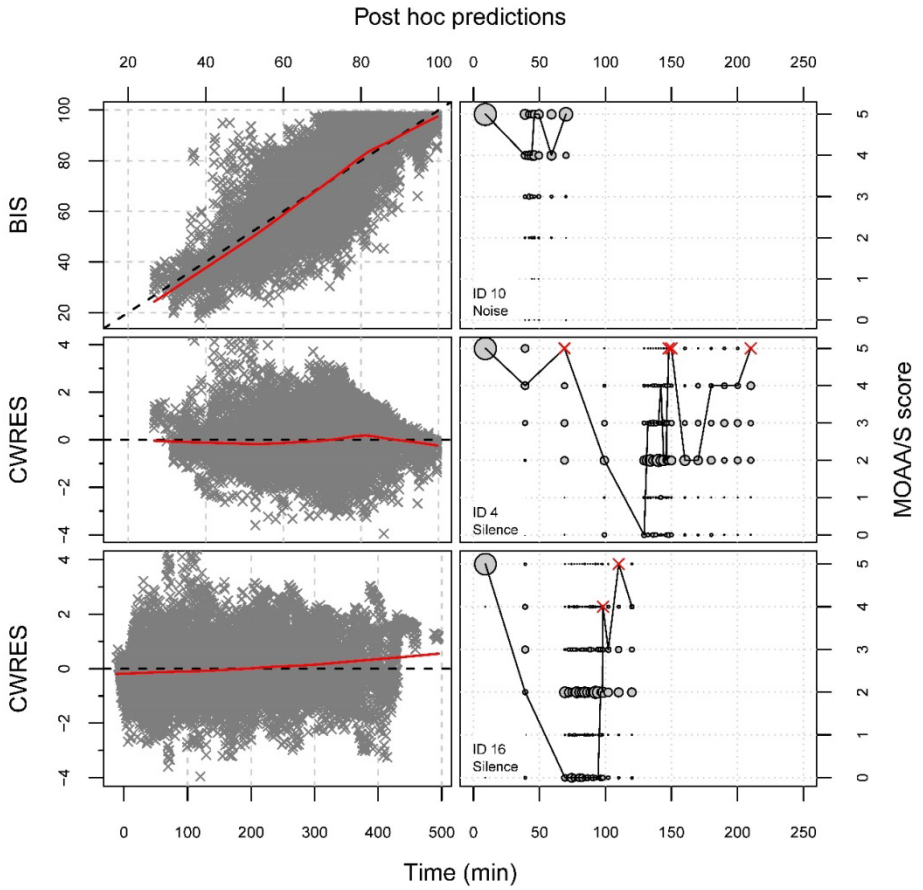

Figure 2. Goodness-of-fit plots for the final model. The left panels show the observed BIS vs *post hoc* predictions and CWRES vs *post hoc* predictions and time. The continuous red line depicts a non-parametric smoother through the data to illustrate lack of bias in the different plots. The right panels show individual GOF plots for the three subjects with the best, median, and worst fit, respectively. The continuous black line shows the observed MOAA/S scores, whereas grey circles denote the probability of observing the MOAA/S scores, with bigger circles having higher probabilities. These probabilities were estimated by simulation using the *post hoc* predicted parameters. Red crosses indicate regions where, according to the simulations, the probability for the observed MOAA/S is < 10%. These points served as 'residuals' to instruct on how to refine the model.

BIS = bispectral index; CWRES = conditionally weighted residuals; GOF = goodness-of-fit; MOAA/S = Modified Observer's Assessment of Alertness/Sedation.

The model illustrates that the effect of stimulation attenuates slowly, with an estimated half-life of 5.3 min. Moreover, the time for the BIS signal to normalize is highly variable within our study population, with 95% of the estimates for the half-life of attenuation between 0.82 and 34.6 min.

Model development for MOAA/S

As a starting point, a linear drug effect model was used to describe dexmedetomidine-induced changes in the logit of the cumulative probabilities. Subsequently, the model was refined by introducing the following: (i) an E_{max} drug effect model (ΔAIC = -173.3) and (ii) inter-individual variability on the baseline logit of observing an MOAA/S score equal to 0 (θ_{LLE0}; ΔAIC = -187.6).

The assumption of proportional odds was challenged by fitting a differential odds model, as described by Kjellsson and colleagues.[11] The differential odds model had a slightly lower AIC (ΔAIC = -6.7) compared with our final model. However, the condition number of the Fisher information matrix (FIM) was high (1110), and no differences were seen between the pcVPCs of both models. Based on these findings, we decided not to implement the differential odds assumption into our final model.

In line with our approach to model the influence of the rousability on the BIS signal, we evaluated a model with an additional E_{max} curve to model potential transient changes in MOAA/S scores attributable to subject stimulation inherent to MOAA/S scoring. This modification led to a marginal improvement in GOF (ΔAIC = -13.9 for two additional parameters). The estimate for the half-life of attenuation was significantly lower than what was found for the BIS model (0.65 vs 5.3 min, respectively), whereas the estimate for the ΔC_{50} was significantly larger (4.21 vs 1.71). The predictive performance, as evaluated by pcVPC, did not improve, and the model suffered from some numerical difficulties, resulting in a high condition number (1203). Overall, these findings led us to the decision not to include a rousability component, describing the time-varying effect of rousability on the MOAA/S, in our final model.

Covariate screening identified session (background silence vs background noise session) as a significant covariate. Inclusion of session as a covariate on the C_{50} led to a significant increase in GOF (ΔAIC = -10.5). The effect of the covariate was confirmed by graphical analysis of the raw data stratified by session. This graphical analysis confirmed that the distribution of MOAA/S scores as a function of TCI targets was different between both sessions (data not shown). Inclusion of the covariate did not increase the condition number of the FIM and was therefore retained in the final model.

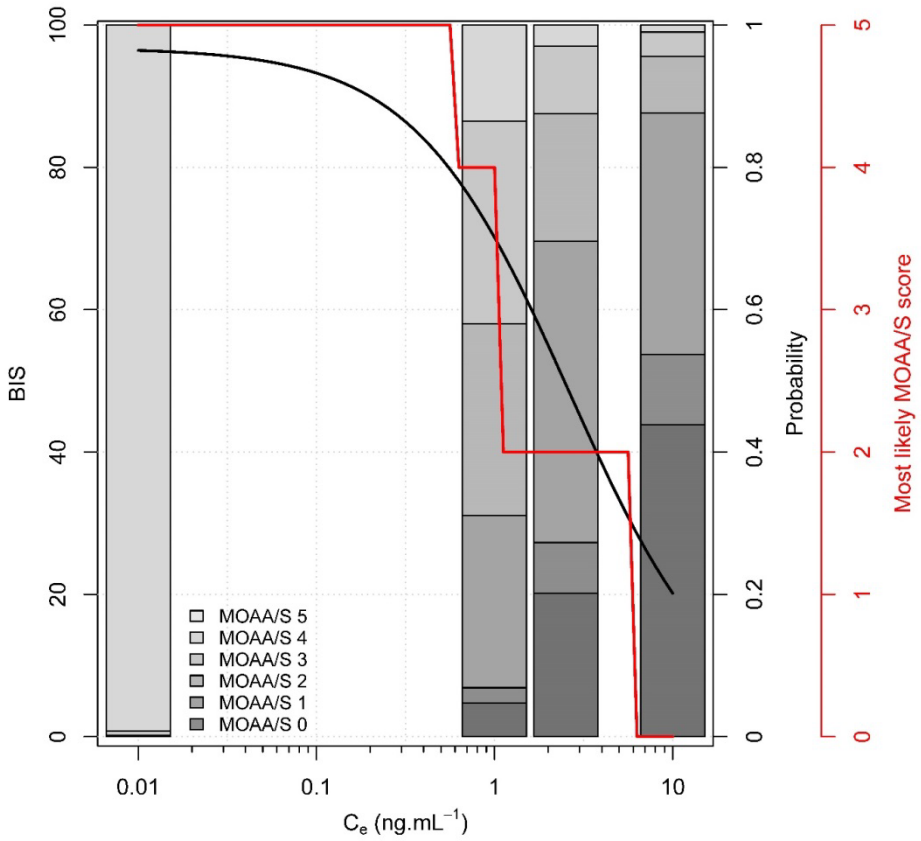

Figure 3. Relationship between effect-site concentrations and BIS and MOAA/S. The continuous black line is the predicted BIS, whereas the MOAA/S with the highest probability is shown with a continuous red line. Stacked bar plots illustrate the distribution of MOAA/S probabilities at effect-site concentrations of 0.01, 1, 2.5 and 10 ng ml^{-1}, corresponding to predicted BIS values of 96, 70, 50 and 20, respectively.

C_e = effect-site concentration; BIS = bispectral index; MOAA/S = Modified Observer's Assessment of Alertness/Sedation.

Age, weight, height, and sex were found not to have a significant impact on the OFV. Furthermore, introduction of inter-occasion variability also did not improve the GOF of the model.

Final model for MOAA/S

The final model parameters and associated standard errors are shown in Table 1. Online Supplementary Figure S3 shows the likelihood profiles for the final model. The GOF of the final model, for three subjects representing the best, median, and worst fit, respectively, is shown in Figure 2 (post hoc predicted vs observed MOAA/S scores as a

function of time for all subjects are shown in Online Supplementary Figure S2). Simulation-based GOF diagnostic plots are favoured here owing to the inability to calculate individually predicted dexmedetomidine plasma concentrations and conditionally weighted residuals-based diagnostic plots for ordered categorical models. A visual predictive check for the final model is shown in Online Supplementary Figure S5. Overall, these diagnostics show that our final model is adequately developed and that the predictive performance is sufficient to characterize our observations.

The equilibration between effect-site concentrations and plasma concentrations for dexmedetomidine is fairly slow, with an estimated half-life for effect-site equilibration of 14 min. Subjects who were deprived of normal ambient background noise from the operating room achieved half of the maximal MOAA/S effect at an effect-site concentration of 0.43 ng ml^{-1}. Volunteers who were exposed to background noises were somewhat more sensitive to the sedative effects of dexmedetomidine and achieved half of the maximal effect at an effect-site concentration that was, on average, 32 % lower (i.e. 0.29 ng ml^{-1}).

According to the model, the difference between the logit of observing an MOAA/S of 0 and an MOAA/S score ≤ 1 is small (Δ_{01} = 0.394). Compared with the other estimates for the differences in logits, this small estimate results in a fairly low predicted probability of observing an MOAA/S 1. This is in line with our observations. Indeed, when we look at the observed proportion of MOAA/S 1 across time (black line in Online Supplementary Figure S5) we see that, as opposed to the other MOAA/S categories, the profile for observing an MOAA/S 1 is relatively flat, not exceeding 10%. An overview of the probability of observing the different MOAA/S scores as a function of effect-site concentration is given in Figure 3 and is commented on further in the discussion.

Discussion

We developed a PKPD model that characterizes the relationship between dexmedetomidine plasma concentrations and the resulting changes in BIS and MOAA/S. Owing to the specific characteristics of dexmedetomidine, our models were built taking into account the time-varying rousability that was introduced by stimulation of the subject during MOAA/S scoring. Furthermore, our study protocol was such that we were able to determine the confounding effect of another type of stimulation, continuous background auditory stimulation, on the sedative properties of dexmedetomidine.

A unique characteristic of our model is that it incorporates the rousability effect on BIS. Stimulation of subjects at the time of MOAA/S scoring induced a transient increase in the BIS signal. The effect of the stimulus diminishes over time and typically disappears within 21 min (4 x t½) in the absence of stimulation. However, if the subject is stimulated more frequently, accumulation occurs and the 'stimulated' state persists for prolonged periods of time.

Our model also explains the potential for an apparent paradoxical response of transiently increasing hypnosis (decreasing BIS) in the presence of decreasing drug concentrations as the individual transitions from a stimulated to an unstimulated pharmacodynamic state. This is visible in Figure 4 where the observed BIS signals during step-up TCI administration and the subsequent recovery for three subjects representing examples of the best, median, and worst fit of our model against the observed data are shown. The good agreement between the observed BIS signal and the post hoc predicted BIS curves (shown in blue) after single and repeated stimulation inspires confidence in the validity of our proposed PKPD model.

The basis for our MOAA/S model is an E_{max} model, using the logit of cumulative probabilities of MOAA/S scores rather than the MOAA/S scores themselves. A time-varying rousability effect similar to the effect found for BIS was not retained in our final PKPD model describing MOAA/S observations. When we tried to estimate the half-life of attenuation, we found an estimate for K_{in} of 1.1 min^{-1}, corresponding to a t½ of 0.65 min, indicating that, for the typical patient, the effect of stimulation disappears within 2.6 min. In the context of our protocol, in which MOAA/S were scored at least 2 min apart, inclusion of the time-varying rousability had no significant impact on the predicted probabilities. However, in other situations, where stimulation occurs more frequently, this might be important, and our suggested approach could be used to take the confounding effect of stimulation into account.

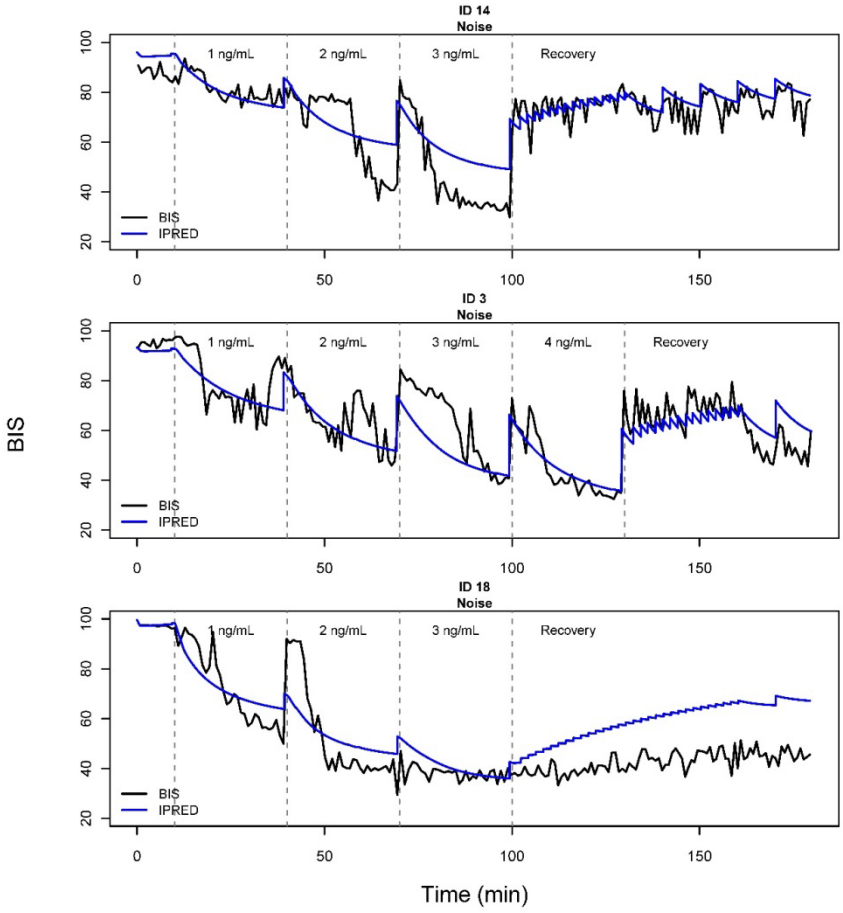

Figure 4. Observed (black lines) and *post hoc* predicted BIS (blue lines) for the individuals with the best, median, and worst fit. The dashed vertical lines indicate when a new TCI target was set. Immediately before this, MOAA/S was assessed.
BIS = bispectral index; MOAA/S = Modified Observer's Assessment of Alertness/Sedation; TCI = target-controlled infusion.

Our analysis showed that the C_{50} for MOAA/S was significantly higher, and thus subjects were more responsive, when deprived of ambient noise in comparison to exposure to ambient operating room noise. This could be because auditory impulses, such as the name of the volunteer being spoken, are more clearly perceived against a silent background. However, our model indicates that even responsiveness towards a painful stimulus was significantly different between sessions. This finding was confirmed by graphical analysis (data not shown) that showed that, after controlling for the TCI target, the frequency of MOAA/S 0 was significantly different between sessions. These results suggest that other more complex physiological phenomena might govern the interaction

between the presence of background noise and the sedative properties of dexmedetomidine.

Surprisingly, we found no influence of age on sensitivity to the sedative effects of dexmedetomidine. Inclusion of age as a covariate on θ_{LLE0} and C_{50} in the MOAA/S and BIS model did not result in a significant decrease in the OFV. In contrast to this finding, Schnider and colleagues[12] and Minto and colleagues[13] found that for propofol and remifentanil the sensitivity to EEG effects increases with age. By including volunteers into our study in age- and sex-stratified cohorts, we maximized the *a priori* possibility of detecting a potential influence of age and sex on the sedative properties of dexmedetomidine. Nevertheless, the limited number of subjects in our study could have obscured an age effect. In contrast, the different receptor pathways involved in dexmedetomidine sedation (α2-receptor agonist) vs propofol ($GABA_A$ receptor agonist) and remifentanil (opioid) sedation might explain the lack of an age effect.

Table 2. BIS_{50} values and corresponding C_e dexmedetomidine for five levels of the MOAA/S score for subjects exposed to and deprived from ambient operating room noise.

	Ambient noise cohort		**Silent cohort**	
	Ce (ng ml^{-1})	BIS_{50}	Ce (ng ml^{-1})	BIS_{50}
Loss of MOAA/S 5	0.29	87	0.43	83
Loss of MOAA/S 4	0.54	80	0.79	74
Loss of MOAA/S 3	0.91	72	1.34	64
Loss of MOAA/S 2	4.10	38	5.99	29
Loss of MOAA/S 1	9.88	20	14.4	15

Our PKPD models allow us to define target effect-site concentrations that maximize the possibility of attaining a particular level of sedation and inform us on the BIS values that correspond to these sedation levels. In a subject exposed to ambient operating room noise, loss of responsiveness to verbal stimulation (i.e. MOAA/S score ≤ 2) is predicted to occur at an effect-site concentration of 0.91 ng ml^{-1}. At this effect-site concentration, BIS immediately before the MOAA/S stimulation is 72. Volunteers deprived of ambient noise lose responsiveness to verbal stimulation at a C_e of 1.3 ng ml^{-1} and BIS value of 64.

Based on a study in healthy volunteers, Kasuya and colleagues[14] found that the correlation between BIS and MOAA/S scales is significantly different between dexmedetomidine and propofol. When considering the same level of sedation, BIS values for dexmedetomidine were generally lower than those in the propofol group. Our

analysis contradicts these findings. The results in Table 2 are in (very) good agreement with earlier work on propofol. Struys and colleagues[15] found that for propofol the BIS values where 50% of the population loses responsiveness (BIS50) to MOAA/S scales 5, 4, and 3 were 85, 74, and 66, respectively. However, earlier findings by Kearse and colleagues[16] and Iselin-Chaves and colleagues[17] showed that the BIS_{50} for loss of responsiveness to verbal stimulation was 65 and 64, respectively. These results are in good agreement with our estimates for dexmedetomidine, indicating that the calibration for BIS is very similar between dexmedetomidine and propofol. Overall, these findings suggest that target BIS values between 60 and 40, which generally indicate adequate general anaesthesia, are appropriate when dexmedetomidine-based deep sedation is required. Between these target BIS values, corresponding to a C_e of 1.6 and 3.6 ng ml^{-1}, loss of responsiveness to verbal stimulation is predicted to occur in 58 and 81% of patients, respectively, and MOAA/S scores will be ≤ 2.

Besides the discrepancy with the work of Kasuya and colleagues,[14] our results are generally in line with earlier reports from experimental studies with dexmedetomidine in healthy volunteers. In a study where healthy volunteers received dexmedetomidine in a step-up TCI titration, Kaskinoro and colleagues[18] found that, on average, loss of responsiveness to verbal stimulation occurred at 1.9 ng ml^{-1}. Although it is not entirely clear whether volunteers were exposed to or deprived of ambient noise, this concentration is in agreement with our predictions, considering the variability associated with assessment of loss of responsiveness to verbal stimulation. In a study where healthy volunteers received a 10 min 6 µg kg^{-1} h^{-1} loading dose followed by a 0.2 or 0.6 µg kg^{-1} h^{-1} i.v. infusion, Hall and colleagues[19] found that BIS decreased by 31% and 36% after 60 min. When we simulated a similar experimental study, we found a 21% and 28% decrease in BIS, which is slightly lower, but still inspires confidence given that we are dealing with an independent data set and that it is not clear whether volunteers in the study by Hall and colleagues[19] were stimulated, which could explain the higher BIS values.

The approach we present, which models the drug effect in both the unstimulated and the stimulated state, was used previously by Heyse and colleagues[20] to account for the differences in hypnotic and analgesic effects between stimulated and unstimulated volunteers receiving sevoflurane-remifentanil anaesthesia. However, in contrast to the analysis of Heyse and colleagues,[20] we used this approach to account for the time-varying effect of stimulation. Correcting for the confounding effect of stimulation is pivotal for modelling dexmedetomidine. Not only does it significantly increase the GOF, without the rousability component in the model a significant bias is seen in estimated PKPD parameters. For example, the C_{50} for BIS, which is the parameter of primary

interest, increases by 82% after stimulation. Dosing regimens taking into account both the pre- and post-stimulation effects with dexmedetomidine, could result in better titration, targeting values with the highest probability for the desired MOAA/S. If deep sedation is required, the target that results in the least increase in BIS without oversedating the patient could be chosen. Whenever BIS is used to target a specific degree of sedation with dexmedetomidine, one should be aware of the confounding effect of stimulation. An applied stimulus is expected to disturb the BIS signal for up to 20 min. Implementing our model into a drug display could correct for this time-varying effect of stimulation and could provide a more robust system to titrate dexmedetomidine-based sedation.

In conclusion, we present a PKPD model that adequately describes the sedative and hypnotic effects of dexmedetomidine in healthy volunteers. This model integrates the well-known rousability associated with dexmedetomidine sedation and accounts for changes in responsiveness between volunteers attributable to repeated auditory stimulation. After validation of our PKPD model in a patient population, our model might be used to transition towards effect-site TCI rather than plasma concentration TCI for dexmedetomidine in clinical practice, thereby allowing tighter control over the desired level of sedation.

Supplementary material

Supplementary material is available at British Journal of Anaesthesia online.

References

1. Jakob SM, Ruokonen E, Grounds RM, Sarapohja T, Garratt C, Pocock SJ, Bratty JR, Takala J: Dexmedetomidine vs midazolam or propofol for sedation during prolonged mechanical ventilation: two randomized controlled trials. JAMA 2012; 307: 1151-60

2. Ziemann-Gimmel, Goldfarb, Koppman, Marema: Opioid-free total intravenous anaesthesia reduces postoperative nausea and vomiting in bariatric surgery beyond triple prophylaxis. Br J of Anaesth 2014; 112: 906-11

3. Ueki M, Kawasaki T, Habe K, Hamada K, Kawasaki C, Sata T: The effects of dexmedetomidine on inflammatory mediators after cardiopulmonary bypass. Anaesthesia 2014; 69: 693–700

4. Hannivoort LN, Eleveld DJ, Proost JH, Reyntjens, KMEM, Absalom AR, Vereecke HEM, Struys, MMRF: Development of an Optimized Pharmacokinetic Model of Dexmedetomidine Using Target-controlled Infusion in Healthy Volunteers. Anesthesiology 2015; 123: 357-67

5. Colin P, Hannivoort LN, Eleveld DJ, Reyntjens, KMEM, Absalom AR, Vereecke HEM, Struys, MMRF: Dexmedetomidine pharmacodynamics in healthy volunteers: 2. Haemodynamic profile. Br J Anaesth 2017; 119: 211-20

6. Dyck JB, Maze M, Haack C, Azarnoff DL, Vuorilehto L, Shafer SL: Computer-controlled infusion of intravenous dexmedetomidine hydrochloride in adult human volunteers. Anesthesiology 1993; 78: 821-8

7. Bergstrand M, Hooker AC, Wallin JE, Karlsson MO: Prediction-corrected visual predictive checks for diagnosing nonlinear mixed-effects models. AAPS J 2011; 13: 143-51

8. Lindbom L, Ribbing J, Jonsson EN: Perl-speaks-NONMEM (PsN)--a Perl module for NONMEM related programming. Comput Methods Programs Biomed 2004; 75: 85-94

9. Keizer RJ, van Benten M, Beijnen JH, Schellens JHM, Huitema ADR: Piraña and PCluster: a modeling environment and cluster infrastructure for NONMEM. Comput Methods Programs Biomed 2011; 101: 72-9

10. Venzon DJ, Moolgavkar SH: A Method for Computing Profile-Likelihood-Based Confidence Intervals. Journal of the Royal Statistical Society. Series C (Applied Statistics) 1988; 37: 87-94

11. Kjellsson MC, Zingmark P, Jonsson EN, Karlsson MO: Comparison of proportional and differential odds models for mixed-effects analysis of categorical data. J Pharmacokinet Pharmacodyn 2008; 35: 483-501

12. Schnider TW, Minto CF, Shafer SL, Gambus PL, Andresen C, Goodale DB, Youngs EJ: The influence of age on propofol pharmacodynamics. Anesthesiology 1999; 90: 1502-16

13. Minto CF, Schnider TW, Egan TD, Youngs E, Lemmens HJ, Gambus PL, Billard V, Hoke JF, Moore KH, Hermann DJ, Muir KT, Mandema JW, Shafer SL: Influence of age and gender on the pharmacokinetics and pharmacodynamics of remifentanil. I. Model development. Anesthesiology 1997; 86: 10-23

14. Kasuya Y, Govinda R, Rauch S, Mascha EJ, Sessler DI, Turan A: The correlation between bispectral index and observational sedation scale in volunteers sedated with dexmedetomidine and propofol. Anesth Analg 2009; 109: 1811-5

15. Struys, MMRF, Jensen EW, Smith W, Smith NT, Rampil I, Dumortier FJE, Mestach C, Mortier EP: Performance of the ARX-derived auditory evoked potential index as an indicator of anesthetic depth: a comparison with bispectral index and hemodynamic measures during propofol administration. Anesthesiology 2002; 96: 803-16

16. Kearse LA, Rosow C, Zaslavsky A, Connors P, Dershwitz M, Denman W: Bispectral analysis of the electroencephalogram predicts conscious processing of information during propofol sedation and hypnosis. Anesthesiology 1998; 88: 25-34

17. Iselin-Chaves IA, Flaishon R, Sebel PS, Howell S, Gan TJ, Sigl J, Ginsberg B, Glass PS: The effect of the interaction of propofol and alfentanil on recall, loss of consciousness, and the Bispectral Index. Anesth Analg 1998; 87: 949-55

18. Kaskinoro K, Maksimow A, Langsjo J, Aantaa R, Jaaskelainen S, Kaisti K, Sarkela M, Scheinin H: Wide inter-individual variability of bispectral index and spectral entropy at loss of consciousness during increasing concentrations of dexmedetomidine, propofol, and sevoflurane. Br J Anaesth 2011; 107: 573-80

19. Hall JE, Uhrich TD, Barney JA, Arain SR, Ebert TJ: Sedative, amnestic, and analgesic properties of small-dose dexmedetomidine infusions. Anesth Analg 2000; 90: 699-705

20. Heyse B, Proost JH, Hannivoort LN, Eleveld DJ, Luginbuehl M, Struys, MMRF, Vereecke HEM: A response surface model approach for continuous measures of hypnotic and analgesic effect during sevoflurane-remifentanil interaction: quantifying the pharmacodynamic shift evoked by stimulation. Anesthesiology 2014; 120: 1390-9

Chapter 4: Dexmedetomidine pharmacodynamics in healthy volunteers: 2. Haemodynamic profile

Modified from *British Journal of Anaesthesia 2017; 119:211-20*

Pieter Colin, Laura N. Hannivoort, Douglas J. Eleveld, Koen M.E.M. Reyntjens, Anthony R. Absalom, Hugo E.M. Vereecke, Michel M.R.F. Struys

Abstract

Background: Dexmedetomidine, a selective α2-adrenoreceptor agonist, has unique characteristics, with little respiratory depression and rousability during sedations. We characterized the haemodynamic properties of dexmedetomidine by developing a pharmacokinetic-pharmacodynamic (PKPD) model with a focus on changes in mean arterial blood pressure (MAP) and heart rate.

Methods: Dexmedetomidine was delivered i.v. to 18 healthy volunteers in a step-up fashion by target-controlled infusion using the Dyck model. Exploratory PKPD modelling and covariate analysis were conducted in NONMEM.

Results: Our model adequately describes dexmedetomidine-induced hypotension, hypertension, and bradycardia, with a greater effective concentration for the hypertensive effect. Changes in MAP were best described by a double-sigmoidal Emax model with hysteresis. Covariate analysis revealed no significant covariates apart from age on the baseline MAP, and the covariates incorporated in the population pharmacokinetic model used to develop this PKPD model. Simulations revealed good general agreement with published descriptive studies of haemodynamics after dexmedetomidine infusion.

Conclusions: The present integrated PKPD model should allow tighter control over the desired level of sedation, while limiting potential haemodynamic side-effects.

Introduction

Dexmedetomidine, a selective α2-adrenoceptor agonist, is widely used in clinical practice as a sedative drug. Owing to its high affinity and selectivity for the α2-adrenoceptors, dexmedetomidine produces a typical biphasic haemodynamic response.[1] At low plasma concentrations, the sympatholytic effect predominates, and dexmedetomidine tends to lower mean arterial blood pressure (MAP) and heart rate (HR) through activation of presynaptic α2-adrenoceptors in the central nervous system and through activation of α2-adrenoceptors in vascular endothelial cells, which causes vasodilation.[2, 3] At higher concentrations, peripheral vasoconstrictive effects attributable to activation of α2-adrenoceptors in vascular smooth muscle become dominant, resulting in an increase in MAP and a further decline in HR.[4, 5]

The haemodynamic effects of dexmedetomidine have been descriptively summarized after short (2, 5 or 10 min) infusions[1, 6-8] at doses between 0.25 and 4 μg kg^{-1} or target-controlled infusion (TCI) systems[4, 5] at target concentrations ranging between 0.5 and 8 ng ml^{-1}. Although a significant dose-response relationship was observed, only very limited pharmacokinetic-pharmacodynamic (PKPD) models exist relating the time course of dexmedetomidine plasma concentrations to its effects on MAP and HR.[6, 8] In order to gain a better understanding and predict these haemodynamic alterations, an integrated PKPD model would be useful to characterize these relationships.

We previously developed a pharmacokinetic model for dexmedetomidine[9] based on data from an extensive healthy volunteer study. In an accompanying paper, we describe the sedative effects of dexmedetomidine, using the EEG-derived bispectral index (BIS®, Medtronic, Dublin, Ireland) and Modified Observer's Assessment of Alertness/Sedation (MOAA/S) scale.[10] In this article, we present a PKPD model describing the haemodynamic effects of dexmedetomidine to characterize the relationship between dexmedetomidine plasma concentrations, effect-site concentrations (C_e) and resulting changes in MAP and HR.

Methods

Study design

This study was approved by the local Medical Ethics Review Committee (METC, University Medical Center Groningen, Groningen, the Netherlands; METC number: 2012/400), and was registered in the ClinicalTrials.gov database (NCT01879865). The study conduct has been described in detail [9] including development of a pharmacokinetic (PK) model based on the study data. In brief, after obtaining written informed consent, 18 healthy volunteers, stratified according to age and sex (18-34, 35-54 and 55-72 yr; three males and three females in each group) received dexmedetomidine i.v. on two separate occasions. Dexmedetomidine was delivered through TCI using the Dyck model,[11] as described in the accompanying paper.[10]

Pharmacodynamic measurements

Continuous arterial blood pressure monitoring was performed *via* an arterial cannula, in the same arm as the i.v. cannula used to deliver the drug. Heart rate was monitored *via* a continuous ECG wave (lead II) that was recorded throughout the study at a frequency of 500 Hz. Vital signs were monitored using a Philips MP50 monitor (Philips, Eindhoven, The Netherlands). Heart rate was derived from the raw ECG wave, by measuring the R-R interval using a Visual Basic macro in Microsoft Excel (Microsoft, Redmond, WA, USA). All monitored parameters and raw waveforms were recorded electronically using RUGLOOP II software (Demed, Temse, Belgium).

Data handling

The final data set contained MAP and HR measurements at a sampling rate of 1Hz, which resulted in > 50,000 observations per session for some individuals. In an attempt to reduce the computational burden during model development, we reduced the number of MAP and HR measurements per subject. We also applied a median filter to reduce the influence of artifacts, outlying data, or both during model development. The width (span) of the median filter was 60 s. Data reduction was performed by retaining only the first out of every 50 consecutive median filtered observations in the data set.

The data set used for modelling contained a median of 458 (range 268-672) MAP measurements and 394 (range 234-542) HR measurements per subject per session, corresponding to a reduced sampling rate of 1 min^{-1}.

Population PKPD modelling

For pharmacodynamic (PD) modelling we used the parameter estimates from the dexmedetomidine PK model published earlier by our group.[9] The individual predicted PK parameters (V1, V2, V3, CL, Q2 and Q3) were fixed for each individual and each session (Hannivoort and colleagues[9] reported that V1 was different between occasions) during further PD modelling.

Different structural models were evaluated to test whether hysteresis exists between the individually predicted dexmedetomidine plasma concentrations ($IPRED_{plasma}$) and the PD measures. Direct models relating $IPRED_{plasma}$ directly to the PD measure were compared against delay drug effect models, such as an effect compartment model or an indirect response model. Drug effects were described using linear, E_{max}, and sigmoid E_{max} models. In the event of numerical difficulties with the estimation algorithm, leading to imprecise estimates of E_{max} and C_{50}, an alternative E_{max} model (shown in equation 1), as described by Schoemaker and colleagues,[12] was evaluated. This equation relies on a parameter (S_0) equal to E_{max}/C_{50} and could be advantageous for PD model estimation when few data are available near the maximal effect.

$$E = \frac{S_0 \times E_{max} \times IPRED_{plasma}}{E_{max} + S_0 \times IPRED_{plasma}} \quad (1)$$

Once the base model structure was established, graphical analysis was conducted to identify potential correlations between post hoc predicted PKPD parameters and subject covariates. The covariates considered were: weight, height, BMI, age, sex and session. Subsequently, these covariates were tested by inclusion in the model, and the resulting change in goodness-of-fit was evaluated. Hereto, for the continuous covariates (age, height and weight) a linear relationship was assumed, whereas for the categorical covariate (sex) an additional parameter was added to the model to differentiate between males and females. Where appropriate, inclusion of model parameters, covariates, or both was tested at the 5% significance level by comparing the decrease in objective function (OFV) against the critical quantile of the corresponding χ^2 distribution (e.g. 3.84 for inclusion or exclusion of a single parameter).

Parameter estimation and model evaluation

The first-order conditional estimation algorithm with interaction (FOCE-I) as implemented in NONMEM® (version 7.3; Icon Development Solutions, Hannover, MD, USA) was used to fit the continuous MAP and HR data. Inter-individual variability (IIV) and inter-occasion variability were modelled using exponential models. Residual unexplained variability was described using additive or proportional error models, or both.

During model building, the goodness-of-fit (GOF) of the different models was compared numerically using the Akaike information criterion (AIC) and the median absolute (population-)prediction error (MdAPE). At each stage, GOF was graphically evaluated by inspecting plots of the individual or population predicted vs observed responses and plots of the conditionally weighted residuals (CWRES) vs individual predictions and time. To ensure numerical stability, only models with a condition number of the estimated variance-covariance matrix < 500 were retained. Finally, models were validated internally using prediction-corrected visual predictive checks (pcVPC) as described by Bergstrand and colleagues.[13]

Models were fitted to the data using PsN[14] and Pirana[15] as back- or front-end, or both, to NONMEM®. The numerical and graphical assessment of the GOF and the construction of the pcVPCs, were conducted in R® (R Foundation for Statistical Computing, Vienna, Austria).

Simulations were performed in a Microsoft Excel® Macro-Enabled Worksheet (Microsoft Office Professional Plus 2013) which is supplied in the Online Supplementary material to this paper. The worksheet depends on the 'PKPD tools for Excel' package developed by T. Schnider and C. Minto, available from http://www.pkpdtools.com/excel (last accessed April 18, 2017).

Statistical analysis

Model parameters are reported as typical values with associated relative standard errors (RSE) and 95% confidence intervals derived from log-likelihood profiling.[16]

Results

Data

Figure 1 shows the median filtered HR and MAP signals for four representative subjects from our study during the step-up TCI administration. The dashed lines indicate when a new TCI target was set. This figure clearly shows the monotonic decrease in HR and the biphasic behaviour of the MAP with increasing dexmedetomidine plasma concentrations.

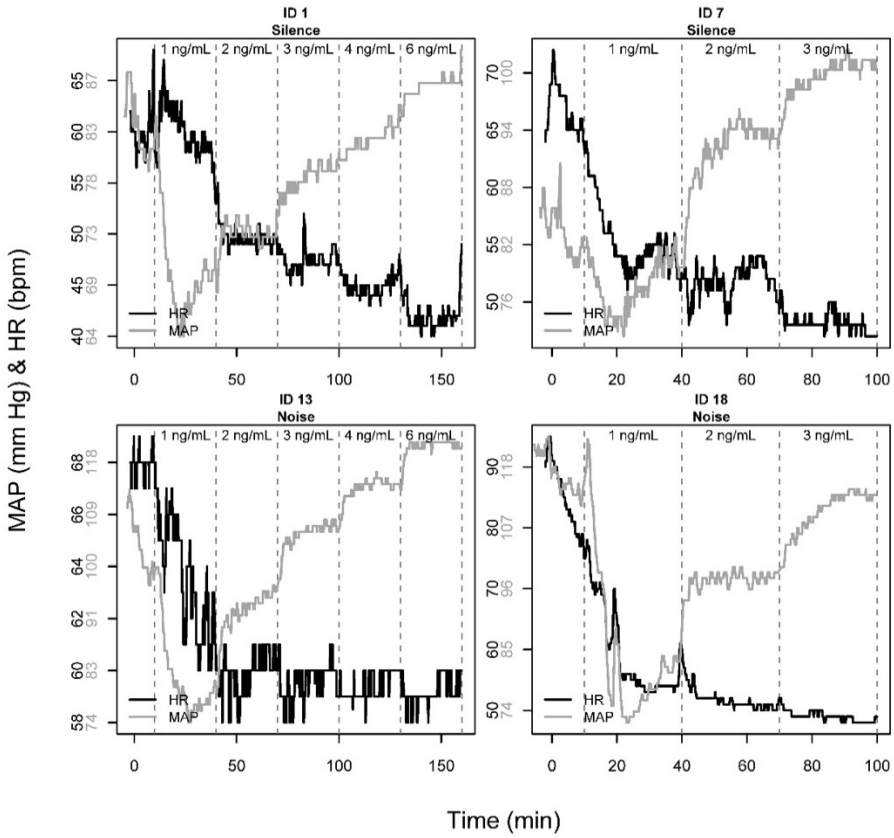

Figure 1. Mean arterial pressure (continuous grey lines; grey y-axis labels) and heart rate (continuous black lines; black y-axis labels) for four representative subjects. The nominal times (as indicated by the study protocol) at which TCI settings were changed are indicated by vertical dashed lines. A bolus infusion was followed by a 10 min recovery period, after which (the first dashed line indicates the end of this phase) TCI targets were increased in a stepwise fashion.
HR = heart rate; MAP = mean arterial pressure; TCI = target-controlled infusion.

Median filtered MAP and HR observations for all subjects throughout the entire study are shown in Online Supplementary Figures S1 and S2.

Mean arterial pressure model development

As a starting point for model building, we used two E_{max} models to characterize the dependency between $IPRED_{plasma}$ and the MAP. This model was deemed necessary to describe the biphasic effect of dexmedetomidine on MAP adequately. As seen in Figure 1, at low dexmedetomidine concentrations the hypotensive effect dominates, whereas at higher concentrations this effect is counteracted and then reversed to profound hypertension.

The model was further modified by fixing the E_{max} term for the hypotensive effect to increase numeric stability (ΔAIC for fixing E_{max} to 1 = -0.8) and by adding a parameter describing the correlation in IIV in baseline MAP ($Base_{MAP}$) and the EC_{50} for the hypertensive effect (ΔAIC = -16). In addition, an effect compartment model was included to characterize the hysteresis between $IPRED_{plasma}$ and MAP. Two effect compartments, with a separate ke0 for the hypotensive ($C_{e,Hypo}$) and the hypertensive effect-site concentrations ($C_{e,Hyper}$), gave the highest improvement in OFV and were retained in the model (ΔAIC = -1552.8). Finally, a specific parameterization, as shown in equation 2, of this double E_{max} model was favoured to ensure that for every subject, the estimated EC_{50} for the hypertensive effect is greater than the EC_{50} for the hypotensive effect.

$$MAP_{ij} = Base_{MAP,i} \times \left(1 - \frac{C_{e,Hypo}}{EC50_{Hypo} + C_{e,Hypo}} + \frac{\left(1 + E_{max,Hyper}\right) \times C_{e,Hyper}}{\left(EC50_{Hypo} + \Delta EC50\right) + C_{e,Hyper}}\right) \quad (2)$$

In the next step, the post hoc predicted parameters for which IIV was included in the model ($Base_{MAP}$, $EC50_{Hypo}$, and ΔEC50) were plotted against the covariates to detect potential covariate relationships. For age a correlation was observed with $Base_{MAP}$. Subsequently, this dependency vs $Base_{MAP}$ was formally tested in the model. Inclusion of age on $Base_{MAP}$ according to equation 3, resulted in a significant improvement in GOF (ΔAIC = -9.6) and a reduction in the population MdAPE from 9.4% to 7.8%.

$$Base_{MAP,i} = Base_{MAP} \times e^{\left(\theta_{age} \times (AGE - 20)\right)} \quad (3)$$

Inclusion of age, weight, height or sex on $EC50_{Hypo}$ or ΔEC50 did not result in a significant decrease in the OFV; therefore, these covariates were not included in the final model.

Table 1. Final model parameters with associated relative standard errors (RSE, %) derived from log-likelihood profiling.

		Final HD model		
	Parameter	Estimate (RSE%[2])	IIV[1] (RSE%[2])	IOV[1] (RSE%[2])
θ_1	$Base_{MAP}$ (mmHg)	80.4 (3.60)	10.9 (16.0)	-
θ_2	θ_{age} (yrs^{-1})	0.00507 (20.2)	-	-
θ_3	$ke0_{MAP,Hypo}$ (min^{-1})	0.0529 (2.80)	-	-
θ_4	$ke0_{MAP,Hyper}$ (min^{-1})	0.0902 (2.80)	-	-
θ_5	$C_{50,Hypo}$ (ng ml^{-1})	0.364 (10.0)	51.1 (16.0) $\rho_{BaseMAP}$: 0.755 (11.8)	-
θ_6	ΔC_{50} (ng ml^{-1})	1.20 (12.0)	41.8 (37.7)	-
θ_7	$E_{max,Hyper}$ (rel.)	0.43 (0.70)	-	-
θ_8	$Base_{HR}$ (bpm)	59.6 (3.30)	13.4 (38.2)	2.24 (42.7)
θ_9	HR_{MIN} (bpm)	22.5 (3.90)	-	-
θ_{10}	$ke0_{HR}$ (min^{-1})	0.396 (7.50)	-	-
θ_{11}	S_0 (bpm ml ng^{-1})	4.37 (22.4)	110 (37.7)	-
θ_{12}	θ_{HRV} (bpm^{-1})	0.0613 (3.10)	-	-
	$\sigma_{RUV,Additive}$ (mmHg)[3]	5.77 (1.10)	-	-
	$\sigma_{RUV,Additive}$ (bpm)[3]	5.58 (11.4)	48.6 (37.6)	-

[1]calculated according to: $\sqrt{e^{\omega}-1} * 100\%$; [2]derived from log-likelihood profiling; [3]expressed as standard deviation.

IIV = interindividual variability; IOV = interoccasion variability; MAP = mean arterial pressure; HR = heart rate; HRV = heart rate variability; ω = estimated variance of the interindividual variability; σ = estimated variance of the residual unexplained variability (RUV)

Final MAP model

The final model parameters are described in Table 1. The likelihood profiles, which were generated to identify potential problems with parameter identification, are shown in Online Supplementary Figure S3. Goodness-of-fit plots, such as post hoc predictions vs observations and CWRES vs time are shown in Online Supplementary Figure S4. Online Supplementary Figure S5 shows the pcVPC. Overall, these figures demonstrate that the presented model adequately describes the observed changes in MAP during dexmedetomidine administration and that all parameters of the model are estimated with acceptable precision. In the recovery phase, there is increased MAP variability around the model predictions. This is seen in the individual post hoc predicted vs observed MAP plots, shown in Online Supplementary Figure S1. As subjects were not restrained during the recovery phase of the experiment, (small) movements probably led to the increased noise in the MAP signal.

The baseline MAP in our study, for a 20-yr-old individual, was estimated to be 80 mmHg and was found to increase by 5.2% for every 10 yr increase in age. The half-lives for effect-site equilibration for the hypotensive and hypertensive effect-site compartments were estimated to be 13 min and 7.7 min, respectively. Furthermore, a significant difference was found between the population typical sensitivity (i.e. EC_{50}) for the hypotensive and hypertensive effects, with the latter being 1.20 ng ml^{-1} higher on average. The difference between both (ΔEC_{50}) sensitivities was positively correlated to the baseline ($\rho = 0.755$). Thus, individuals with a higher baseline MAP, tend to show a more profound hypotensive phase compared with individuals having a lower baseline MAP.

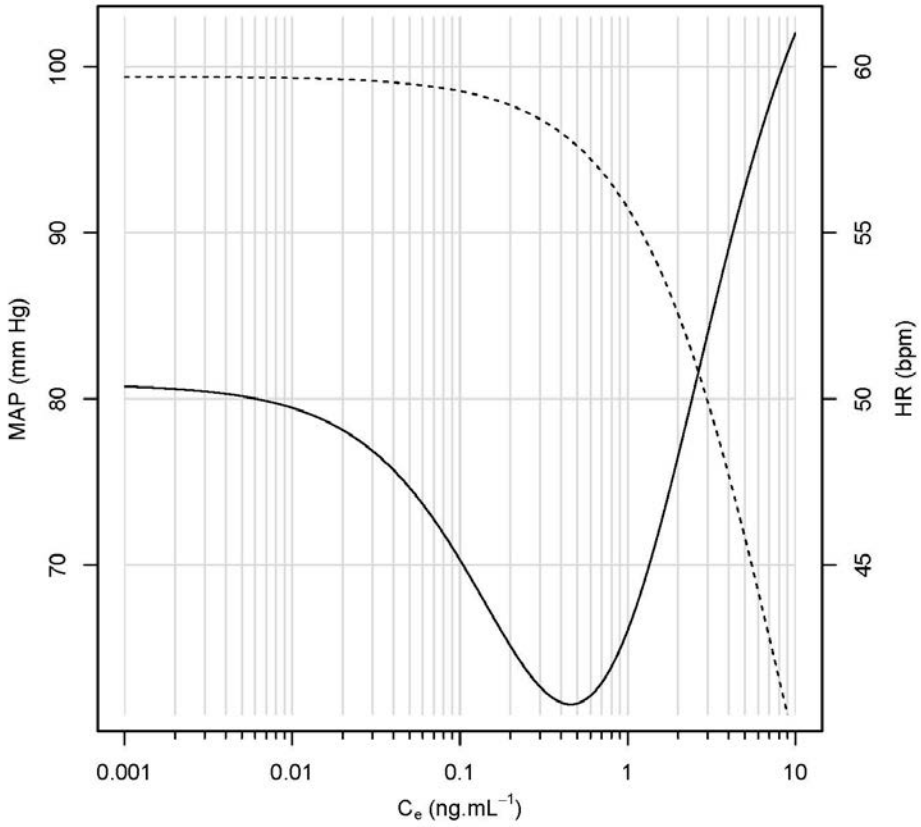

Figure 2. Change in mean arterial pressure (continuous black line) and heart rate (dashed black line), for a typical 20-yr-old individual, as a function of the respective effect-site concentrations. C_e = effect-site concentration; HR = heart rate; MAP = mean arterial pressure.

A graphical presentation of the change in MAP according to C_e, for a typical 20-yr- old individual, is shown in Figure 2. The MAP decreases below baseline at low dexmedetomidine C_e, followed by a return to baseline at 2.4 ng ml^{-1}. Above this concentration, dexmedetomidine induces hypertension, with a maximal MAP 43% higher than the initial baseline.

Heart rate model development

Initially, HR data were analysed using a model that assumed a linear decrease in HR as a function of $IPRED_{plasma}$. The model modifications that led to a significant decrease in AIC were as follows: (i) use of a non-linear drug effect model according to Schoemaker and colleagues[12] (ΔAIC = -731.1), (ii) inclusion of an effect compartment model as opposed to a direct model (ΔAIC = -448.9) and (iii) the use of a model that assumed exponentially decreasing HR variability (HRV), as shown in equation 4 (ΔAIC = -817.5).

$$SD_{ij} = \sigma_{RUV,Additive,i} \times e^{\left(-\theta_{HRV} \times (Base_{HR,i} - IPRED_{HR,ij})\right)} \quad (4)$$

This error model was evaluated to give more weight to lower HR values which, in light of a potential dexmedetomidine-induced bradycardia, are clinically more important. The residual unexplained variability (RUV) was described by an additive error model with an SD for subject i at time j (SD_{ij}) that exponentially decreased, at a rate equal to θ_{HRV}, with the difference between baseline HR ($BASE_{HR,i}$) and the predicted HR at time j ($IPRED_{HR,ij}$). The baseline RUV (i.e. before the start of the dosing) for each subject ($\sigma_{RUV,Additive,i}$) was adequately described by a population SD with an exponential inter-individual variability term.

The relationship between dexmedetomidine effect-site concentrations and HR was best described by an adaptation of the model described by Schoemaker and colleagues.[12] In our version of this model, as illustrated in equation 5, the maximal drug effect was dependent on the individual baseline HR and a population parameter describing the minimal attainable HR during dexmedetomidine administration (HR_{MIN}). Other approaches to model the drug effect, using an E_{max} or a sigmoid E_{max} model, failed as a result of numerical instability of the estimation algorithm.

$$E_{max} = Base_{HR,i} - HR_{MIN} \quad (5)$$

A graphical exploration of the *post hoc* predicted PKPD parameters ($Base_{HR}$, S_0, and SD) from this base model vs subject covariates revealed no apparent correlations. Inclusion of age, weight, height or sex on S_0 did not result in a significant decrease in the OFV, therefore, no covariates were included in the final model.

Final HR model

The final model adequately describes the time course of HR during/after dexmedetomidine administration (Online Supplementary Figure S4). This conclusion is further supported by the pcVPC shown in Online Supplementary Figure S5. The final model parameters and associated standard errors (derived from the log-likelihood-profiles in Online Supplementary Figure S3) are presented in Table 1. Again, *post hoc* predicted vs observed HR as a function of time for all individuals in the study are shown in Online Supplementary Figure S2.

In the final model, baseline HR variability was described by a combination of inter-individual and inter-occasion variability, accounting for 13% and 2.2% of baseline variability, respectively. Changes in dexmedetomidine plasma concentrations induced relatively rapid changes in HR, with a half-life for effect-site equilibration of 1.75 min ($\frac{\ln 2}{ke0_{HR}}$ = 1.75).

The estimated lower boundary for the HR during dexmedetomidine therapy was found to be 22 bpm and was significantly different from zero (the OFV increased by 226 when this lower boundary was fixed to zero). The slope parameter (S_0) was estimated to be 4.37 bpm ml ng^{-1} and had considerable inter-individual variability (110%).

The RUV in HR at baseline was relatively high and variable between subjects. We found a population SD for the RUV of 5.6 bpm and an inter-individual variability of 48%, respectively. On an individual level, the RUV varied between 2.9 bpm and 12.5 bpm at baseline. During dexmedetomidine administration, HRV was found to be correlated with the *post hoc* predicted HR, with an approximate reduction in RUV of 45% with every 10 bpm decrease in HR.

Effects of infusion duration and dose on MAP and HR

To get a clearer clinical picture of the effects of dexmedetomidine on MAP and HR, several drug infusions with varying infusion durations and doses were simulated. The top and bottom panels of Figure 3 show the influence of increasing dexmedetomidine doses and infusion duration on the MAP (left panels) and HR (right panels) for doses ranging from 0.25 to 4.0 µg kg^{-1} for a 27-yr-old healthy volunteer weighing 77 kg (the Excel® worksheet used to simulate these dosing regimens is available from the Online Supplementary material of Colin and colleagues).[10]

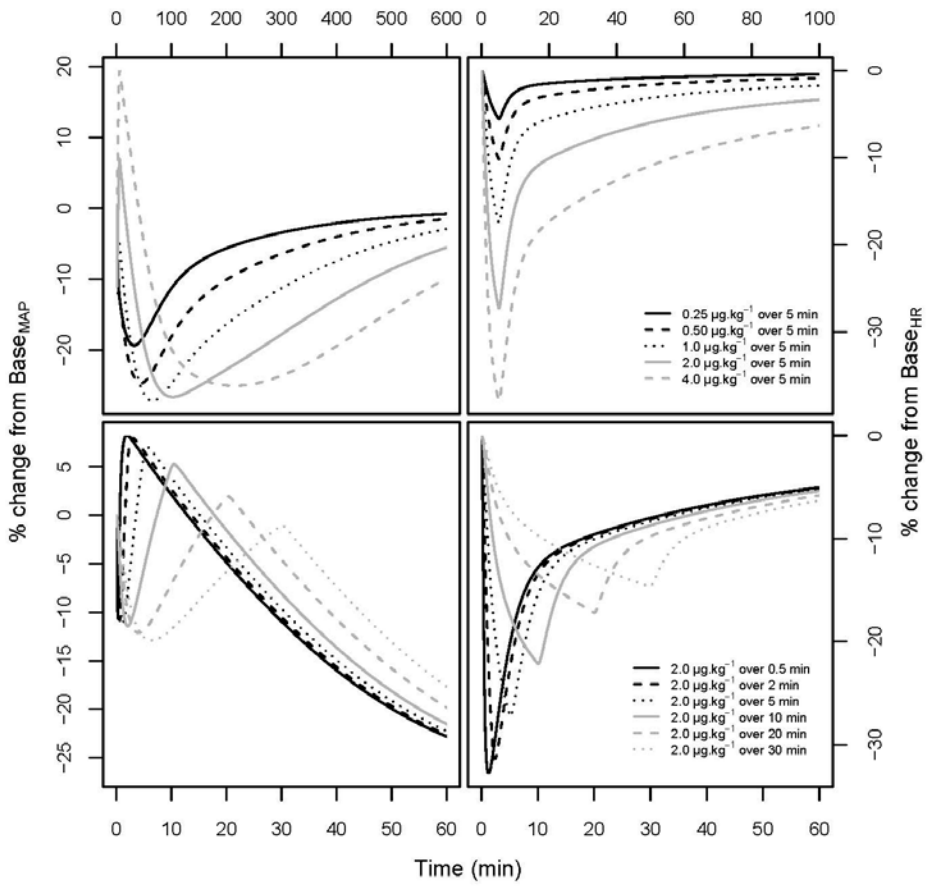

Figure 3. Influence of dexmedetomidine dose (top panels) and infusion duration (lower panels) on mean arterial pressure (left panels) and heart rate (right panels) for short (30 min at most) infusions.

$Base_{HR}$ = baseline heart rate; $Base_{MAP}$ = baseline mean arterial pressure.

For MAP, dexmedetomidine administration up to 1 µg kg^{-1} over 5 min causes no hypertension, but with higher doses (2 and 4 µg kg^{-1}), profound hypertension occurs, with an increase from baseline MAP of 7% and 19%, respectively (Table 2). For all simulated drug regimens, profound postinfusion hypotension is predicted, although the decrease in MAP levels off at around 25-27% below baseline, even at increasing doses. Furthermore, our model predicts that the recovery period (time necessary to return to baseline MAP once the infusion is stopped) increases from 3.7 to 13 h for the 0.25 and 4.0 µg kg^{-1} dose, respectively.

Table 2. Influence of dexmedetomidine dose and infusion duration on various PK and PD end points.

Dose ($\mu g\ kg^{-1}$)	Infusion duration (min)	C_{max} ($ng\ ml^{-1}$)	T_{max} (min)	HR_{min} (%)	$T_{HR,min}$ (min)	$T_{HR,base}$ (min)	MAP_{max} (%)	$T_{MAP,max}$ (min)	MAP_{min} (%)	$T_{MAP,min}$ (min)	$T_{MAP,base}$ (hr)
0.25	5	1.1	5.0	-5.5	5.0	6.0	-	-	-19	32	3.7
0.50	5	2.1	5.0	-10	5.0	10	-	-	-25	44	5.9
1.0	5	4.2	5.0	-17	5.0	24	-	-	-27	66	8.1
2.0	5	8.5	5.0	-27	5.1	63	7	5.7	-27	102	10.4
4.0	5	17.0	5.0	-38	5.1	132	19	5.7	-25	214	12.6
2.0	0.5	47	0.5	-33	1.2	61	8	1.9	-27	100	10.3
2.0	2	18	2.0	-31	2.3	61	8	3.0	-27	101	10.3
2.0	5	8.5	5.0	-27	5.1	63	7	5.7	-27	102	10.4
2.0	10	5.2	10	-22	10	65	5	10.5	-27	105	10.4
2.0	20	3.4	20	-17	20	71	2	20.3	-27	110	10.5
2.0	30	2.7	30	-15	30	76	-	-	-27	116	10.6

C_{max} = maximum concentration; T_{max} = time to maximum concentration; HR_{min} = maximum decrease in heart rat; $T_{HR,min}$ = time to maximum heart rate decrease; $T_{HR,base}$ = time necessary to return to return to ± 5% from the initial baseline value; MAP_{max}; maximum increase in mean arterial pressure (MAP); $T_{map,max}$; time to maximum MAP increase; MAP_{min}; maximum decrease in MAP; $T_{MAP,min}$ = time to maximum MAP decrease; $T_{MAP,base}$ = time necessary to return to ± 5% from the initial baseline value;

For HR, there is a clear dose-response relationship between infused dose and infusion duration and decrease in HR (Table 2). For increasing doses from 0.25 to 4.0 µg kg^{-1} over 5 min, the decrease in HR increases from 5.5% to 38% from baseline. Increasing the infusion duration gives a smaller effect on HR decrease, and increases the time until maximal HR reduction is reached.

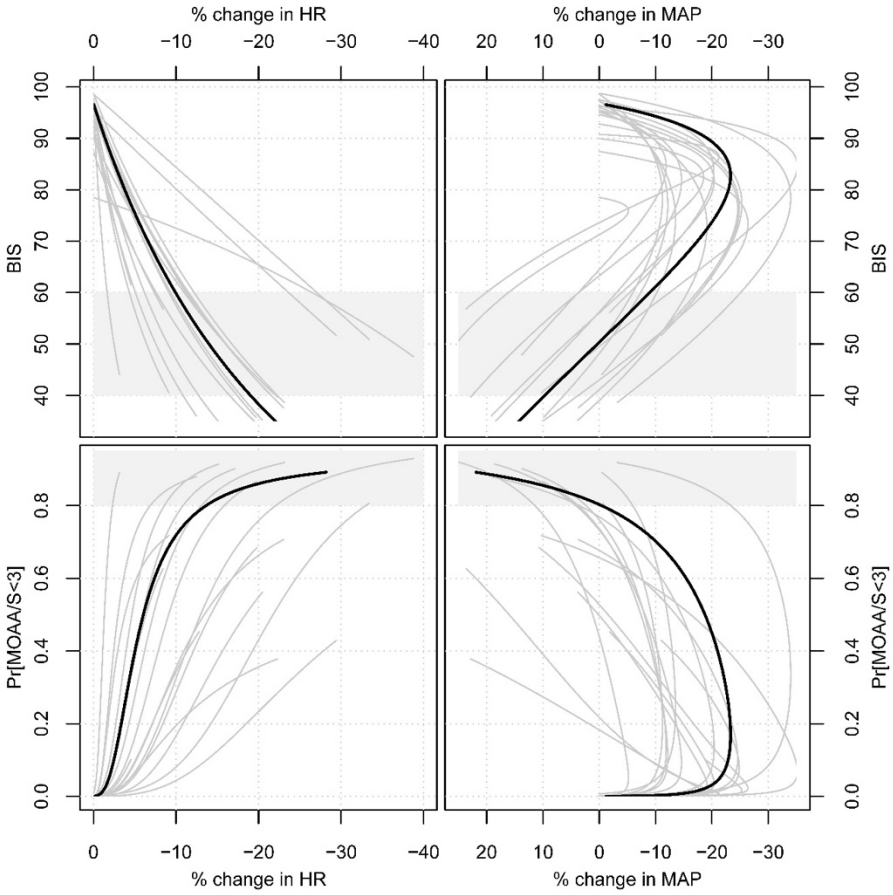

Figure 4. *Post hoc* predicted change in BIS (top panels) and probability for loss of MOAA/S 3 (bottom panels) as a function of the simultaneous change in heart rate (left panels) and mean arterial pressure (right panels). The individually predicted trajectories for all subjects are shown with grey continuous lines. The population average trajectory is shown with a thick continuous black line. Clinically interesting targets for BIS and probability for loss of MOAA/S 3 are shown with grey shaded areas.

BIS = bispectral index; HR = heart rate; MAP = mean arterial pressure; MOAA/S = Modified Observer's Assessment of Alertness/Sedation; Pr = predicted,

Comparison between the haemodynamic and sedative properties of dexmedetomidine

We used our combined PKPD model to investigate whether the haemodynamic responses after dexmedetomidine administration could be used as a surrogate marker for the sedative effects.[10] The individual responses across different end points were predicted from the *post hoc* PKPD parameters, and plasma concentrations, effect-site concentrations and the resulting haemodynamic and sedative effects were predicted for all subjects during the time course of the study. In order to increase the interpretability of these results, differences in baseline MAP and HR across subjects had to be accounted for. This was achieved by expressing the changes in haemodynamic end points relative to individually predicted baseline values.

The decrease in BIS and the increase in the probability of achieving an MOAA/S < 3 (i.e. loss of responsiveness) are shown in Figure 4 as a function of the simultaneous changes in HR and MAP. For HR,a straightforward correlation is seen with the predicted sedative effects. For the typical individual, we expect that BIS values between 60 and 40 are accompanied by a decrease in HR of 10% and 20%, respectively. This HR reduction corresponds to a high probability (i.e. ≥ 80%) for loss of responsiveness.

The relationship between MAP and the sedative effects of dexmedetomidine is less straightforward. Nevertheless, for the typical individual, the point where MAP normalizes, (after the hypotensive phase and before the hypertensive phase), appears to indicate sufficient sedation depth. At this point, BIS is predicted to be between 60 and 40, and the probability of loss of responsiveness is high (i.e. ≥ 80%).

Discussion

We present a PKPD model describing dexmedetomidine-induced changes in mean arterial pressure and heart rate in healthy volunteers. Knowledge of these relationships is crucial for optimizing dexmedetomidine drug administration profiles to avoid undesirable haemodynamic side–effects. Dexmedetomidine-induced changes in MAP were best described by a double-sigmoidal E_{max} model, which characterizes the biphasic effect of hypotension at low concentrations and hypertension at higher concentrations. We also found a hysteresis between plasma concentration and both hypotensive and hypertensive effects, and this hysteresis is different for both effects. This results in two effect compartments with two different equilibration constants, k_{e0}. This can be physiologically explained by the hypertensive and hypotensive effects occuring at different receptor sites. The hypertensive effect is thought to originate from α2-receptor activation in the vascular smooth muscle, whereas the hypotensive effect is mediated by α2-receptor activation in the vascular endothelium and in the central nervous system. The concentration at which the hypertensive effect overcame the hypotensive effect was 2.4 ng ml^{-1}, in good agreement with information from other groups. For example, the assessment report of the European Medicines Agency[17] on dexmedetomidine and Ebert and colleagues[5] report significant hypertension starting at plasma concentrations of 3.2 and 1.9 ng ml^{-1}, respectively. The only covariate found was the effect of age on baseline MAP, where older volunteers had a higher baseline MAP, but no effect was found between age and dexmedetomidine-induced MAP changes.

The effect of dexmedetomidine on HR was best described by a non-linear model, as described by Schoemaker and colleagues.[12] This model provides greater numerical stability compared with the E_{max} model, when estimating maximal effect from observations made predominantly around C_{50}. The increased precision in the estimated maximal drug effect (i.e. the lower HR range) is also clinically the most important range to evaluate, as bradycardia could be one of the limiting factors in dexmedetomidine administration at higher concentrations. This is especially true in patients with pre-existing bradycardia or in patients who perform better with a higher HR, such as patients with dilated cardiac failure. A narrow hysteresis was found between plasma concentration and HR effects, with a high k_{e0}, describing a fast change in HR in response to changes in plasma concentration. No covariates were found to be associated with baseline HR or dexmedetomidine-induced HR changes.

Our MAP model resembles the model presented by Potts and colleagues,[8] with a few important differences. While both models include a double-sigmoidal E_{max} model, describing both the sympatholytic and the vasoconstrictor effects of dexmedetomidine,

our model uses an effect-site compartment for both the hypertensive and hypotensive effects, whereas the Potts model describes an effect-site compartment only for the hypotensive effects. Possible explanations are the usually shorter delays in drug effects in children, and less frequent non-invasive monitoring of blood pressure (every 5 min), obscuring the hysteresis for the vasoconstrictor effects. Also, Potts and colleagues[8] included a parameter describing the maximal sympatholytic effect, whereas we chose to omit this parameter from the model because it resulted in numerical difficulties with model estimation. The differences in parameter values between the Potts model and our model are small, despite the fact that the Potts model describes paediatric data. In our model, the EC_{50} values for the hypotensive (0.36 ng ml^{-1}) and hypertensive (1.6 ng ml^{-1}) effects are only slightly higher than in the Potts model (0.10 and 1.1 ng ml^{-1}, respectively). Furthermore, the maximal decrease and subsequent increase in MAP are similar between populations, where we found a decrease and increase of 27% and 43%, respectively, and Potts and colleagues[8] described a decrease and increase of 15% and 62%. The k_{e0} values for the hypo- and hypertensive responses were 0.053 min^{-1} (t½ = 12.1 min) and 0.090 min^{-1} (t½ = 7.68 min), respectively, whereas Potts and colleagues[8] estimated a k_{e0} for the sympatholytic effect of 0.072 min^{-1} (t½ = 9.65 min), corresponding to a slightly longer equilibration half-time for our adult volunteer model compared with the paediatric model.

Yoo and colleagues[6] used a mechanism-based PKPD model to describe changes in blood pressure and HR after dexmedetomidine administration. Several important differences can be noted here. Firstly, the dexmedetomidine dose resulted only in low plasma concentrations, below 2.4 ng ml^{-1}, therefore, no hypertensive reaction was seen in their study, and also not modelled. Secondly, the predicted lower boundary for the HR was 50.5 bpm, which is clearly inconsistent with our data, as several volunteers reached heart rates of 40 bpm.

Our simulations are in good agreement with the observations described by Bloor and colleagues[1] and Dyck and colleagues[7] on the effects of dexmedetomidine on HR in healthy volunteers. Bloor and colleagues[1] found that at 2 min infusions of 1.0 and 2.0 µg kg^{-1} dexmedetomidine, HR decreased from 59 bpm at baseline to 49 and 44 bpm 2-3 min postinfusion. From our simulations we found a change from baseline of -21% and -31%, respectively. When taking into account a baseline HR of 59 bpm, this results in a predicted minimal HR of 47 and 41 bpm, which is very similar to the results from Bloor and colleagues.[1] Dyck and colleagues[7] found that after a 5 min infusion of 2 µg kg^{-1} dexmedetomidine HR decreased to 27% below baseline 4-5 min postinfusion. This is in good agreement with what is predicted by our model (-27% change from baseline at 5.1 min after the start of the infusion).

For the predicted effects of dexmedetomidine on the MAP, especially for the hypertensive phase, our model somewhat underachieves. For the dexmedetomidine infusions of 2 μg kg^{-1} studied by Bloor and colleagues[1] and Dyck and colleagues,[7] our model predicts an increase in MAP of 7% and 8%, respectively, which is lower than the 22% and 24% increase observed. In contrast, when we simulate the experimental work described by Snapir and colleagues[4] and Ebert and colleagues,[5] who used TCI administration to study the haemodynamic effects of dexmedetomidine at steady-state plasma concentrations of 5.1 and 8 ng ml^{-1}, we predict an increase in MAP of 15% and 23%, which is higher than the 10% and 12% increase reported. The fact that the model predictions are not biased when comparing against these independent data sets (i.e. not always over- or underpredicting) inspires confidence. Nevertheless, this aspect has the potential for improvement as more data become available.

Our model adequately describes dexmedetomidine-induced postinfusion hypotension, which is well known from the work of Bloor and colleagues[1] and Dyck and colleagues.[7] These studies found that MAP was reduced (-17% and -22% for the 2 μg kg^{-1} infusion, respectively) up to 4 and 5.5 h after the start of the infusion. Our predicted decreases in MAP of -16% and -21% are in good agreement with these findings. Based on our model, we expect that it would take 10.4 h for MAP to return to within 5% of its baseline value. As the previously mentioned studies ended 4 and 5.5 h after the start of the dexmedetomidine infusion, this aspect of the model remains to be validated.

Based on our PKPD models, we were able to study the interplay between the sedative and haemodynamic effects of dexmedetomidine. Dexmedetomidine-induced changes in HR and MAP are reflected in the sedative properties and could therefore, at least in theory, be used as surrogate markers for the degree of sedation.For the typical individual, a HR decrease of 10-20% and a normalization of MAP after the initial hypotensive phase could serve as a surrogate marker to target a shallow state of sedation (i.e. BIS between 60 and 40 and ≥ 80% chance of loss of responsiveness). Individual variability in sensitivity to the sedative and haemodynamic responses means that these haemodynamic targets will be associated with some variability in sedation. A larger study should be conducted to refine and validate these targets in a population context. Depending on the precision of the haemodynamic monitoring system used, these targets might be obscured by measurement noise and, as such, might be of limited clinical use in some instances.

Strengths of our study include the use of stratified age groups, a relatively wide range of individual heights and weights, and both male and female volunteers, increasing our chances of detecting relevant covariates. However, apart from an effect of age on

baseline MAP, we found no other covariates for baseline values or dexmedetomidine effects on MAP and HR. This is in line with other PKPD analyses,[6, 8] which also did not find a significant influence of patient characteristics on estimated PKPD parameters.

Use of healthy volunteers allowed development of a PKPD model that avoids confounding influences of concomitant medications or patient co-morbidity. For example, a study by Talke and colleagues[2] showed that the sympatholytic effect of dexmedetomidine is attenuated under general anaesthesia, while the vasoconstrictive effect remains. It is uncertain whether co-morbidity and concomitant medications might limit or, conversely, increase the haemodynamic effects of dexmedetomidine.

The volunteers in our study mostly did not return to baseline values of HR and MAP. One reason may be the long-lasting effect that dexmedetomidine has on haemodynamics, and our recovery period of 5 h was too short for a full return to baseline, as is also shown in our simulations. Another explanation may be that 'baseline' is not the true baseline at rest, and nervousness and stress may cause volunteers to have higher HR and MAP before the start of the study than in the recovery period.

Given that our infusion rate was limited to 6 or 10 µg kg^{-1} h^{-1}, our simulations with higher infusion rates are not validated. One of the characteristics of our model is that even at high infusion rates, there is initial hypotension, followed rapidly by a hypertensive reaction. This phenomenon is not described in the literature. Although this could be explained by the fact that blood pressure monitoring is often too slow to capture this effect, it could also simply be an artifact of the model, and that, physiological feedback mechanisms prevent this phenomenon in vivo. Attempts to incorporate such feedback mechanisms in our PKPD model failed because of numerical issues with the estimation algorithm. Further research, focusing on high-resolution haemodynamic monitoring during different infusion rates, is required to validate this effect.

In conclusion, we developed a PKPD model for dexmedetomidine effects on HR and MAP in healthy volunteers. The model accurately describes the reduced HR and the clear biphasic effect on MAP, with two effect-site compartments corresponding to different physiological α2-receptor effects. No additional subject covariates beyond those that were already included in the previously developed PK model[9] had an impact on dexmedetomidine-induced changes in the haemodynamics. The sedative and haemodynamic effects of dexmedetomidine are highly correlated, so our model provides surrogate haemodynamic markers to guide dexmedetomidine sedation. Further prospective clinical validation should be conducted to assess the performance of our model and the proposed surrogate haemodynamic markers.

Supplementary material

Supplementary material is available at British Journal of Anaesthesia online.

References

1. Bloor BC, Ward DS, Belleville JP, Maze M: Effects of intravenous dexmedetomidine in humans. II. Hemodynamic changes. Anesthesiology 1992; 77: 1134-42

2. Talke P, Lobo E, Brown R: Systemically administered alpha2-agonist-induced peripheral vasoconstriction in humans. Anesthesiology 2003; 99: 65-70

3. Figueroa XF, Poblete MI, Boric MP, Mendizábal VE, Adler-Graschinsky E, Huidobro-Toro JP: Clonidine-induced nitric oxide-dependent vasorelaxation mediated by endothelial alpha(2)-adrenoceptor activation. Br J Pharmacol 2001; 134: 957-68

4. Snapir A, Posti J, Kentala E, Koskenvuo J, Sundell J, Tuunanen H, Hakala K, Scheinin H, Knuuti J, Scheinin M: Effects of low and high plasma concentrations of dexmedetomidine on myocardial perfusion and cardiac function in healthy male subjects. Anesthesiology 2006; 105: 70

5. Ebert TJ, Hall JE, Barney JA, Uhrich TD, Colinco MD: The effects of increasing plasma concentrations of dexmedetomidine in humans. Anesthesiology 2000; 93: 382-94

6. Yoo H, Iirola T, Vilo S, Manner T, Aantaa R, Lahtinen M, Scheinin M, Olkkola KT, Jusko WJ: Mechanism-based population pharmacokinetic and pharmacodynamic modeling of intravenous and intranasal dexmedetomidine in healthy subjects. Eur J Clin Pharmacol 2015; 71: 1197-207

7. Dyck JB, Maze M, Haack C, Vuorilehto L, Shafer SL: The pharmacokinetics and hemodynamic effects of intravenous and intramuscular dexmedetomidine hydrochloride in adult human volunteers. Anesthesiology 1993; 78: 813-20

8. Potts AL, Anderson BJ, Holford NH, Vu TC, Warman GR: Dexmedetomidine hemodynamics in children after cardiac surgery. Paediatr Anaesth 2010; 20: 425-33

9. Hannivoort LN, Eleveld DJ, Proost JH, Reyntjens, Koen M E M, Absalom AR, Vereecke HEM, Struys, Michel M R F: Development of an Optimized Pharmacokinetic Model of Dexmedetomidine Using Target-controlled Infusion in Healthy Volunteers. Anesthesiology 2015; 123: 357-67

10. Colin P, Hannivoort LN, Eleveld DJ, Reyntjens KMEM, Absalom AR, Vereecke HEM, Struys MMRF: Dexmedetomidine pharmacokinetic-pharmacodynamic modeling in healthy volunteers: 1. Influence of arousal on bispectral index and sedation. Br J Anaesth 2017; 119: 200-10

11. Dyck JB, Maze M, Haack C, Azarnoff DL, Vuorilehto L, Shafer SL: Computer-controlled infusion of intravenous dexmedetomidine hydrochloride in adult human volunteers. Anesthesiology 1993; 78: 821-8

12. Schoemaker RC, van Gerven JM, Cohen AF: Estimating potency for the Emax-model without attaining maximal effects. J Pharmacokinet Biopharm 1998; 26: 581-93

13. Bergstrand M, Hooker AC, Wallin JE, Karlsson MO: Prediction-corrected visual predictive checks for diagnosing nonlinear mixed-effects models. AAPS J 2011; 13: 143-51

14. Lindbom L, Ribbing J, Jonsson EN: Perl-speaks-NONMEM (PsN)--a Perl module for NONMEM related programming. Comput Methods Programs Biomed 2004; 75: 85-94

15. Keizer RJ, van Benten M, Beijnen JH, Schellens JHM, Huitema ADR: Piraña and PCluster: a modeling environment and cluster infrastructure for NONMEM. Comput Methods Programs Biomed 2011; 101: 72-9

16. Venzon DJ, Moolgavkar SH: A Method for Computing Profile-Likelihood-Based Confidence Intervals. Journal of the Royal Statistical Society. Series C (Applied Statistics) 1988; 37: 87-94

17. European Medicines Agency. European Public Assessment Report. 2016. Available from: http://www.ema.europa.eu/docs/en_GB/document_library/EPAR_-_Product_Information/human/ 002268/WC500115631.pdf (lase accessed April 18, 2017)

Chapter 5: A response surface model approach for continuous measures of hypnotic and analgesic effect during sevoflurane–remifentanil interaction

Quantifying the pharmacodynamic shift evoked by stimulation

Modified from *Anesthesiology 2014; 120:1390-9*

Bjorn Heyse†, Johannes H. Proost†, Laura N. Hannivoort, Douglas J. Eleveld, Martin Luginbühl, Michel M. R. F. Struys, Hugo E. M. Vereecke

† Both authors contributed equally to this study and should both be seen as first authors.

Abstract

Background: The authors studied the interaction between sevoflurane and remifentanil on bispectral index (BIS), state entropy (SE), response entropy (RE), Composite Variability Index, and Surgical Pleth Index, by using a response surface methodology. The authors also studied the influence of stimulation on this interaction.

Methods: Forty patients received combined concentrations of remifentanil (0 to 12 ng/ml) and sevoflurane (0.5 to 3.5 vol%) according to a crisscross design (160 concentration pairs). During pseudo–steady-state anesthesia, the pharmacodynamic measures were obtained before and after a series of noxious and nonnoxious stimulations. For the "prestimulation" and "poststimulation" BIS, SE, RE, Composite Variability Index, and Surgical Pleth Index, interaction models were applied to find the best fit, by using NONMEM 7.2.0. (Icon Development Solutions, Hanover, MD).

Results: The authors found an additive interaction between sevoflurane and remifentanil on BIS, SE, and RE. For Composite Variability Index, a moderate synergism was found. The comparison of pre- and poststimulation data revealed a shift of $C50_{SEVO}$ for BIS, SE, and RE, with a consistent increase of 0.3 vol%. The Surgical Pleth Index data did not result in plausible parameter estimates, neither before nor after stimulation.

Conclusions: By combining pre- and poststimulation data, interaction models for BIS, SE, and RE demonstrate a consistent influence of "stimulation" on the pharmacodynamic relationship between sevoflurane and remifentanil. Significant population variability exists for Composite Variability Index and Surgical Pleth Index.

Introduction

Two important components of general anesthesia are hypnosis and analgesia: The hypnotic component may be defined as probability of tolerance to a nonnoxious stimulus (*e.g.*, name calling or shake and shout), whereas the analgesic component (also called: the balance between nociception and antinociception) may be considered as the probability of tolerance to a noxious stimulus.[1] Tolerance means "the absence of a response" being either a somatic response (*e.g.*, movement, sweating, eye opening), a hemodynamic response (increase in heart rate or blood pressure), or an arousal on the electroencephalogram of the frontal cortex, which is a reflection of a decreased cerebral hypnotic drug effect due to an insufficient analgesic effect. This "component" definition is based on the notion that tolerance to verbal and noxious stimulation will be mediated through different neuronal networks, which are located in the higher cortical *versus* subcortical structures of the brain, respectively.[1] These networks are independently affected by the interaction between a hypnotic and an analgesic drug. As an example of this, Heyse *et al*.[2] showed different response surface models for tolerance to nonnoxious and noxious stimulation.

In addition to the dichotomous observations of tolerance to stimulation, several neurophysiology-derived measures of anesthesia effect have been developed to monitor the anesthesia state of the patient in a continuous way. Electroencephalographic measures, such as bispectral index (BIS; Covidien, Boulder, CO), state entropy (SE), and response entropy (RE) (M-Entropy; GE Healthcare, Helsinki, Finland), have a stronger correlation with the hypnotic component than with the analgesic component of anesthesia.[3] More recently, new continuous measures with different neurophysiological background, such as the Surgical Pleth Index (SPI; GE Healthcare) and the Composite Variability Index (CVI; Covidien), attempt to quantify the balance between nociception and antinociception.[4, 5] All these continuous surrogate measures of hypnotic or analgesic effect are influenced by the interaction between hypnotic and analgesic drugs and should therefore be studied with this multidrug reality in mind. Eventually, the ultimate goal of continuous monitoring is to effectively counter deviating measurements with an adequate change in the balance between opioids and hypnotics so that better clinical results are obtained. This performance can only be expected if a well-described dose-response relationship exists between the measurements and the applied drug combinations.

To depict this dose-response relationship in the presence of multiple drugs, it is common to use population-derived response surface interaction models.[2] For BIS, SE, RE, CVI, and

SPI, the interaction between sevoflurane and remifentanil on continuous measures has not yet been described.

Therefore, the primary goal of this study was to develop response surface models that best describe the dose-response relationship between the combined administration of sevoflurane and remifentanil *versus* BIS, SE, RE, CVI, and SPI. Overall, we hypothesized that the nature of the various interactions should be synergistic for the continuous measures as this is in concordance with the interaction on dichotomous clinical endpoints as described by Heyse *et al*.[2] The secondary goal of the study was to investigate whether noxious stimulation significantly affects the model structure or the model parameters.

Materials and Methods

The data presented in this article were collected during a previous study as published by Heyse *et al*.[2] This study presents the results of a secondary analysis focusing on the continuous measurements of drug effect, whereas the previous study focused on dichotomous endpoints of anesthetic effect (clinical signs of responsiveness). The studied patients, the crisscross study design, and drug administration methods applied in this study have been described elsewhere in detail.[2]

Subjects

After obtaining Institutional Review Board (Ghent University Hospital Ethics Committee, Gent, Belgium) approval and prospective trial registration at ClinicalTrials.gov (NCT00522587) and after obtaining written informed consent, 40 patients with American Society of Anesthesiologists status I or II, aged 18 to 60 yr, and scheduled to undergo surgery requiring general anesthesia were included. Exclusion criteria were weight less than 70% or more than 130% of ideal body weight, neurological disorders, diseases involving the cardiovascular system, pulmonary diseases, gastric diseases, endocrine diseases, and recent use of psychoactive medication or use of more than 20 g of alcohol daily. The complete study was executed in a quiet operating room before the start of the surgical procedure.

Study Design

This study was performed as a randomized, prospective, open-label study. No participant of the study received premedication. After the patients arrived in the operating room, standard monitors (electrocardiogram, noninvasive blood pressure, and hemoglobin oxygen saturation), M-Entropy using a Datex S/5 Anesthesia Monitor (GE Healthcare), and BIS using an Aspect A-2000 monitor (Covidien) were connected, and a large forearm vein was cannulated. Thereafter, the patients were preoxygenated with 6 l/min of O_2 at an $F_I = 1.0$ for 5 min using a tightfitting face mask, which also served to sample exhaled air for end-tidal carbon dioxide measurement. Vital signs and end-tidal sevoflurane concentrations, respiratory data (tidal volume, minute volume, and end-tidal carbon dioxide), and infusion-related data (predicted concentrations and infused volumes) were continuously recorded on a computer hard disk using RUGLOOP II data-recording software (Demed, Temse, Belgium).

Drug Administration

Technical Aspects. Remifentanil was administered by a target-controlled infusion technique by using RUGLOOP II TCI software (Demed) based on a three-compartment model with an effect-site compartment as published by Minto *et al*.[6, 7] Sevoflurane was

administered in 50% O_2 and 50% air by using a standard out-of-circle vaporizer and a standard breathing circuit of an ADU anesthesia workstation (Datex/Ohmeda; GE Healthcare).

Dosing Regimen. We randomized 40 patients to receive four prespecified combinations of sevoflurane (0.5 to 3.5 vol%) and remifentanil (0 to 12 ng/ml) according to a modification of the crisscross design proposed by Short *et al*.[8] In half of the patients, remifentanil was held constant, and sevoflurane was stepwise increased; in the other half, sevoflurane was held constant and remifentanil was stepwise increased. The dosing schedule is shown in table 1 in the study by Heyse *et al*.[2] No muscle relaxants were administered throughout the study.

Assessment of Clinical Response

For each concentration step, the clinical response was assessed 12 min after reaching the target concentrations to allow for plasma effect-site equilibration. The patient was exposed to the following series of stimuli, with increasing intensity: (1) verbal and nonpainful tactile stimuli according to the Modified Observer's Assessment of Alertness/ Sedation (OAA/S) score[9]; (2) a tetanic stimulus of the ulnar nerve for 5 s by using the standard neurostimulator; (3) insertion of a laryngeal mask airway (size 3 for women and 4 for men, LMA Unique® [The Surgical Company, Amersfoort, The Netherlands]); and (4) laryngoscopy aiming at full visualization of the vocal cords by using a size-3 curved Macintosh- type blade (HEINE Optotechnik GmbH & Co KG, Herrsching, Germany). All stimuli – Including laryngoscopy – were performed by a single anesthesiologist (B.H.) to minimize interindividual variability in stimulation. Between each stimulus, a 1-min delay was maintained to evaluate the somatic responsiveness on each stimulus. If there was no response to a stimulus, the next stimulus was applied 1 min after the response assessment of the previous stimulus.

In this study, we only compared data before OAA/S score (unstimulated state) with data after laryngoscopy (stimulated state). For the data that were obtained in between stimuli, we did not estimate separate models. We could not exclude a bias evoked by influences of the preceding stimulus on the next one. However, by performing simultaneous model estimations on data before and after the sequence of four clinically relevant stimulations, we explore pharmacodynamic differences between a generally "unstimulated" *versus* a "stimulated" anesthesia state.

Data Acquisition and Management

BIS, SE, and RE. The spectral entropy monitor (M-Entropy; GE Healthcare) calculated SE and RE. BIS was simultaneously derived from the frontal electroencephalogram (At-Fpzt) by using a quatro BIS™ sensor with four electrodes (Covidien). The smoothing time

of the BIS monitor was set at 15 s. All data were recorded electronically using RUGLOOP II software (Demed) with a 5-s time interval.

The median of the recorded values during 1 min before the assessment of the OAA/S score was used for the analysis of the BIS, SE, and RE data.

CVI. The raw electroencephalographic signal was captured by the BIS™ monitor with a 128-Hz sample rate and allowed *post hoc* calculation of CVI. The calculation of CVI has been described by Mathews *et al*.[5] The CVI is a composite index that combines the variability in BIS with frontal electromyographic changes over time. A high CVI reflects activation of the frontal electromyography and increased input of sensory information from deep brain structures to the cortex. A low CVI reflects an adequate inhibition of this sensory input and adequate analgesia. The CVI was calculated with a 5-s time interval. The median of the recorded values during 1 min before the assessment of the OAA/S score was used for the analysis. In the case that one or more values were missing during the last minute before the assessment of OAA/S score due to a technical reason, the CVI was regarded as a missing value and was not taken into account in the analysis.

SPI. The SPI is derived from plethysmographic pulse wave characteristics combined with heart rate variability and is a surrogate measure of the orthosympathetic and parasympathetic nervous system response to noxious stimulation. The calculation of SPI has been described by Huiku *et al*.[4] The SPI was calculated with a 1-s time interval. The median of the recorded values during 1 min before the assessment of the OAA/S score was used for the analysis. In the case that there were less than seven values during the last minute before the assessment of OAA/S score, the SPI was regarded as a missing value and was not taken into account in the analysis.

Data after Stimulation. A moving median technique was applied on the raw data measured during 1 min after laryngoscopy. For the NONMEM analysis, the highest value of the moving median over several consecutive values was used. By doing so, the effect of single outlier values on the average behavior of each measurement was minimized without losing sensitivity for detecting a relevant response on BIS, SE, RE, CVI, and SPI after stimulation. For measurements that were logged every 5 s (BIS, SE, RE, and CVI), or every second (SPI), we performed the moving median technique over a sequence of respectively five or seven consecutive values. In the case that there were less than five or seven consecutive values during 1 min after application of laryngoscopy, or if laryngoscopy was not applied because the patient was responsive to a previous stimulus (see the study by Heyse *et al*.[2]), the measurement was considered as missing and was not taken into account in the analysis.

Pharmacodynamic Analysis of the Continuous Variables

For the continuous data, a negative sigmoid E_{max} model was used[10]:

$$Effect = E_0 - (E_0 - REST) \times \left(\frac{U^{\gamma}}{1 + U^{\gamma}}\right) \quad (1)$$

where E_0 is the baseline value in the absence of drug, REST is a nonsuppressible effect (the lowest possible value of the effect variable), U represents the normalized combined potency of one or more drugs, and γ is the slope parameter reflecting the steepness of the concentration–effect relationship. The normalized combined potency U is a function of the drug effect-site concentrations and model parameters, as described in detail in the appendix in the study by Heyse *et al*.[2] The following models were tested:

a. Greco model

$$U = \frac{C_{SEVO}}{C50_{SEVO}} + \frac{C_{REMI}}{C50_{REMI}} + \alpha \times \frac{C_{SEVO}}{C50_{SEVO}} \times \frac{C_{REMI}}{C50_{REMI}} \quad (2)$$

where C_{SEVO} is the effect-site concentration of sevoflurane, C_{REMI} is the effect-site concentration of remifentanil, $C50_{SEVO}$ is the effect-site concentration of sevoflurane with 50% effect, $C50_{REMI}$ is the effect-site concentration of remifentanil with 50% effect, and α is a dimensionless interaction parameter.

b. Reduced Greco model without effect of the opioid alone

$$U = \frac{C_{SEVO}}{C50_{SEVO}} \times \left(1 + \frac{C_{REMI}}{C50_{REMI}}\right) \quad (3)$$

c. Minto model[11]

$$U = \frac{\frac{C_{SEVO}}{C50_{SEVO}} + \frac{C_{REMI}}{C50_{REMI}}}{1 - \beta_{U50} \times \theta \times (1 - \theta)} \quad (4)$$

where β_{U50} is a dimensionless interaction parameter, and θ is defined by:

$$\theta = \frac{\frac{C_{SEVO}}{C50_{SEVO}}}{\frac{C_{SEVO}}{C50_{SEVO}} + \frac{C_{REMI}}{C50_{REMI}}} \quad (5)$$

d. Hierarchical model

$$U = \frac{C_{SEVO}}{C50_{SEVO}} \times \left(1 + \left(\frac{C_{REMI}}{C50_{REMI}}\right)^{\gamma_O}\right) \quad (6)$$

where γ_O is the slope parameter reflecting the steepness of the concentration–effect relationship for remifentanil.

Because each pharmacodynamic endpoint was analyzed separately, the Scaled $C50_O$ and Fixed $C50_O$ Hierarchical models are identical.[2]

For BIS, SE, and RE, it was assumed that the measure approaches zero for high concentrations of sevoflurane or remifentanil, so REST is zero, reducing the model to a fractional E_{max} model.[10] For CVI and SPI, the nonsuppressible effect REST was modeled as a function of the drug concentrations according to the procedure described by Minto *et al.*[11]:

$$REST = REST_{SEVO} \times \theta + REST_{REMI} \times (1 - \theta) - \beta_{REST} \times \theta \times (1 - \theta) \quad (7)$$

where $REST_{SEVO}$, $REST_{REMI}$, and β_{REST} are model parameters.

Parameter Estimation

The model parameters were estimated using NONMEM 7.2.0 (Icon Development Solutions, Hanover, MD), using first-order conditional estimation. Platform was Windows XP (Microsoft, Redmond, WA) and compiler was G95. For all parameters, interindividual variability was assumed either to be absent or to have a lognormal distribution. It was tested whether a single value for the individual deviation from the typical value (eta in NONMEM) could be used for C50 of sevoflurane and remifentanil, in accordance with the assumption that this value reflects the sensitivity of that individual for hypnotic and opioid drugs. Residual intraindividual variability of the continuous variables was modeled using standard additive or proportional error models.

Parameters were tested for significance by comparing the objective function which is minus two times log-likelihood (−2LL). Significance level for hypothesis tests was 0.01 (chi-square test), or a 6.84 difference in the −2LL adding one parameter for nested models. The goodness-of-fit for the models was also assessed by visual inspection of the predicted *versus* observed plots and the distribution of residuals for each of the continuous endpoints.

Model building was performed starting with the simplest form of each model and expanding the model with parameters and interindividual variability until the decrease

of the objective function value was not statistically significant using the chi-square test. In addition, model building was started with the most complex model, reducing the model by fixing parameters to zero. The NONMEM analysis was performed with various values for initial estimates and boundary values. The results were accepted as valid only if both minimization and covariance steps were successful, unless stated otherwise.

To evaluate the final model, a bootstrap analysis was performed, based on 2,000 sets of 40 patients each, randomly selected from the available 40 patients, using a custom program written in c. Results were analyzed in Excel (Microsoft) to obtain nonparametric 95% CIs.

The poststimulation data after laryngoscopy were analyzed by using an identical modeling approach as applied on the prestimulation data. To investigate the effect of the stimulations on the model parameters, we performed a simultaneous fitting of the data before OAA/S (= unstimulated anesthesia state) and after laryngoscopy (= stimulated anesthesia state) in a stepwise model-building process, starting with fixed common parameters for both data sets, followed by testing the addition of parameters for the difference between before OAA/S and after laryngoscopy.

Statistical Analysis

All model parameters are reported as typical values with relative standard error (in % of the typical value) within parentheses, and clinical data are given as mean and SD or as median and range, when appropriate.

Table 1. Population Model Estimates for BIS, SE, RE and CVI

	BIS	SE	RE	CVI
Interaction Model	Greco/Minto	Greco/Minto	Greco/Minto	Reduced Greco
$C50_{REMI}$ (ng/ml)	27.3 (13%) (20.4-37.7)	16.2 (19%) (11.0-27.9)	18.2 (21%) (12.6-31.9)	7.56 (32%) (4.01-17.7)
$C50_{SEVO}$ (vol%)	1.99 (6%) (1.68-2.23)	1.82 (8%) (1.49-2.11)	1.88 (7%) (1.58-2.14)	1.09 (97%) (0.08-3.28)
γ	1.88 (10%) (1.53-2.27)	1.87 (9%) (1.54-2.26)	2.08 (8%) (1.76-2.40)	1.16 (29%) (0.77-2.15)
E_0	89.5 (4%) (83.5-99.1)	97.1 (5%) (84.3-110)	103 (4%) (95-113)	4.32 (57%) (2.35-19.9)
IIV ($C50_{REMI}$)	20% (14%) (14-25%)	59% (19%) (33-86%)	67% (19%) (43-99%)	0*
IIV ($C50_{SEVO}$)	20%†	22% (22%) (8-30%)	25% (19%) (13-34%)	18% (24%) (0-26%)
Residual SD	6.2‡ (9%) (5.0-7.2)	9.5‡ (10%) (7.5-11.1)	9.6‡ (10%) (7.5-11.2)	27%§ (11%) (22-33%)
$\Delta C50_{SEVO}$ (vol%)	0.30 (18%) (0.20-0.41)	0.31 (22%) (0.18-0.46)	0.36 (20%) (0.23-0.52)	||

Values are typical values, relative standard error (% of the typical value) and 95% CI obtained by bootstrapping.

* Not significantly different from 0; † Common value for remifentanil and sevoflurane; ‡ Additive error; § Proportional error; || Could not be estimated (for detail, see text).

BIS = bispectral index; SE = state entropy; RE = response entropy; CVI = Composite Variability Index; C50REMI = effect-site concentration of remifentanil with 50% effect; C50SEVO = effect-site concentration of sevoflurane with 50% effect; ΔC50SEVO = increase of C50SEVO after laryngoscopy, as obtained in a separate analysis (see text); E0 = baseline value in absence of drugs; γ = model parameter reflecting the steepness of the concentration-effect relationship; IIV(C50REMI) and IIV(C50SEVO) = interindividual variability for C50REMI and C50SEVO, respectively (calculated as the square root of interindividual variance, multiplied by 100%); Residual SD = SD of the differences between the observed and predicted responses (calculated as the square root of the residual variance).

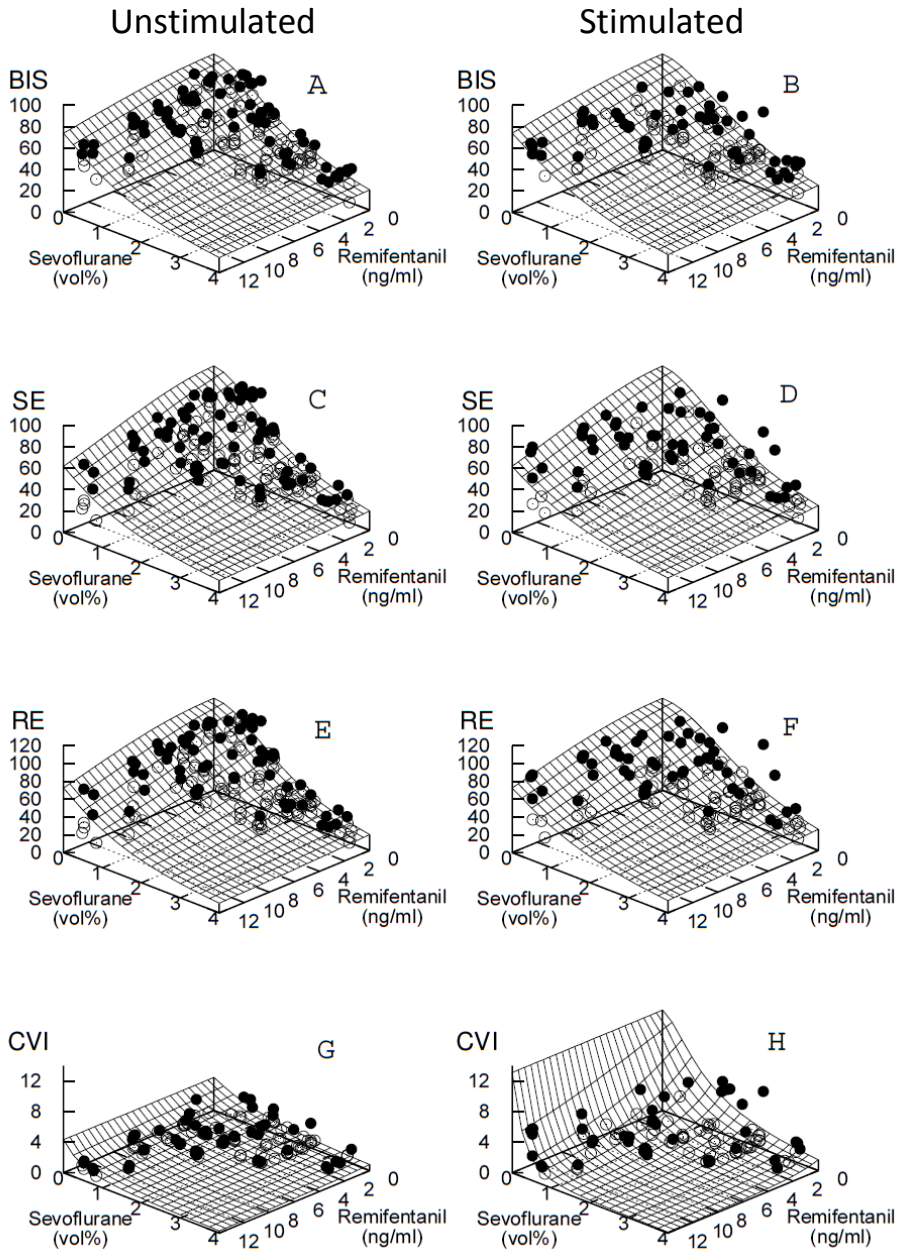

Figure 1. Response surface for electroencephalographic endpoints before stimulation (A, C, E, G) and after stimulation (B, D, F, H) was applied: Bispectral index (BIS), state entropy (SE), response entropy (RE), and Composite Variability Index (CVI), as a function of the end-tidal steady-state sevoflurane concentration and the predicted remifentanil effect-site concentration, calculated from the data listed in table 1. Measured values above the surface are shown as filled circles and below the surface as open circles.

Results

In total, 40 patients (26 women and 14 men) were included in this study. The demographics are as follows: body weight, 66 ± 11 kg; height, 172 ± 8 cm; and age, 30 ± 11 yr. All patients were classified as American Society of Anesthesiologists status I.

Data

In total, the data sets contained 159 periods of testing (40 patients with 4 periods per patient minus 1 missing period where no stimulus was given).

Model Development for BIS

Initially, BIS data were analyzed using the Greco, Reduced Greco, Minto, and Hierarchical models, using a fractional E_{max} model (REST = 0). For both the Greco model and the Minto model, the interaction term for C50 did not differ significantly from zero. Similarly, the interaction term for γ in the Minto model did not differ significantly from zero. Consequently, both models yield identical results. The objective function value for the Greco model (808.5) was markedly lower than that for the Reduced Greco model (823.0) and Hierarchical model (822.2), and therefore, the Greco model was considered as the most appropriate method. The additional error model fitted better to the data than the proportional error model, as concluded from the objective function value and diagnostic plots of residuals.

Final Model for BIS

The final results for this model are shown in table 1. In the final model, interindividual variability was included in $C50_{REMI}$ and $C50_{SEVO}$ with a common *eta*. The value for C50 for remifentanil (27.3 ng/ml) exceeds the upper range of concentrations in the study (12 ng/ml), but its precision was satisfactory (relative standard error 12%).

The response surface of the final model is shown in figure 1. Figure 2 depicts the observed BIS values (filled symbols) and predicted BIS (solid line) *versus* the normalized combined potency U_{BIS}, which has a sigmoidal E_{max} relationship.

Model Development for SE and RE

The Greco model was found to be the most appropriate model for SE and RE, in accordance with the best model for BIS.

Final Models for SE and RE

The results of the final models are summarized in table 1. The variability in SE and RE is larger than for the BIS data, as reflected in larger relative standard errors, larger interindividual variability, and larger residual SD.

The response surfaces of the final models for SE and RE are shown in figure 1. Figures 3 and 4 depict the observed (filled symbols) and predicted (solid line) SE and RE *versus* the normalized combined potencies U_{SE} and U_{RE}, respectively, which also have a sigmoidal E_{max} relationship.

Model Development for CVI

In four patients, the CVI could not be calculated due to missing data. In 17 patients, the CVI could not be calculated from the available electroencephalogram registration in one or more periods. In total, 122 CVI values in 36 patients were available.

For CVI, the objective function value of the Reduced Greco model was lower than for the Greco model and Minto model. The proportional error model fitted better to the data than the additional error model, as concluded from the objective function value and diagnostic plots of residuals. Using the Hierarchical model, the slope factor γ for remifentanil (0.289) and $C50_{SEVO}$ (0.266 vol.%) was very low, E_0 (10.2) was much higher than the highest observed CVI value, and standard errors were high; therefore, this model was not accepted as a valid model.

Final Model for CVI

The results for the final Reduced Greco model are shown in table 1. The residual error of 27% is large and the CIs for the model parameters are wide, reflecting the poor fit.

The response surface of the final model for CVI is shown in figure 1. Figure 5 depicts the observed (filled symbols) and predicted CVI values (solid line) *versus* the normalized combined potency U_{CVI}. The CVI has a sigmoidal E_{max} relationship with U_{CVI}, which is comparable in behavior to BIS, SE, and RE.

Model Development for SPI

In two patients, the SPI could not be calculated due to missing data. In four patients, the SPI could not be calculated from the available plethysmography data in one or more periods. In total, SPI data from 145 periods in 38 patients were available.

Modeling of the SPI data did not result in reliable results. Plotting the SPI data against the sevoflurane or remifentanil concentration revealed that the SPI value is hardly affected by sevoflurane or remifentanil, in contrast to the BIS, SE, RE, and CVI (data not shown).

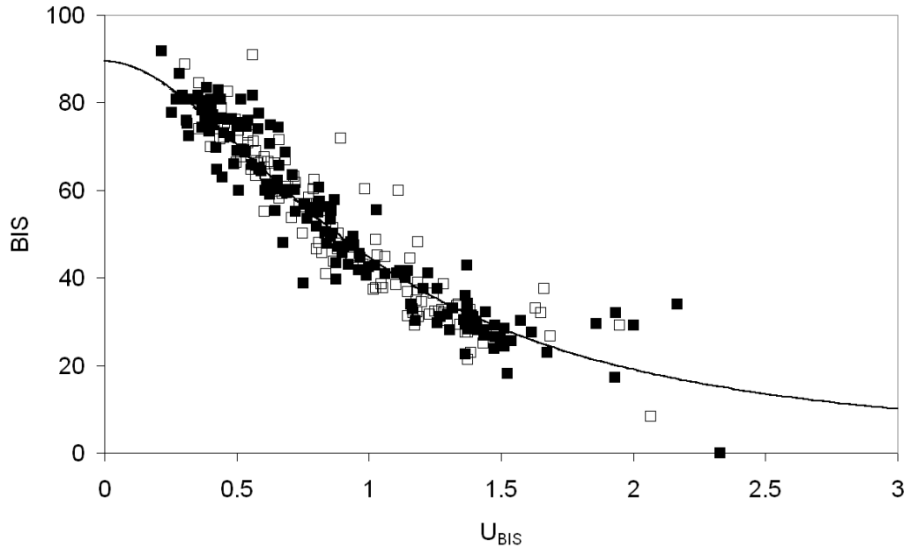

Figure 2. Relationship between the normalized combined potency U_{BIS} according to the Greco model and the observed bispectral index (BIS) (squares, n = 159) and predicted BIS (solid line; calculated from the data listed in table 1) for unstimulated (filled symbols) and stimulated (open symbols).

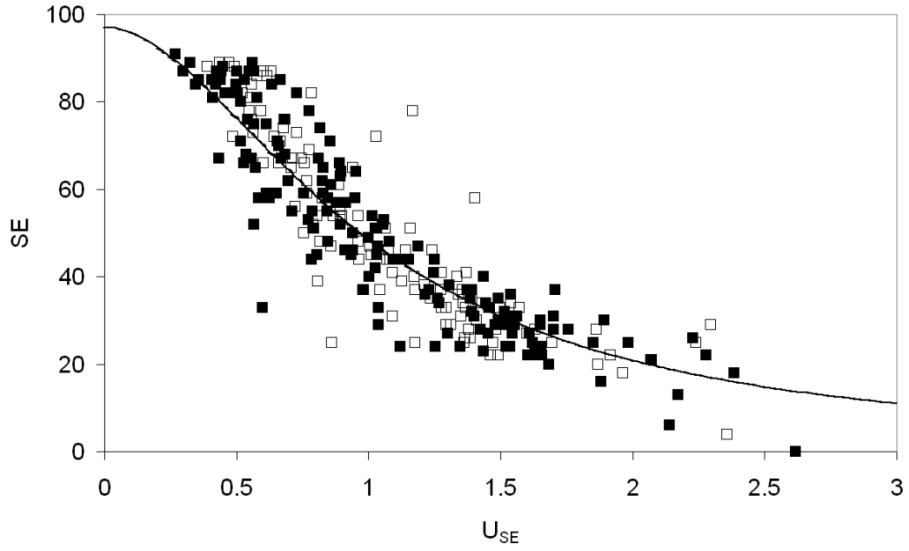

Figure 3. Relationship between the normalized combined potency U_{SE} according to the Greco model and the observed state entropy (SE) (squares, n = 159) and predicted SE (solid line; calculated from the data listed in table 1) for unstimulated (filled symbols) and stimulated (open symbols).

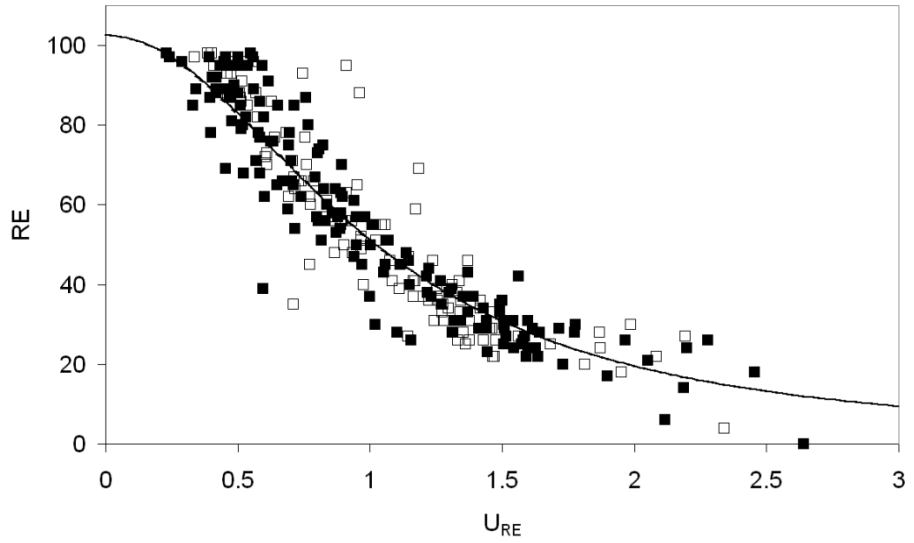

Figure 4. Relationship between the normalized combined potency U_{RE} according to the Greco model and the observed response entropy (RE) (squares, n = 159) and predicted RE (solid line; calculated from the data listed in table 1) for unstimulated (filled symbols) and stimulated (open symbols).

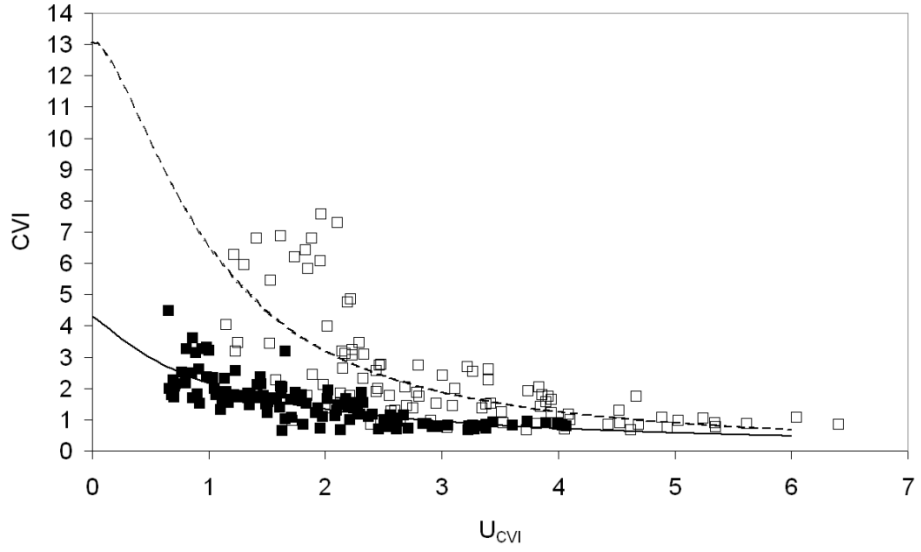

Figure 5. Relationship between the normalized combined potency U_{CVI} according to the Reduced Greco model and the observed Composite Variability Index (CVI) (squares, n = 122) and predicted CVI (lines; calculated from the data listed in table 1) for unstimulated (filled symbols, solid line) and stimulated (open symbols, dashed line).

Data after Stimulation

The data after stimulation were first analyzed using an identical modeling approach as applied on the unstimulated data. For BIS, SE, and RE, the number of data points was 114 (in 45 periods, laryngoscopy was not applied for ethical or other reasons). The optimal models were identical and the parameters were broadly comparable with the results before the assessment of OAA/S, except for $C50_{SEVO}$, which was consistently higher after the series of stimulation (data not shown).

Next, to investigate this effect of stimulation on the model parameters, we performed a simultaneous fitting of the data before OAA/S (= unstimulated anesthesia state) and after laryngoscopy in a model-building process (= stimulated anesthesia state), starting with fixed common parameters for both data sets, followed by adding parameters for the difference between before OAA/S and after laryngoscopy. This analysis revealed that $C50_{SEVO}$ was significantly higher after laryngoscopy for BIS, SE, and RE, with an average increase of 0.3 vol% sevoflurane (table 1), whereas the other parameters did not change. The response surfaces of the final models for BIS, SE, and RE are shown in figure 1. Figures 2–4 depict the observed values (open symbols) and predicted values (solid line) *versus* the normalized combined potency U for BIS, SE, and SE, respectively. Because the baseline values, maximal effect and steepness of the model are not affected by the stimulation, the relationship between U and predicted value is not affected, and the solid line is identical for unstimulated and stimulated conditions. For each combination of sevoflurane and remifentanil, the value U_{BIS} (similar for U_{SE} and U_{RE}) after stimulation is lower compared with the unstimulated state as a result of the higher $C50_{SEVO}$. Consequently, the predicted BIS after stimulation will be higher than in the unstimulated state, reflecting a reduction of the combined drug effect. In other words, stimulation moves U_{BIS} to the left, and the predicted BIS upwards along the solid lines of figures 2–4.

In contrast, simultaneous analysis of the CVI data before OAA/S and after laryngoscopy, with parameters fixed to the values from the analysis of the data before OAA/S alone (table 1), resulted in a lower value for $C50_{REMI}$ (3.09 ng/ml; CI, 1.78 to 4.68 ng/ml), a higher value for γ (1.62; CI, 1.28 to 1.79), and E_0 (13.1; CI, 9.4 to 17.2). Also, the residual SD (46%; CI, 37 to 53%) after stimulation was higher, indicating an even larger variability in the dose–response relationship of CVI compared with the unstimulated condition. Figure 5 depicts the observed values (open symbols) and predicted CVI (dashed line) *versus* the normalized combined potency U_{CVI}, respectively. Figure 5 also shows the shift in dose–response relationship of CVI *versus* U_{CVI} between the unstimulated (solid line) and stimulated condition (dashed line). Because the baseline and steepness are affected by the stimulation, the relationship between U_{CVI} and predicted value is different for the

unstimulated and stimulated data. The response surface for CVI after stimulation is shown in figure 1.

The SPI data after stimulation (104 valid SPI values) were analyzed using the same approaches. Similar to the unstimulated data, the SPI values after stimulation were hardly affected by sevoflurane or remifentanil, and modeling did not result in reliable results (data not shown).

Isoboles

In figure 6, the isoboles of BIS values from 10 to 80 are depicted for the unstimulated (solid lines) and stimulated (dashed lines) condition. The additive nature of the interaction results in linear isoboles for the complete range of BIS values. The isoboles are shifted upwards after stimulation, reflecting the increase in $C50_{SEVO}$.

In figure 7, the isoboles of CVI values from 0.5 to 3 are depicted for the unstimulated (solid lines) and stimulated (dashed lines) condition, showing a synergistic nature of the interaction, as reflected by the Reduced Greco model. For low CVI values, the isoboles of the stimulated condition intersect the isoboles of the unstimulated condition.

For SPI, no isoboles could be depicted, as we could not fit an appropriate response surface model to the data.

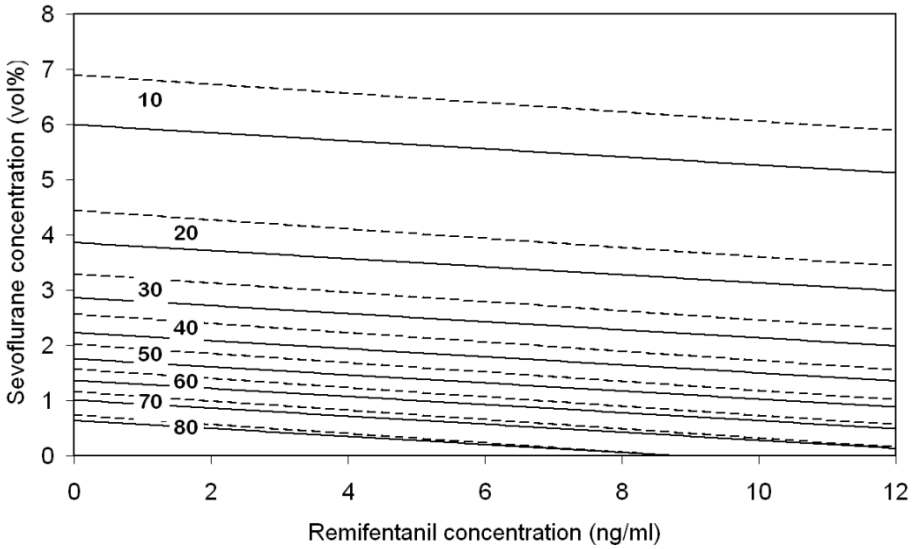

Figure 6. Isoboles for bispectral index values of 10, 20, 30, 40, 50, 60, 70, and 80 for the unstimulated (solid lines) and stimulated (dashed lines) data, as a function of the end-tidal sevoflurane concentration and the predicted remifentanil effect-site concentration, calculated from the data listed in table 1.

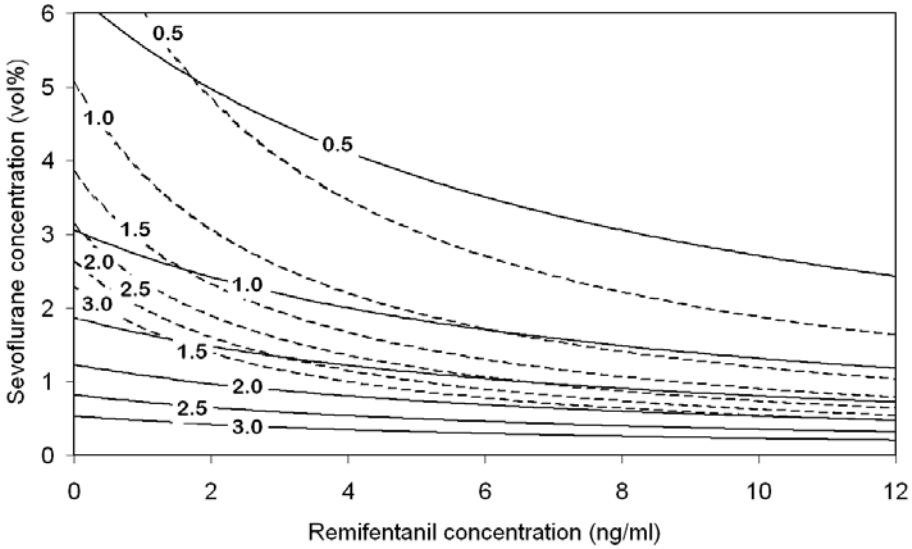

Figure 7. Isoboles for Composite Variability Index values of 0.5, 1, 1.5, 2, 2.5, and 3 for the unstimulated (solid lines) and stimulated (dashed lines) data, as a function of the end-tidal sevoflurane concentration and the predicted remifentanil effect-site concentration, calculated from the data listed in table 1.

Discussion

We describe the interaction between sevoflurane and remifentanil on BIS, SE, RE, CVI, and SPI. Although opioids have a rather weak effect on the electroencephalogram, we found an additive effect of remifentanil on reduction of BIS, SE, and RE by sevoflurane. The effect on CVI was synergistic. The SPI was not affected by sevoflurane or remifentanil. The Greco model provided the best fit of the data for BIS, SE, and RE, whereas the reduced Greco model best described CVI. Interestingly, the structural interaction model was not affected by noxious stimulation, but noxious stimulation did increase the $C50_{SEVO}$ for BIS, SE, and RE by 20%, whereas the $C50_{REMI}$ did not change. In contrast, for CVI all model parameters changed except $C50_{SEVO}$.

The findings on (unstimulated) BIS, SE, and RE are in agreement with that reported in previous literature. Nieuwenhuijs *et al.*[12] presented an interaction model during sevoflurane–alfentanil anesthesia, suggesting additivity for BIS. During propofol anesthesia, Vanluchene *et al.*[3] found that remifentanil evoked an increase in the threshold for loss of consciousness on BIS, SE, and RE in a dose-dependent way, but no conclusion was drawn on the nature of this interaction. Bouillon *et al.*[13] found additivity for BIS during propofol–remifentanil anesthesia. Schumacher *et al.*[10] found an additive interaction on BIS for combined propofol and sevoflurane. Conversely, the interaction of sevoflurane and remifentanil on clinical endpoints of effect, as published by Heyse *et al.*,[2] was not additive but synergistic. Also, $C50_{REMI}$ was 10-fold higher for BIS, SE, and RE compared with $C50_{REMI}$ for dichotomous endpoints.[2] Apparently, the opioid effect on the electroencephalogram is weak, despite a strong effect on patient responsiveness. This may explain why electroencephalographic variables are poor predictors of responsiveness to noxious stimuli.

According to the parameter estimates (table 1), BIS is least opioid sensitive, followed by SE, RE, and CVI, whereas BIS, SE, and RE are equally sensitive to sevoflurane, but less than CVI. The slope of the response surfaces is similar for BIS, SE, and RE, but steeper than the slope for CVI (fig. 5). The interaction model for BIS is characterized by the lowest interindividual (table 1: IIV [$C50_{REMI}$]) and residual variability.

Interaction models not only define combined effects of sevoflurane and remifentanil as a response surface but also allow expression of the potency of a combination of drugs as one dimensionless number. For this purpose, we introduced “U” being units of combined potency related to each of the investigated effects variables. For example, U_{BIS} is the sum of the sevoflurane and remifentanil concentration both normalized to the respective C50s of the BIS dose-response curve (equations 2 and 4). The potency U_{BIS} =

1 can be achieved by 1.99 vol% of sevoflurane (=$C50_{SEVO}$) or (*e.g.*) by 1.49 vol% of sevoflurane (=0.75 × $C50_{SEVO}$) plus 6.8 ng/ml of remifentanil (=0.25 × $C50_{REMI}$). As C50 is specific for each electroencephalographic variable, one given sevoflurane and remifentanil concentration does not yield identical values of "U" for BIS, SE, RE, or CVI. According to the final models (table 1), 1.5 vol% of sevoflurane combined with 5 ng/ml of remifentanil yields a U_{BIS}, U_{SE}, U_{RE}, and U_{CVI} of 0.94, 1.13, 1.07, and 2.29, respectively.

In concordance with Minto *et al.*,[11] we consider the combination of two drugs as a virtual new drug. "U" can be used as if it was a drug concentration of that virtual new drug on the x-axis of a two-dimensional concentration–response curve (figs. 2–5). With the selected interaction models, the combined potency "U" predicted the effect on BIS, SE, and RE with an error of approximately 10%, which is comparable to that reported in the previous studies.[13]

"U" as a number represents potency of a combination of sevoflurane and remifentanil to suppress the electroencephalographic variable and has similarities with the Noxious Stimulation Response Index.[14] The Noxious Stimulation Response Index is based on the suppression of a response to laryngoscopy, using the Hierarchical interaction model. The $C50_{REMI}$ (1.16 ng/ml) in this model is much lower than the $C50_{REMI}$ in the current study (7.5 to 27.3 ng/ml, depending on the type of electroencephalographic variable). This makes Noxious Stimulation Response Index much more opioid sensitive compared with "U," which is in agreement with the fact that hypnotics have a stronger effect on electroencephalogram than the effects of opioids on electroencephalogram. The clinical utility of any of the "U"s or Noxious Stimulation Response Index to titrate opioids and hypnotics remains to be determined.

The CVI as a potential indicator of nociception behaved similar as dichotomous endpoints in the previous study[2]: the interaction was synergistic. The best fit was found with the reduced Greco model. As expected, the concentration–response curve of CVI was affected by noxious stimulation (figs. 5 and 7), especially due to a substantial increase in baseline effect (E_0), probably due to an increase in electromyographic activity. The dose-response curve was rather flat, and a ceiling effect was observed at the level of a CVI of approximately 1 (fig. 5). This explains why a larger increase of the sevoflurane concentration is needed to lower CVI from 1 to 0.5 than that required to lower CVI from 3 to 2.5 (fig. 7). Although noxious stimulation and opioids evoke a greater effect on CVI than on BIS, SE, and RE, CVI may offer lower discriminating capacity compared with BIS, SE, and RE. Even in our best-fitted model, the differences between estimated and observed CVI were high, especially after noxious stimulation (figs. 1 and 5).

The poststimulation data set represents a population that is in a pharmacological pseudosteady state (at similar drug concentrations as before stimulation), where the applied stimuli may have disrupted the balance between drug concentrations and effect variables. Assuming that noxious stimulation might induce an arousal response on the electroencephalographic variables, we hypothesized that the parameter estimates from the poststimulation data could be different from those of the prestimulation data. We expected larger differences in model estimates for CVI and SPI compared with BIS, SE, and RE, as the arousal response in BIS is already suppressed by rather low remifentanil concentrations.[15]

For all poststimulation response surface models, the structural model with the lowest objective function was identical to the prestimulation model. For BIS, SE, and RE, the model parameters hardly changed, except for $C50_{SEVO}$ (consistently 0.3 vol% higher after laryngoscopy). This pharmacodynamic shift is consistent for BIS and entropy and it is only little smaller than the difference between $C50_{SEVO}$ for tolerance of shake and shout and laryngoscopy, found in the previous article (0.53 vol%).[2] Typical accuracy for measuring sevoflurane end-tidal concentrations is ±0.15 vol% + 5% of reading. The time between nonstimulation and poststimulation sampling did not exceed 6 min and therefore was assumed to be constant. Therefore, we consider 0.3 vol% (or 14% of 1 minimal alveolar concentration) as clinically relevant. The sevoflurane and remifentanil concentrations mentioned above (1.5 vol% and 5 ng/ml) yield a poststimulation U for BIS, SE, and RE which is approximately 10% lower than the prestimulation U. Therefore, both single-model parameters (*e.g.*, C50s) and combined potency U could be used as surrogate measures of stimulus intensity.

For CVI, the changes in the poststimulation model are complex. $C50_{REMI}$ decreased to 3.09 ng/ml. Gamma and the baseline effect (E_0) increased. The increased steepness of the dose-response curve and the larger difference between baseline and maximal effect suggest an improved descriptive capacity for CVI in stimulated compared with unstimulated conditions. However, the residual SD and the standard errors of the parameters indicate a larger variability in the dose-response relationship compared with the unstimulated condition. Our finding is in agreement with the notion that a noxious stimulus is mandatory to measure the balance between nociception and antinociception accurately.

For SPI, we were not able to extract plausible parameter estimates from our data, neither from prestimulation nor from poststimulation observations. Either SPI is hardly affected by sevoflurane and remifentanil or the inter- and intraindividual variability of SPI hides a minimal dose– response relationship. The sympathetic and parasympathetic

nerve system may be affected by many confounding factors apart from noxious stimulation and anesthetic drug dosages. The inability to detect any dose–response relationship in steady-state conditions, both with or without noxious stimulation, lowers the expectations for SPI as a guide for titrating sevoflurane and remifentanil anesthesia.

In conclusion, sevoflurane and remifentanil are additive on BIS and entropy, but they act synergistic on CVI. SPI is not correlated to drug concentrations. Noxious stimulation did not change structural models but increased the C50 of sevoflurane related to BIS and entropy, whereas a more complex parameter shift was found for CVI.

References

1. Glass PS: Anesthetic drug interactions: an insight into general anesthesia--its mechanism and dosing strategies. Anesthesiology 1998; 88: 5-6

2. Heyse B, Proost JH, Schumacher PM, Bouillon TW, Vereecke HE, Eleveld DJ, Luginbuhl M, Struys MM: Sevoflurane remifentanil interaction: comparison of different response surface models. Anesthesiology 2012; 116: 311-23

3. Vanluchene ALG, Struys, M M R F, Heyse BEK, Mortier EP: Spectral entropy measurement of patient responsiveness during propofol and remifentanil. A comparison with the bispectral index. Br J Anaesth 2004; 93: 645-54

4. Huiku M, Uutela K, van Gils M, Korhonen I, Kymäläinen M, Meriläinen P, Paloheimo M, Rantanen M, Takala P, Viertiö-Oja H, Yli-Hankala A: Assessment of surgical stress during general anaesthesia. Br J Anaesth 2007; 98: 447-55

5. Mathews DM, Clark L, Johansen J, Matute E, Seshagiri CV: Increases in electroencephalogram and electromyogram variability are associated with an increased incidence of intraoperative somatic response. Anesth Analg 2012; 114: 759-70

6. Minto CF, Schnider TW, Egan TD, Youngs E, Lemmens HJ, Gambus PL, Billard V, Hoke JF, Moore KH, Hermann DJ, Muir KT, Mandema JW, Shafer SL: Influence of age and gender on the pharmacokinetics and pharmacodynamics of remifentanil. I. Model development. Anesthesiology 1997; 86: 10-23

7. Minto CF, Schnider TW, Shafer SL: Pharmacokinetics and pharmacodynamics of remifentanil. II. Model application. Anesthesiology 1997; 86: 24-33

8. Short TG, Ho TY, Minto CF, Schnider TW, Shafer SL: Efficient trial design for eliciting a pharmacokinetic-pharmacodynamic model-based response surface describing the interaction between two intravenous anesthetic drugs. Anesthesiology 2002; 96: 400-8

9. Chernik DA, Gillings D, Laine H, Hendler J, Silver JM, Davidson AB, Schwam EM, Siegel JL: Validity and reliability of the Observer's Assessment of Alertness/Sedation Scale: study with intravenous midazolam. J Clin Psychopharmacol 1990; 10: 244-51

10. Schumacher PM, Dossche J, Mortier EP, Luginbuehl M, Bouillon TW, Struys MM: Response surface modeling of the interaction between propofol and sevoflurane. Anesthesiology 2009; 111: 790-804

11. Minto CF, Schnider TW, Short TG, Gregg KM, Gentilini A, Shafer SL: Response surface model for anesthetic drug interactions. Anesthesiology 2000; 92: 1603-16

12. Nieuwenhuijs DJ, Olofsen E, Romberg RR, Sarton E, Ward D, Engbers F, Vuyk J, Mooren R, Teppema LJ, Dahan A: Response surface modeling of remifentanil-propofol interaction on cardiorespiratory control and bispectral index. Anesthesiology 2003; 98: 312-22

13. Bouillon TW, Bruhn J, Radulescu L, Andresen C, Shafer TJ, Cohane C, Shafer SL: Pharmacodynamic interaction between propofol and remifentanil regarding hypnosis, tolerance of laryngoscopy, bispectral index, and electroencephalographic approximate entropy. Anesthesiology 2004; 100: 1353-72

14. Luginbuhl M, Schumacher PM, Vuilleumier P, Vereecke H, Heyse B, Bouillon TW, Struys MM: Noxious stimulation response index: a novel anesthetic state index based on hypnotic-opioid interaction. Anesthesiology 2010; 112: 872-80

15. Guignard B, Menigaux C, Dupont X, Fletcher D, Chauvin M: The effect of remifentanil on the bispectral index change and hemodynamic responses after orotracheal intubation. Anesth Analg 2000; 90: 161-7

Chapter 6: Probability to tolerate laryngoscopy and noxious stimulation response index as general indicators of the anaesthetic potency of sevoflurane, propofol, and remifentanil

Modified from *British Journal of Anaesthesia 2016; 116:624-31*

Laura N. Hannivoort†, Hugo E. M. Vereecke†, Johannes H. Proost, Bjorn E. K. Heyse, Douglas J. Eleveld, Thomas W. Bouillon, Michel M. R. F. Struys and Martin Luginbühl

† Both authors contributed equally to this study and should both be regarded as first author.

Abstract

Background: The probability to tolerate laryngoscopy (P_{TOL}) and its derivative, the noxious stimulation response index (NSRI), have been proposed as measures of potency of a propofol–remifentanil drug combination. This study aims at developing a triple drug interaction model to estimate the combined potency of sevoflurane, propofol, and remifentanil in terms of P_{TOL}. We compare the predictive performance of P_{TOL} and the NSRI with various anaesthetic depth monitors.

Methods: Data from three previous studies (n=120) were pooled and reanalysed. Movement response after laryngoscopy was observed with different combinations of propofol–remifentanil, sevoflurane–propofol, and sevoflurane–remifentanil. A triple interaction model to estimate P_{TOL} was developed. The NSRI was derived from P_{TOL}. The ability of P_{TOL} and the NSRI to predict observed tolerance of laryngoscopy (TOL) was compared with the following other measures: (i) effect-site concentrations of sevoflurane, propofol, and remifentanil (Ce_{SEVO}, Ce_{PROP}, and Ce_{REMI}); (ii) bispectral index; (iii) two measures of spectral entropy; (iv) composite variability index; and (v) surgical pleth index.

Results: Sevoflurane and propofol interact additively, whereas remifentanil interacts in a strongly synergistic manner. The effect-site concentrations of sevoflurane and propofol at a P_{TOL} of 50% (Ce50; standard error) were 2.59 (0.13) vol% and 7.58 (0.49) µg ml^{-1}. A Ce_{REMI} of 1.36 (0.15) ng ml^{-1} reduced the Ce50 of sevoflurane and propofol by 50%. The common slope factor was 5.22 (0.52). The P_{TOL} and NSRI predict the movement response to laryngoscopy best.

Conclusions: The triple interaction model estimates the potency of any combination of sevoflurane, propofol, and remifentanil expressed as either P_{TOL} or NSRI.

Introduction

Adequate anaesthesia can be defined as the combination of an accurate level of hypnosis with sufficient analgesia to avoid response to a noxious stimulation, where 'response' includes a variety of modalities, such as movement, haemodynamic response, or arousal. Most contemporary anaesthetic depth monitors are based on the processed EEG and correlate mainly with hypnotic drug effect; however, they do not reliably predict a response to noxious stimulation.[1, 2] Recent attempts to measure analgesia, based on the variability of the processed EEG signal[3] or on changes in the autonomic nervous system as measured by pulse plethysmography,[4, 5] were only partly successful. Similar decreasing accuracy was found for the propofol effect-site concentration (Ce_{PROP}) as a measure of drug effect in the presence of opioids.[1, 2]

For decades, the probability of response to skin incision, defined as the minimal alveolar concentration (MAC), has been used to quantify and compare the potency of volatile agents.[6-9] More recently, Bouillon and colleagues[10] defined tolerance of laryngoscopy (TOL) as an absence of movement response to laryngoscopy, and they proposed the probability to tolerate laryngoscopy (P_{TOL}) as an alternative to MAC when using propofol instead of volatile agents. For ergonomic reasons and in order to cope with the clinical conformity of standard depth of anaesthesia monitoring, Luginbühl and colleagues[11] normalized and calibrated P_{TOL} towards a new index called the noxious stimulation response index (NSRI). The NSRI is a numerical depth of anaesthesia indicator that is directly derived from P_{TOL} and was first described for propofol and remifentanil anaesthesia. The NSRI and P_{TOL} are therefore interchangeable; they merely differ in scale. The NSRI is scaled between 100 (when no anaesthetic drugs are administered) and zero (indicating extensive combined drug effects), whereas P_{TOL} scales from zero to one.

Until now, specific P_{TOL} results have been found in three different drug interaction studies, resulting in separate response surface models for propofol–remifentanil,[10] sevoflurane–propofol,[12] and sevoflurane–remifentanil.[13] In order to use P_{TOL} (and NSRI) as general probabilistic parameters to represent the lack of responsiveness to a noxious stimulation in both i.v. and volatile anaesthesia conditions, supplemented with opioids, one needs to solve the problems of whether synergy of remifentanil with propofol is stronger than synergy with sevoflurane and whether the slope of the propofol–remifentanil and the sevoflurane–remifentanil response surfaces are different. This may be clarified by developing a triple interaction surface model, merging the information from the previously published dual drug models,[10, 12, 13] hereby also rescaling and expanding previously published P_{TOL} and NSRI scales.

For clinicians, a general P_{TOL} and its derivative, NSRI, would enable estimation of the concentration of sevoflurane that is equipotent to a given propofol concentration when used in combination with remifentanil.

The primary purpose of the present study was to define a triple interaction response surface model to express the potency of any combination of sevoflurane, propofol, and remifentanil in terms of P_{TOL} and NSRI by merging the raw data from three previously published studies.[10, 12, 13] The secondary purpose was to test the ability of P_{TOL} and NSRI, calculated with the new triple interaction model parameters, to predict the observed TOL. We compared the performance of P_{TOL} and NSRI with other measures, such as single drug effect-site concentrations of sevoflurane, propofol, and remifentanil (Ce_{SEVO}, Ce_{PROP}, and Ce_{REMI}), current hypnotic effect monitors, such as the EEG-derived bispectral index (BIS; Covidien, Boulder, CO, USA)[14] and two measures of the EEG-derived spectral entropy, state entropy and response entropy (SE and RE; GE Healthcare, Helsinki, Finland),[15] and newer analgesic effect monitors, such as the BIS-derived composite variability index (CVI; Covidien)[3, 16] and pulse plethysmograph-derived surgical pleth index (SPI; GE Healthcare).[5]

Methods

We performed a response surface analysis of the pooled raw data from three previously published studies on interactions between sevoflurane, propofol, and remifentanil.[10, 12, 13, 17] The Ethics' Committees from these original studies (Ghent University Hospital, Gent, Belgium and Stanford University, Stanford, CA, USA) both agreed that the anonymized original databases could be re-used for this analysis. As the original studies were executed and published long before the introduction of the public registration requirements, no registration of the original studies was possible.

The characteristics of the study populations are summarized in Supplementary File 1 and in the Results section. The study design and drug administration protocol have been described in detail in each of the studies. Briefly, combinations of propofol–remifentanil,[10] sevoflurane–propofol,[12] and sevoflurane– remifentanil[13, 17] were administered using a modified crisscross design according to Short and colleagues.[18] Propofol and remifentanil were administered as computer-controlled infusions targeting effect-site or plasma concentrations using the pharmacokinetic and pharmacodynamic models by Schnider[19, 20] and Minto,[21, 22] respectively. While Bouillon and colleagues[10] used targeted plasma concentrations and observed an equilibration time of 15 min, Schumacher and colleagues[12] and Heyse and colleagues[13, 17] applied target effect-site concentrations with an equilibration time of 12 min. Sevoflurane was titrated to achieve predetermined end-tidal concentrations using an ADU ventilator with an integrated AS3 monitor (GE Healthcare). These equilibration times are considered sufficient for all drugs to allow equilibration between the plasma and effect-site concentration. Acceptable prediction errors of the Schnider and Minto models were confirmed in the propofol–remifentanil study by means of repetitive blood sample analysis for propofol and remifentanil published previously.[23] A steady state for sevoflurane was confirmed through end-tidal measurements of sevoflurane concentrations. In all three studies, after equilibration of plasma and effect-site concentrations, a series of stimuli was applied and the presence or absence of movement response recorded. However, only TOL was used in our final analysis after initial model validation (see Results section).

The following drug effect monitors were used: BIS (BIS Version 3.22, A1000; Covidien) by Bouillon and colleagues;[10] BIS (Version 4.0, A-2000; Covidien); and SE and RE (M-Entropy; GE Healthcare) by Schumacher and colleagues[12] and Heyse and colleagues.[17] Additionally, Heyse and colleagues[17] computed the composite variability index (CVI; Covidien) and the surgical pleth index (SPI; GE Healthcare) off-line from the recorded

raw EEG and pulse plethysmograph data, respectively. Detailed information can be found in the original publications.

Pharmacodynamic model

The synergistic interactions between propofol and remifentanil and between sevoflurane and remifentanil were best described by the modified hierarchical model,[10, 13, 23] whereas the additive interaction between sevoflurane and propofol was best described by the Greco model.[12] We therefore postulated that the interaction of the three compounds could be described by considering any combination of the three drugs as a virtual new drug with the potency 'U'.[13, 24]

Equation (1) is the sigmoidal response function for a dichotomous effect:

$$P_{TOL} = \frac{U^{\gamma}}{1 + U^{\gamma}} \quad (1)$$

where P_{TOL} is the probability of TOL, γ is the slope parameter that represents the steepness of the concentration–effect relationship, and U is the combined potency of the drugs according to equation (2):

$$U = \left(\frac{Ce_{SEVO}}{Ce50_{SEVO}} + \frac{Ce_{PROP}}{Ce50_{PROP}}\right) \times \left(1 + \left(\frac{Ce_{REMI}}{Ce50_{REMI}}\right)^{\gamma_o}\right) \quad (2)$$

where Ce_{SEVO}, Ce_{PROP}, and Ce_{REMI} are the effect-site concentrations of sevoflurane, propofol, and remifentanil, respectively, $Ce50_{SEVO}$ and $Ce50_{PROP}$ are the effect-site concentrations of sevoflurane and propofol, respectively, resulting in P_{TOL} =0.5 if given alone, $Ce50_{REMI}$ is the effect-site concentration of remifentanil that results in an increase of U by a factor of 2 or an apparent decrease of the $Ce50_{SEVO}$ and $Ce50_{PROP}$ by 50%, and γ_o represents the steepness of the concentration–effect relationship of the opioid.

According to the parameter estimates of the original studies (Table 1), our hypothesis was that $Ce50_{REMI}$, γ_o, and γ were different for sevoflurane and propofol, and we assumed a linear interpolation. The null hypothesis was that these parameters were similar. Linear interpolation was performed according to equations (3)–(5):

$$Ce50_{REMI} = Ce50_{REMI(SEVO)} \times SF + Ce50_{REMI(PROP)} \times (1 - SF) \quad (3)$$

$$\gamma_o = \gamma_{o(SEVO)} \times SF + \gamma_{o(PROP)} \times (1 - SF) \quad (4)$$

$$\gamma = \gamma_{(SEVO)} \times SF + \gamma_{(PROP)} \times (1 - SF) \quad (5)$$

where SF is the sevoflurane fraction defined in equation (6):

$$SF = \frac{Ce_{SEVO}/Ce50_{SEVO}}{Ce_{SEVO}/Ce50_{SEVO} + Ce_{PROP}/Ce50_{PROP}} \quad (6)$$

Thus, SF=0 if Ce_{SEVO}=0, and SF=1 if Ce_{PROP}=0, and SF is between zero and one for mixtures of sevoflurane and propofol. Note that the final models in the three original studies[10, 12, 13, 17] are equivalent to equations (1)–(6), with the following specific constraints: γ_o =1 in the study by Bouillon and colleagues,[10] and γ(SEVO)=γ(PROP) in Schumacher's study.[12]

The purpose of the model developed from the data is to predict P_{TOL} of random individuals in a population. Similar to the MAC, a P_{TOL} of 50% is the concentration where 50% of a population tolerates laryngoscopy without movement response (TOL). The individual concentration–response of the 'typical subject' was therefore not the focus of the study, and inter-individual variability was not included in the parameter estimation (naive pooling approach).

Selection of the final model and parameter estimation

In the first step, the data from each study were separately fitted to the model [equations (1)–(6)] in order to determine the effect of considering only TOL instead of the whole series of stimuli as previously published. In the second step, a fit of the pooled TOL data was performed. In the pooled fit, the parameters $Ce50_{SEVO}$, $Ce50_{PROP}$, $Ce50_{REMI}$, γ1, and γ_o were estimated assuming that the parameters $Ce50_{REMI}$, γ_o, and γ were identical for the two hypnotics sevoflurane and propofol. Then we tested whether different values for $Ce50_{REMI}$, γ_o, or γ for sevoflurane and propofol significantly improved the fit. In addition, we tested whether γ_o was significantly different from one. The results were accepted as valid only if both minimization and covariance steps were successful, unless stated otherwise.

The model parameters were estimated using NONMEM 7.2.0 (Icon Development Solutions, Hanover, MD, USA), using the Laplace method. The software was installed on a GNU Fortran 95 compiler (http://gcc.gnu.org) with Windows XP operating system (Microsoft, Redmond, WA, USA). PLT Tools (PLTsoft, San Francisco, CA, USA) was used as graphical user interface.

To determine the final model, non-parametric 95% confidence intervals (CIs) were calculated, using a bootstrap analysis based on 2000 sets, stratified according to the original studies. Assuming a χ2 distribution with one degree of freedom, an improvement of the objective function value of 3.84, corresponding to a value of P<0.05, was considered significant.

The P_{TOL} was calculated from equation (1) and NSRI from equation (7):

$$NSRI = \frac{100}{1 + \left(\frac{P_{TOL}}{1 - P_{TOL}}\right)^{s}} \quad (7)$$

where s is a constant (s=0.63093).

For further information on the transformation of P_{TOL} to NSRI, see Supplementary File 2.

Model evaluation

The data of responders and non-responders were plotted together with the 50 and 90% isoboles, derived from the original models,[10, 12, 13, 17] and the final model for visual inspection of the goodness of fit. Additionally, we plotted the observed P_{TOL} against the P_{TOL} predicted by all models to compare the ability of the final model for P_{TOL} with the previously published models. The observed P_{TOL} was obtained from the raw data according to the following procedure. For each observation (response or no response to laryngoscopy), the predicted P_{TOL} was calculated from the effect-site concentrations and model parameters (Table 1) using equations (1) and (2). Then the predicted P_{TOL} of each observation and the related true response (0 or 1) were sorted with increasing value of predicted P_{TOL}. The observed P_{TOL} was defined as the average of the response of the index observation and the next 10 observations with a lower and a higher predicted P_{TOL}. The observed P_{TOL} is thus a moving average over 21 observations, where the missing values at the lower and upper end were omitted. The resulting plots allow a visual inspection of the goodness of fit, as shown in Supplementary File 3. The mean absolute prediction error (MAPE) was calculated as the mean of the absolute value of the difference between the observed and predicted P_{TOL}. For clarification to the reader, the 'observed P_{TOL}' is used only for this specific model validation. Otherwise in this work, 'P_{TOL}' always refers to the 'predicted P_{TOL}'.

In a second validation, we used the raw data of two original studies for parameter estimation and the raw data of the third study for model validation, as shown in the Supplementary File 4.

Assessment of prediction probability

The prediction probability (P_K) is based on multiple comparisons of two data points from the total data set, to investigate the degree of association between each predictor and the observed tolerance. A P_K value of 0.5 implies no association, thus a poor prediction probability; a value of one implies complete association, thus an excellent prediction probability.[25, 26]

We used P_K to assess the performance of predicted P_{TOL}, its derivative, NSRI, and the observed BIS, SE, RE, CVI, and SPI to predict TOL. For comparison, the P_K values of the single drug concentrations (Ce_{SEVO}, Ce_{PROP}, and Ce_{REMI}) were also determined. Using single drug concentrations as estimates of the likelihood of tolerance does not take into account the effect of simultaneously administered drugs; therefore, we hypothesized that they are less accurate than the predicted P_{TOL} as a result of this limitation.

The drug concentrations, their related variables, and the monitor records immediately before the stimulus series were used as independent variables to predict the response.

To ensure that the predicted P_{TOL} and its derivative, NSRI, are independent of the observed P_{TOL}, the calculation of P_K for P_{TOL} and NSRI was performed by a two-fold cross-validation procedure. The total data set was divided into two subsets, each containing 60 patients, randomly drawn from the propofol–remifentanil[10] (10 patients), sevoflurane–propofol[12] (30 patients), and sevoflurane–remifentanil[13] (20 patients) studies. In each subset, a population interaction model was modelled and used for calculating P_{TOL} and NSRI in the other subgroup. The parameter estimates for calculating P_{TOL} and NSRI from one subgroup were thus used to validate the prediction in the other subgroup.

Bootstrapping (1000 replicates) was used to determine 95% CIs of the P_K values for each predictor and also the difference between the P_K values of each combination of two predictors. Significance was achieved if the 95% CI of the difference did not include zero ($p<0.05$).

All P_K calculations were performed in Excel 2003 (Microsoft) using VBA macros.

Statistical analysis

In all patients, we were able to compare the predictive performance of predicted P_{TOL}, NSRI, Ce_{SEVO}, Ce_{PROP}, Ce_{REMI}, and BIS to predict TOL (P_K performance comparison 1). In data obtained from the sevoflurane–propofol and the sevoflurane–remifentanil studies, SE and RE were additionally available as predictors (P_K performance comparison 2). In the data obtained from the sevoflurane– remifentanil study, SPI and CVI were also evaluated, as predictors of TOL (P_K performance comparison 3). Results of each performance comparison should be seen as a separate test of performance because the data sets are different.

Statistical significance is set to $P<0.05$ unless stated otherwise. All model parameters are reported as typical values with standard error within parentheses. Clinical data are given as mean and standard deviation or as median and range, when appropriate.

Table 1. Comparison of model parameters of tolerance of laryngoscopy from three studies[10, 12, 13]

	Propofol–remifentanil (Bouillon et al.)		Sevoflurane–propofol (Schumacher et al.)		Sevoflurane–remifentanil (Heyse et al.)		Pooled data
Number of patients	20		60		40		120
Number of observations	95		274		152		521
	Published	Reanalysis	Published	Reanalysis	Published	Reanalysis	Reanalysis
$Ce50_{SEVO}$ (vol%)	-	-	2.83 (0.19)	2.76 (0.19)	2.00 (0.15)	2.11 (0.20)	2.59 (0.13) [2.36-2.91]
$Ce50_{PROP}$ (μg ml^{-1})	8.48 (1.98)	7.81 (1.76)	6.55 (0.51)	7.24 (0.60)	-	-	7.58 (0.49) [6.71-8.84]
$Ce50_{REMI}$ (ng ml^{-1})	1.16 (0.48)	1.31 (0.57)	-	-	1.69 (0.35)	1.91 (0.32)	1.36 (0.15) [1.06-1.67]
SEVO/PROP ratio	-	-	0.43*	0.381*	-	-	0.342*
γ	3.46 (0.83)	3.85 (1.10) [2.54-9.45]	17.6 (2.69)†	5.70 (0.69)‡ [4.56-7.51]	7.41 (0.86)	5.82 (0.97) [4.46-9.39]	5.22 (0.52)‡ [4.22-6.51]
$γ_o$	1¶	1¶	-	-	0.718 (0.085)	1¶	1¶
IIV ($Ce50_{SEVO}$)	-	-	32%	||	20%	||	||
IIV ($Ce50_{PROP}$)	§	||	31%	||	-	-	||
IIV ($Ce50_{REMI}$)	§	||	-	-	§	||	||

Pooled data are observations from all three studies. Typical values (standard error) [95% confidence interval] as published, from reanalysis using laryngoscopy data only, and from reanalysis of the pooled laryngoscopy data.

IIV = inter-individual variability; SEVO/PROP ratio (vol% ml $μg^{-1}$)=$Ce50_{SEVO}$/$Ce50_{PROP}$. $Ce50_{SEVO}$, $Ce50_{PROP}$ = effect-site concentrations of sevoflurane and propofol, respectively, resulting in P_{TOL}=0.5 if given alone; $Ce50_{REMI}$ = effect-site concentration of remifentanil, resulting in an apparent decrease of the $Ce50_{SEVO}$ and $Ce50_{PROP}$ by 50%; γ = slope parameter of the concentration-effect relationship of sevoflurane and propofol; $γ_o$ = slope parameter of the concentration-effect relationship of the opioid. *Calculated from $Ce50_{SEVO}$/$Ce50_{PROP}$. †Assumed to be equal for sevoflurane and propofol. ‡Not significantly different for sevoflurane and propofol. ¶Not significantly different from one. §Not significantly different from 0. ||Inter-individual variability was not included in the analysis

Results

Study population

The characteristics of the populations of the three studies were comparable. The mean (range) weight was 69 (50–120), 66 (50– 102), and 64 (50–103) kg in the propofol–remifentanil,[10] the sevoflurane–propofol,[12] and the sevoflurane–remifentanil[13] trial, respectively. The mean height was 169 (155–184), 172 (150– 190), and 172 (157–186) cm, the mean age 34 (20–43), 30 (18–58), and 26 (18–54) yr, and the gender ratio (female/male) 10/10, 33/27, and 26/14, respectively.

Common response surface of sevoflurane, propofol, and remifentanil

The results of the reanalysis of the three studies by separate and pooled analysis of the laryngoscopy data are summarized in Table 1, together with the results reported in the original papers. The separate reanalysis of each study gave slightly different results from those reported in the original paper, because only the laryngoscopy data were included and because inter-individual variation of the parameter estimates was not included in our analysis.

In the pooled analysis of the laryngoscopy data from the three studies, we could not confirm the hypothesis that $Ce50_{REMI}$ and γ are different for sevoflurane and propofol. In addition, γ_o was not significantly different from one. When the $Ce50_{REMI}$ was allowed to vary between sevoflurane and propofol, the parameter estimates were 1.37 and 1.33 ng ml^{-1}, respectively, with an 'improvement' of the NONMEM objective function of 0.018. When γ was allowed to vary between sevoflurane and propofol, the parameter estimates (standard error) were 5.55 (0.74) and 4.71 (0.87), respectively, with an improvement of the NONMEM objective function of 0.420. As a result, the data of the three studies can be well described with only four model parameters ($Ce50_{SEVO}$, $Ce50_{PROP}$, $Ce50_{REMI}$, and γ), with good precision (i.e. the standard error values were smaller than in the original papers and in the separate analysis; Table 1). Equation (2) may therefore be simplified to:

$$U = \left(\frac{Ce_{SEVO}}{Ce50_{SEVO}} + \frac{Ce_{PROP}}{Ce50_{PROP}}\right) \times \left(1 + \frac{Ce_{REMI}}{Ce50_{REMI}}\right) \quad (8)$$

also known as the reduced Greco model.[7, 17] Equation (8) is thus the final model of the combined effect of sevoflurane, propofol, and remifentanil.

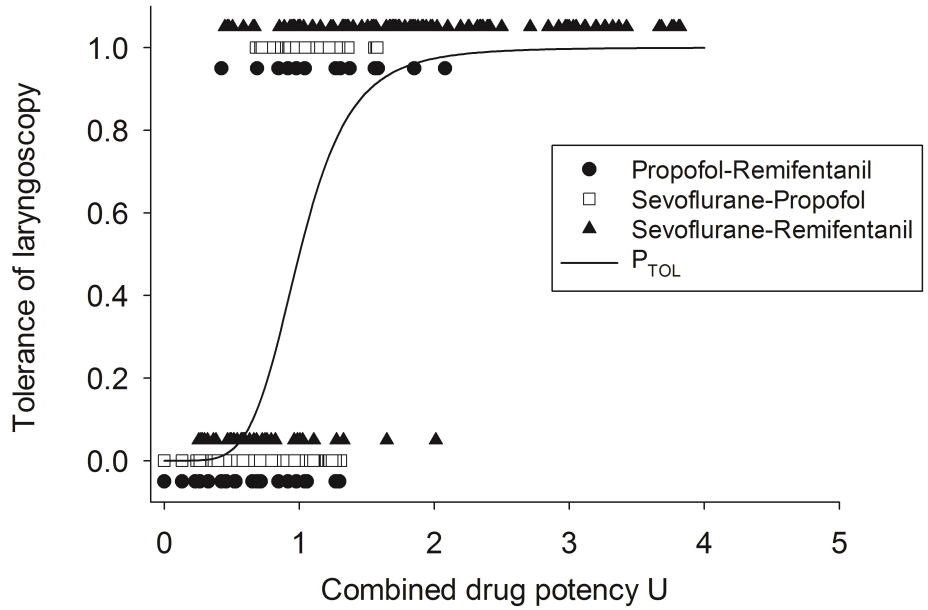

Figure 1. The observed movement response and non-response to laryngoscopy is presented as a function of the total potency of the drug combination expressed as 'U' [equation (8)]. A value of one denotes tolerance of laryngoscopy (no movement); a value of zero denotes movement response. Data are from the propofol–remifentanil study,[10] sevoflurane–propofol study,[12] and sevoflurane–remifentanil study.[13] The sigmoid concentration–response curve represents equation (1) with the final model.

The CIs calculated from the bootstrap analysis are presented in Table 1. In order to calculate P_{TOL} using equation (1), U was calculated using equation (8) by entering the parameter estimates of the pooled analysis in the formula (Table 1). Figure 1 shows the presence or absence of TOL as a function of U.

Model evaluation

The 50 and 90% TOL isoboles and the raw data of responders and non-responders are shown in Figure 2A-C. The MAPE was calculated for the following three models: (i) a model as published (i.e. computed from the raw data of each single study including the response to all applied stimuli); (ii) a model reanalysed from the data of each single study including the response to laryngoscopy only; and (iii) the final model computed from the pooled data of all three studies including response to laryngoscopy only. For propofol–remifentanil, the MAPEs of the predicted P_{TOL} of the resulting models were 1.8, 2.3, and 3.9%, respectively. For sevoflurane–propofol, the MAPEs were 14.6, 6.8, and 6.9%, and for sevoflurane–remifentanil, the MAPEs were 5.3, 3.0, and 4.1%, respectively. Thus, the MAPE values of the triple interaction model are close to those of the separate reanalysis

of each study and are lower than those obtained from the published models, except for propofol–remifentanil, where MAPE is low for all models. The reason for the rather large MAPE for the sevoflurane–propofol data is visible in Figure 1. In the absence of remifentanil, the maximal U was only 1.56, which was only little above the range of U where responders and non-responders were observed. A plot of observed vs predicted P_{TOL} allowing for a visual inspection of the goodness of fit is presented in Supplementary File 3. The result of the cross-validation based on parameter estimation from the raw data of two studies and validation with the raw data of the third study is presented in Supplementary File 4.

Prediction probability

Table 2 shows the results for P_K to assess the performance of P_{TOL}, its derivative, NSRI, and the observed BIS, SE, RE, CVI, and SPI to predict TOL. For comparison, the P_K values of the single drug concentrations (Ce_{SEVO}, Ce_{PROP}, and Ce_{REMI})were also determined and are shown in Table 2.

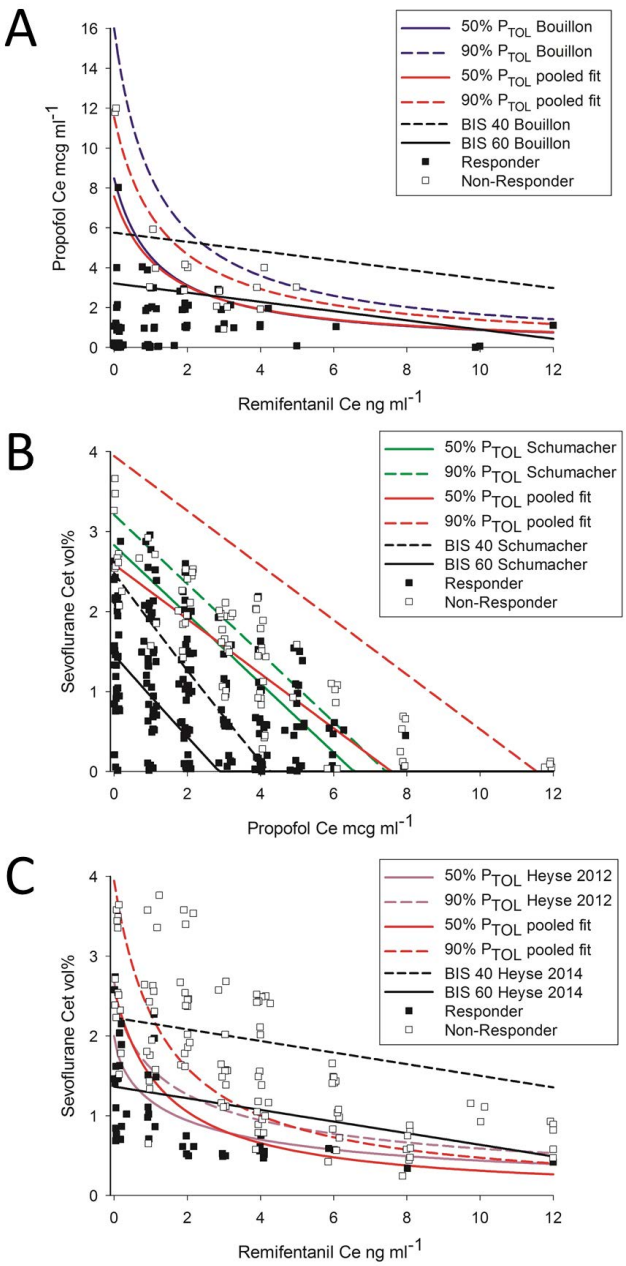

Figure 2. Goodness-of-fit plot of the tolerance of laryngoscopy isoboles (P_{TOL}) for propofol–remifentanil (a), sevoflurane–propofol (b), and sevoflurane–remifentanil (c) combinations. Non-responders and responders to laryngoscopy are indicated. To avoid superposition of multiple responses at the same point, concentration values were slightly modified by adding a random value with mean zero and SD 0.1. The 50% (continuous lines) and 90% (dashed lines) isoboles calculated with the original models (blue, green, purple, respectively)[10, 12, 13] and the new interaction model (green; Table 1) are plotted with the BIS 40 (pink dashed line) and BIS 60 (pink continous line) isoboles according to the original response surface model.[10, 12, 17] For remifentanil concentrations >2 ng ml^{-1}, the 90% P_{TOL} isobole is between the BIS 40 and BIS 60 isobole, which corresponds to clinical dosing practice. The additive isobole for the sevoflurane and propofol interaction (straight lines) are well above the BIS 40 isobole, which reflects the fact that the EEG-suppressing effect of the two hypnotic drugs is much stronger than the potency to suppress the response to laryngoscopy.

Ce = effect-site concentration; Cet = end-tidal concentration; BIS = bispectral index.

Table 2. Prediction probabilities (P_K) of all studied measures to detect tolerance of laryngoscopy.

Ce_{SEVO}	Ce_{PROP}	Ce_{REMI}	BIS	SE	RE	CVI	SPI	P_{TOL} & NSRI
Whole population (n=120)								
0.73* (0.68-0.77)	0.46 (0.41-0.51)	0.67* (0.61-0.72)	0.71* (0.66-0.77)	-	-	-	-	**0.92**† (0.90-0.94)
Subgroups sevoflurane–propofol and sevoflurane–remifentanil (n=100)								
0.71* (0.66-0.76)	0.41 (0.35-0.47)	0.70* (0.65-0.74)	0.65* (0.59-0.71)	0.69* (0.63-0.75)	0.69* (0.63-0.75)	-	-	**0.92**‡ (0.89-0.94)
Subgroup sevoflurane–remifentanil (n=40)								
0.76¶ (0.68-0.84)	-	0.72 (0.64-0.80)	0.78¶ (0.69-0.86)	0.78¶ (0.68-0.86)	0.77¶ (0.67-0.86)	0.74 (0.62-0.84)	0.57 (0.48-0.69)	**0.95**§ (0.91-0.98)

Numbers are prediction probabilities according to Smith et al.[25] estimated from the data (95% confidence intervals estimated from a bootstrap analysis). The best predictor for each stimulus is highlighted (bold).

P_{TOL} = 'predicted P_{TOL}' calculated from the effect-site concentrations and model parameters; Ce_{SEVO}, Ce_{PROP}, Ce_{REMI} = effect-site concentrations of sevoflurane, propofol and remifentanil, respectively; BIS = bispectral index; SE = state entropy; RE = response entropy; CVI = composite variability index; SPI = surgical pleth index.

*$p < 0.05$ compared with Ce_{PROP}; †$p < 0.05$ compared with Ce_{SEVO}, Ce_{PROP}, Ce_{REMI} and BIS; ‡$p < 0.05$ compared with Ce_{SEVO}, Ce_{PROP}, Ce_{REMI}, BIS, SE and RE; ¶$p < 0.05$ compared with SPI; §$p < 0.05$ compared with Ce_{SEVO}, Ce_{REMI}, BIS, SE, RE, CVI and SPI

Discussion

With a pooled analysis of data from three previously published studies of similar design on dual drug interactions, a triple interaction model was developed to describe the anaesthetic potency of combinations of sevoflurane, propofol, and remifentanil in terms of P_{TOL} and its derivative, the NSRI. The model that fits the data best can be interpreted as an extension of the hierarchical hypnotic–opioid interaction model published previously.[10, 12, 13, 23] We found that the interaction between sevoflurane and propofol is additive when their concentrations are normalized to their respective effect-site concentration inducing TOL in 50% of the population. This is a confirmation of earlier work.[12, 27, 28] Remifentanil has a strong but equally synergistic effect on sevoflurane and propofol. In contrast to original publications,[10, 12, 13] the pooled analysis did not support different Ce50 values for remifentanil nor different slope factors for sevoflurane and propofol. This is not surprising, because the standard error values of both parameters were ~20% in the study by Heyse and colleagues[13] and ~40% in the study by Bouillon and colleagues[10] for $Ce50_{REMI}$, and the 95% CIs for the slopes were overlapping in all three studies. As such, our common $Ce50_{REMI}$ and slope are within the standard error of the values published previously (Table 1).

Various model validation methods were applied and proved that our final model describes the data accurately and represents clinical reality. In Figure 2, the 50 and 90% P_{TOL} isoboles calculated with the triple interaction model and with the previous two-drug interaction model.[10, 12, 13] are plotted together with the raw data from the three studies to demonstrate the goodness of fit. Additionally, the clinically used BIS 40 and BIS 60 isoboles as predicted from previous studies are shown.[10, 17] The difference in the shape of the isoboles is related to the difference in Ce50 values and the different slopes between current and previously published models (Table 1). For remifentanil concentrations >2 ng ml^{-1}, the 90% P_{TOL} isobole is between the BIS 40 and BIS 60 isobole, which corresponds to clinical dosing practice. This is consistent with previous data on the sevoflurane–remifentanil interaction by Manyam and colleagues,[29] who demonstrated that the 95% isobole for suppressing response to tetanic stimulation was between the BIS 60 and 70 isobole at remifentanil concentrations greater than ~3 ng ml^{-1}. The additive 50 and 90% isoboles for the sevoflurane and propofol interaction (straight lines) are well above the BIS 40 isobole, which reflects the fact that the EEG-suppressing effect of the two hypnotic drugs is much stronger than the potency to suppress the response to laryngoscopy.

In a general sense, P_{TOL} can be considered an extension of the clinically applied MAC concept.[6] For the first time, the potency of inhaled and i.v. hypnotic drugs can be

compared uniformly. Using our triple interaction model, the potency of any combination of sevoflurane, propofol, and remifentanil can be expressed as P_{TOL} or its derivative, NSRI. For example, a Ce_{REMI} of 3 ng ml^{-1} combined with either a Ce_{PROP} of 3 µg ml^{-1} or a Ce_{SEVO} of 1.03 vol% will yield a P_{TOL} of 0.7 or an NSRI of 31 and are thus considered equipotent. A more detailed clinical application is shown in Supplementary File 5. In a simulated anaesthesia induction with a bolus of propofol and a remifentanil target-controlled infusion, the time when sevoflurane needs to be administered depends on the size of the propofol bolus and the remifentanil concentration. The interaction model allows compensation for the decay of the propofol effect-site concentration by increasing the effect-site concentration of sevoflurane, in order to maintain a predefined total potency of the drugs in terms of P_{TOL}.

In the population, TOL was best predicted by P_{TOL} and NSRI (Table 2), whereas Ce_{SEVO}, Ce_{PROP}, Ce_{REMI}, and BIS were intermediate (0.7) and Ce_{PROP} was a poor predictor of TOL. In data obtained from the sevoflurane–propofol and the sevoflurane–remifentanil studies, SE and RE were also available and showed a moderate predictive accuracy, similar to BIS. In the data obtained from the sevoflurane–remifentanil study, CVI was found to be a moderately accurate predictor of TOL. The SPI was not able to predict TOL. Both P_{TOL} and NSRI outperformed the other measures in both sub-analyses.

A limitation of our study is that our triple interaction model is based on pooled data from three independently performed two- drug interaction studies, so no patient was given a combination of all three drugs. As a result, our model neither detects nor excludes a superimposed triple interaction in patients who receive all three drugs simultaneously. In a large triple interaction study on midazolam, propofol, and alfentanil, Minto and colleagues[24] found significant synergistic interactions of each pair of these compounds but no additional triple interaction when three drugs were combined. A significant and relevant triple interaction does not therefore seem likely, considering the additive interaction between sevoflurane and propofol, and the strong and similar synergistic interaction of remifentanil with both hypnotic drugs. Our model does produce predictions about P_{TOL} when all three drugs are administered simultaneously, and these predictions are open to hypothesis testing. Outside of our model, these predictions are not available because no other triple interaction model exists for these drugs in current literature.

In conclusion, our response surface interaction model allows estimation of the potency of any combination of sevoflurane, propofol, and remifentanil as the probability to tolerate laryngoscopy. The P_{TOL} and its derivative, the NSRI, are good predictors of TOL.

Clinical applicability needs further validation in a prospective study, with surgical and other standardized stimuli.

Supplementary material

Supplementary material is available at British Journal of Anaesthesia online.

References

1. Vanluchene ALG, Struys, M M R F, Heyse BEK, Mortier EP: Spectral entropy measurement of patient responsiveness during propofol and remifentanil. A comparison with the bispectral index. Br J Anaesth 2004; 93: 645-54

2. Vanluchene AL, Vereecke H, Thas O, Mortier EP, Shafer SL, Struys MM: Spectral entropy as an electroencephalographic measure of anesthetic drug effect: a comparison with bispectral index and processed midlatency auditory evoked response. Anesthesiology 2004; 101: 34-42

3. Sahinovic MM, Eleveld DJ, Kalmar AF, Heeremans EH, De Smet T, Seshagiri CV, Absalom AR, Vereecke HEM, Struys, Michel M R F: Accuracy of the composite variability index as a measure of the balance between nociception and antinociception during anesthesia. Anesth Analg 2014; 119: 288-301

4. Huiku M, Uutela K, van Gils M, Korhonen I, Kymäläinen M, Meriläinen P, Paloheimo M, Rantanen M, Takala P, Viertiö-Oja H, Yli-Hankala A: Assessment of surgical stress during general anaesthesia. Br J Anaesth 2007; 98: 447-55

5. Rantanen M, Yli-Hankala A, van Gils M, Yppärilä-Wolters H, Takala P, Huiku M, Kymäläinen M, Seitsonen E, Korhonen I: Novel multiparameter approach for measurement of nociception at skin incision during general anaesthesia. Br J Anaesth 2006; 96: 367-76

6. Eger EI, Saidman LJ, Brandstater B: Minimum alveolar anesthetic concentration: a standard of anesthetic potency. Anesthesiology 1965; 26: 756-63

7. de Jong RH, Eger EI: MAC expanded: AD50 and AD95 values of common inhalation anesthetics in man. Anesthesiology 1975; 42: 384-9

8. Zbinden AM, Maggiorini M, Petersen-Felix S, Lauber R, Thomson DA, Minder CE: Anesthetic depth defined using multiple noxious stimuli during isoflurane/oxygen anesthesia. I. Motor reactions. Anesthesiology 1994; 80: 253-60

9. Zbinden AM, Petersen-Felix S, Thomson DA: Anesthetic depth defined using multiple noxious stimuli during isoflurane/oxygen anesthesia. II. Hemodynamic responses. Anesthesiology 1994; 80: 261-7

10. Bouillon TW, Bruhn J, Radulescu L, Andresen C, Shafer TJ, Cohane C, Shafer SL: Pharmacodynamic interaction between propofol and remifentanil regarding hypnosis, tolerance of laryngoscopy, bispectral index, and electroencephalographic approximate entropy. Anesthesiology 2004; 100: 1353-72

11. Luginbuhl M, Schumacher PM, Vuilleumier P, Vereecke H, Heyse B, Bouillon TW, Struys MM: Noxious stimulation response index: a novel anesthetic state index based on hypnotic-opioid interaction. Anesthesiology 2010; 112: 872-80

12. Schumacher PM, Dossche J, Mortier EP, Luginbuehl M, Bouillon TW, Struys MM: Response surface modeling of the interaction between propofol and sevoflurane. Anesthesiology 2009; 111: 790-804

13. Heyse B, Proost JH, Schumacher PM, Bouillon TW, Vereecke HE, Eleveld DJ, Luginbuhl M, Struys MM: Sevoflurane remifentanil interaction: comparison of different response surface models. Anesthesiology 2012; 116: 311-23

14. Rampil IJ: A primer for EEG signal processing in anesthesia. Anesthesiology 1998; 89: 980-1002

15. Viertiö-Oja H, Maja V, Särkelä M, Talja P, Tenkanen N, Tolvanen-Laakso H, Paloheimo M, Vakkuri A, Yli-Hankala A, Meriläinen P: Description of the Entropy algorithm as applied in the Datex-Ohmeda S/5 Entropy Module. Acta Anaesthesiol Scand 2004; 48: 154-61

16. Mathews DM, Clark L, Johansen J, Matute E, Seshagiri CV: Increases in electroencephalogram and electromyogram variability are associated with an increased incidence of intraoperative somatic response. Anesth Analg 2012; 114: 759-70

17. Heyse B, Proost JH, Hannivoort LN, Eleveld DJ, Luginbuehl M, Struys, Michel M R F, Vereecke HEM: A response surface model approach for continuous measures of hypnotic and analgesic effect during sevoflurane-remifentanil interaction: quantifying the pharmacodynamic shift evoked by stimulation. Anesthesiology 2014; 120: 1390-9

18. Short TG, Ho TY, Minto CF, Schnider TW, Shafer SL: Efficient trial design for eliciting a pharmacokinetic-pharmacodynamic model-based response surface describing the interaction between two intravenous anesthetic drugs. Anesthesiology 2002; 96: 400-8

19. Schnider TW, Minto CF, Gambus PL, Andresen C, Goodale DB, Shafer SL, Youngs EJ: The influence of method of administration and covariates on the pharmacokinetics of propofol in adult volunteers. Anesthesiology 1998; 88: 1170-82

20. Schnider TW, Minto CF, Shafer SL, Gambus PL, Andresen C, Goodale DB, Youngs EJ: The influence of age on propofol pharmacodynamics. Anesthesiology 1999; 90: 1502-16

21. Minto CF, Schnider TW, Egan TD, Youngs E, Lemmens HJ, Gambus PL, Billard V, Hoke JF, Moore KH, Hermann DJ, Muir KT, Mandema JW, Shafer SL: Influence of age and gender on the pharmacokinetics and pharmacodynamics of remifentanil. I. Model development. Anesthesiology 1997; 86: 10-23

22. Minto CF, Schnider TW, Shafer SL: Pharmacokinetics and pharmacodynamics of remifentanil. II. Model application. Anesthesiology 1997; 86: 24-33

23. Bouillon TW: Hypnotic and opioid anesthetic drug interactions on the CNS, focus on response surface modeling, Handbook of Experimental PharmacologyEdited by Anonymous Germany, 2008, pp 471-87

24. Minto CF, Schnider TW, Short TG, Gregg KM, Gentilini A, Shafer SL: Response surface model for anesthetic drug interactions. Anesthesiology 2000; 92: 1603-16

25. Smith WD, Dutton RC, Smith NT: Measuring the performance of anesthetic depth indicators. Anesthesiology 1996; 84: 38-51

26. Smith WD, Dutton RC, Smith NT: A measure of association for assessing prediction accuracy that is a generalization of non-parametric ROC area. Stat Med 1996; 15: 1199-215

27. Sebel LE, Richardson JE, Singh SP, Bell SV, Jenkins A: Additive effects of sevoflurane and propofol on gamma-aminobutyric acid receptor function. Anesthesiology 2006; 104: 1176-83

28. Harris RS, Lazar O, Johansen JW, Sebel PS: Interaction of propofol and sevoflurane on loss of consciousness and movement to skin incision during general anesthesia. Anesthesiology 2006; 104: 1170-5

29. Manyam SC, Gupta DK, Johnson KB, White JL, Pace NL, Westenskow DR, Egan TD: When is a bispectral index of 60 too low?: Rational processed electroencephalographic targets are dependent on the sedative-opioid ratio. Anesthesiology 2007; 106: 472-83

Chapter 7: Summary, discussion and future perspectives

Summary and discussion

Apart from the ever-continuing development of new anesthetic drugs, advances in anesthetic pharmacology and its application in clinical anesthetic practice have in recent years focused on more accurate titration of anesthesia. This research consists of exploration of the pharmacokinetic (PK) and pharmacodynamic (PD) properties of anesthetic drugs, development of PKPD models, exploration of the interactions between different drugs and modeling these interactions as well. This knowledge and these models can then be used in anesthetic practice through the use of target-controlled infusion (TCI) systems, and interaction drug displays to increase accuracy of (multi-)drug titration. The main aim of this thesis is to contribute to several components of these advancements: the development of PKPD models, complex interaction models using multiple drugs, and also expanding on an interaction parameter which can be used in clinical practice to guide anesthesia.

Chapter 1 provides a basic overview on what is currently known about pharmacokinetics, pharmacodynamics, PK-, PD- and PKPD-modeling, interactions and interaction modeling, and an overview of dexmedetomidine, a drug which is investigated extensively in this thesis.

Chapter 2 starts off at the basis of all modeling, the development of an optimal PK model, as no PD modeling or interaction modeling can be performed without an adequate PK model. In the case of dexmedetomidine, several PK models already exist, but these have several flaws that limit their use in clinical practice. As explained in Chapter 1, a model is only as good as the data which it describes. Several tactics were used to provide optimal conditions for developing a good model: 1) the experiment involved healthy volunteers to exclude drug interactions and comorbidities, 2) the inclusion of a broad range of subject weight, height and age, 3) the use of arterial blood sampling, 4) the use of TCI drug infusion and 5) using simulations before the start of the study to determine the best dosing scheme and sampling times to allow for good estimation of model parameters. We also studied each volunteer twice, which enabled us to investigate whether factors such as stress and ‘uncertainty of the unknown’ in session 1 compared to session 2 influences pharmacokinetics of dexmedetomidine, perhaps through changes in hemodynamics.

This resulted in the development of a three-compartment PK model, with allometric weight scaling on the volumes of all three compartments and elimination clearance. The intercompartmental clearances were found to be better scaled allometrically to the

volumes of their respective compartments, rather than to weight. Age, height and fat-free mass were not found to be covariates for the model.

One problem with compartmental pharmacokinetic modeling for intravenous drugs is that it assumes immediate mixing of a bolus dose in the central compartment. This is however not compatible with reality, as a drug injected in a vein is not immediately mixed in the whole bloodstream, but has to circulate before it is fully mixed, all the while peripheral distribution already takes place (mainly in the lungs as the drug passes through the pulmonary circulation before reaching the arterial sampling site). This process is called front-end kinetics. Avram et al.[1] investigated how to set up a compartmental PK study that will accurately describe front-end kinetics as modeled by a recirculatory model. They found that data collected during and after a brief infusion instead of a bolus may describe front-end kinetics better than a bolus assuming instantaneous mixing and no distribution at t=0, combined with early sampling. This can prevent extensive back-extrapolation to t=0 and helps to correctly determine the central compartment volume. Very early sampling may however introduce inaccuracies due to incomplete mixing of the drug in the blood stream. In our study, by using a priori simulations to determine the best dosing scheme and sampling times, we were able to determine that an initial short infusion and early sampling after this initial infusion would enable us to optimally describe the volume of the central compartment, V1. This likely enabled us to describe front-end kinetics more accurately than standard dosing would.

An interesting finding in Chapter 2 was that the variability between sessions (interoccasion variability) was greater than interindividual variability for the central compartment volume V1. We did not find a systematic change between session 1 and session 2, but the greater interoccasion variability does suggest that unknown factors changing over time have a greater influence on pharmacokinetics of dexmedetomidine than differences between individuals. What these factors are, can only be guessed at.

Chapters 3 and 4 expand on the pharmacokinetic model that was developed in chapter 2, by adding several pharmacodynamic profiles to the model, resulting in PKPD models of both sedative and hemodynamic effects. These are the first PKPD models that have been developed for dexmedetomidine.

Chapter 3 focusses on the sedative effects, and describes two pharmacodynamic models, which are linked to the PK model through the use of two effect-site compartments each with their own equilibration rate constant. The first model is based on the effect of dexmedetomidine on the bispectral index (BIS), an EEG-derived hypnotic monitor, the second model is based on the Modified Observer's Assessment of

Alertness/Sedation score (MOAA/S), a score which assesses the level of sedation based on responses to verbal, tactile and noxious stimuli.

The unique sedative effects of dexmedetomidine in maintaining rousability provided its challenges. Not only was this the case for 'planned' stimuli, when MOAA/S scores were assessed, but also other uncontrollable stimuli, both external (sudden loud sounds filtering through the headset) and internal (thirst, pruritus etc.). As a result of these stimuli, the BIS would increase, and as the study subject settled down again, the BIS would slowly decrease again. A second form of (continuous) stimulation performed during the study, was the presence or absence of recorded operating room background noise.

The effect of dexmedetomidine on BIS is best described by an Emax model, with a $C50_{BIS}$ of 2.63 ng/ml and a rather slow effect-site equilibration rate ($ke0_{BIS}$ of 0.120 min^{-1}; T½ 5.8 min). We were able to implement the phenomenon of increased BIS due to sudden stimulation by introducing a stimulated and unstimulated state, where a subject would immediately go into a stimulated state after MOAA/S scoring with a 2.7-fold increase in $C50_{BIS}$, and over time revert back to an unstimulated state when no further stimulation took place, with a half-time of 5.3 minutes. We did not find an effect of the continuous background noise on the BIS model, neither did we find other covariates for the model (inter-occasion variability, age, weight, height, gender).

The MOAA/S model is different from most models, because the MOAA/S score is not dichotomous like the probability of tolerance of laryngoscopy, nor is it a continuous scale such as the BIS, MAP or HR, but an ordinal parameter. Therefore, we used logit transformations and assessed cumulative probabilities (i.e. probability of MOAA/S ≤ 3). The effect of dexmedetomidine on MOAA/S is best described by an E_{max} model, with a $C50_{MOAA/S}$ of 0.428 ng/ml and a $ke0_{MOAA/S}$ of 0.0428 min^{-1} (T½ 16.2 min). Contrary to the BIS model, we found that adding effects of a previous stimulation only minimally improved the model for MOAA/S, without increase in predictive value and with increased numerical difficulties during modeling; therefore, we did not include this in the model. As for the BIS-model, inter-occasion variability, age, weight, height and gender were not significant covariates.

In contrast, however, we found that background noise did influence the MOAA/S model. Whereas our initial hypothesis was that the presence of background noise would lessen the effect of dexmedetomidine by increasing the C50 (the noise would keep the volunteer 'more awake'), we found that noise increased the effect of dexmedetomidine, and the C50 was increased for the sessions where background noise was absent. A possible theory is that the auditory stimuli (volunteer's name being spoken) produce a

greater change in relative volume against a silent environment than against the presence of background noise, thereby causing the subject to be more responsive. However, we found that the difference remained for noxious stimuli, with a difference in frequency of MOAA/S 0 (no response to trapezius squeeze), suggesting that other mechanisms may modulate the effect of background noise on responsiveness during dexmedetomidine sedation.

An interesting finding was that the probability of observing an MOAA/S score of 1 (the subject responds to a noxious stimulus but not to a non-noxious (tactile) or verbal stimulus) was very small. The model thus shows that subjects are far more likely to either respond to a non-noxious stimulus (MOAA/S ≥ 2) or tolerate a noxious stimulus (MOAA/S = 0). During the study, a MOAA/S score of 1 was rare (about 10% of all observations), and we commonly observed a subject progressing from MOAA/S 2 (response to shake and shout) directly to a MOAA/S 0 (no response to trapezius squeeze) with increasing dexmedetomidine concentrations. Clinically, this would indicate that although subjects sedated with dexmedetomidine remain rousable at relatively higher doses, once they no longer respond to verbal or tactile stimuli, they are unlikely to respond to noxious stimuli.

In contrast to PD models for other anesthetic drugs such as propofol[2] and remifentanil[3], in our study age was not found to be a significant covariate for the relationship between dexmedetomidine concentration and either BIS or MOAA/S. By using age-stratified inclusion of volunteers, we assumed a high a priori chance of identifying whether age is a covariate for the sedative effects of dexmedetomidine. The fact that age was not a significant covariate in our model, may be due to the small number of subjects, or perhaps there truly is no effect of age. It might be that whereas the neuronal pathways that mediate sedation caused by propofol and other sedatives are influenced by age-related factors, the different pathways mediating dexmedetomidine-induced sedation are not.

Chapter 4 focusses on modeling the hemodynamic side effects of dexmedetomidine, namely mean arterial pressure (MAP) and heart rate (HR).

For the MAP model, we were able to model the biphasic effect through the use of two E_{max} models with two different effect-sites for hypotension and hypertension. The effect-site for hypertension has a faster k_{e0} and a higher C50 and E_{max} than the effect-site for hypotension. This allows for a mathematical explanation of the clinical observation that a bolus or rapid infusion of dexmedetomidine results initially in a short hypertensive phase, changing to hypotension after a few minutes, as well as the biphasic effect in that at higher concentrations, the hypertensive effect is stronger than the

hypotensive effect. This is also compatible with the physiologic substrate of the biphasic effect: the hypertensive effect is mainly through receptors in the arterial smooth muscle cells, while the hypotensive effect is partly through receptor activation in the vascular endothelium, and in a large part by activation of adrenoceptors in the central nervous system. It is likely that the effect-site for hypertension rises faster than the concentration in the central nervous system. The 'turning point' was reached at an average concentration of 2.4 ng/ml, where the MAP returned to baseline, and at higher concentrations changed to hypertension. There was a correlation between the baseline MAP and size of effect on hypotension, where subjects with higher baseline MAP experienced a more profound hypotensive effect. The maximum hypertensive effect was 43% above baseline. The only covariate found was an effect of age on baseline MAP, where MAP increased by 5.2% for every 10 years. No other covariates (weight, height, gender) were found for the MAP model.

Our model also describes the lengthy duration of hypotension after termination of dexmedetomidine infusion adequately. It is known from previous publications[4, 5] that the hypotensive effects persist for up to 4-5.5 hours after the start of infusion. Extrapolation of our model, as seen in Table 2 of Chapter 4 shows that it could take up to 10 hours for MAP to return to within 5% of baseline. As there are no studies, including our own, with a follow-up beyond 5-6 hours after termination of dexmedetomidine infusion, the time to recovery of MAP remains to be validated.

Applying an E_{max} or sigmoid E_{max} model for HR resulted in numerical instability. The use of a non-linear effect model according to Schoemaker[6] resulted in better goodness of fit than a linear model. The Schoemaker model stabilizes the modeling when data near E_{max} is sparse, as is the case in this study, where we found a lower boundary of HR of 22.5 bpm while HR in our subjects did not reach below 40, as that was a criterium for stopping dexmedetomidine infusion. The effect-site equilibration rate constant was relatively high, indicating faster changes in heart rate with changes in plasma concentration. None of the possible covariates, age, weight, height and gender, were found to be significant covariates.

Chapter 4 also focusses in part on the combined PKPD of sedation and hemodynamics by demonstrating through the use of simulations – which are available in the online supplement – how certain dosing strategies affect dexmedetomidine plasma concentrations, BIS, MOAA/S scores, MAP and HR. This simulation can help to determine the best dosing strategies, considering the need for fast clinical sedative effect, without compromising safety in the form of hemodynamic problems. The simulations also allow for different infusion rates, to determine the effects on mainly heart rate and

hypertension of rapid infusions or bolus doses. Although our model does show an initial hypertension from rapid infusions as is compatible with clinical data, it is still an extrapolation from the study, as we only used 6 – 10 µg kg^{-1} h^{-1} as maximum infusion rates, and these simulations should be considered with that in mind.

Chapter 5 moves away from single-drug modeling, and advances into the realm of drug interaction modeling. The study is an extension of a previous sevoflurane-remifentanil interaction study. In the initial study, the interaction between these two drugs on the tolerance of several stimuli (both non-noxious and noxious) was assessed. In Chapter 5, the effect of the drug combinations on continuous parameters was investigated. The continuous parameters consist of 3 measurements marketed as (mainly) hypnotic monitors, namely the electroencephalograph (EEG) derived bispectral index (BIS), state entropy (SE) and response entropy (RE), and 2 marketed as (mainly) analgesic monitors, the composite variability index (CVI) and the surgical pleth index (SPI). CVI is calculated from BIS variability and frontal electromyographic activity, whereas the SPI is derived from plethysmographic pulse wave characteristics and heart rate variability.

Response surface modeling methodology was used to describe the interaction between sevoflurane and remifentanil for each continuous parameter. For this, several different interaction models were explored, as explained in detail in the Appendix of the original interaction study by Heyse et al.[7], and in short in Chapter 1 of this thesis. These models result in a parameter U, which is the combined potency of both drugs, normalized to their own C50s, and may be seen as a 'virtual' new drug with concentration U. U can then be used to describe the concentration-effect relationship.

For the three hypnotic monitors, BIS, SE and RE, the interaction was found to be additive, and best described by the Greco model, and the effect was best described by a sigmoid E_{max} model. The C50s for remifentanil for each of these monitors was high, especially in the case of BIS, where the C50 exceeded the concentrations used in the study (27.3 ng/ml). This suggests that EEG, in particular BIS, is only minimally influenced by remifentanil. Similar C50s for sevoflurane suggest that all three parameters are equally sensitive for sevoflurane. For CVI, the interaction was found to be moderately synergistic, and best described by the reduced Greco model. The effect was also best described by a sigmoid E_{max} model. This model had large variability and a poorer fit than the hypnotic monitors. SPI modeling did not result in reliable parameters, and plotting of the SPI with sevoflurane and remifentanil concentrations showed no reliable influence of either drug on SPI.

The effect of (noxious) stimulation, namely laryngoscopy, on the continuous parameters was also assessed, and the same modeling techniques were applied to the post-

stimulation data, to explore changes in model parameters after noxious stimulation. For the BIS, SE and RE, all model parameters were found to be similar, except for the $C50_{SEVO}$, which was consistently higher post-stimulation, by an average of 0.3 vol%. In contrast, for CVI, the $C50_{SEVO}$ was the only parameter that remained the same post-stimulation, whereas $C50_{REMI}$ decreased, and γ and E_0 increased. The already large variability of CVI increased further after stimulation. The increased slope and larger difference between baseline effect and maximal effect post-stimulation suggest that for CVI, noxious stimulation is necessary to be able to assess the balance between nociception and antinociception. SPI post-stimulation remained the same, and like pre-stimulation, modeling did not provide reliable results.

Whereas the interaction between sevoflurane and remifentanil is known to be synergistic for clinical dichotomous endpoints such as tolerance of noxious stimuli, this study shows the interaction on continuous hypnotic monitors to be additive, with only a small effect of remifentanil on these parameters. This is consistent with previous findings, not only on the interaction between sevoflurane and opioids[8], but also between propofol and opioids.[9, 10] This may explain why EEG-derived parameters in general are poor predictors of these clinical dichotomous endpoints when hypnotic-opioid combinations are used.

Chapter 6 investigates the triple interaction between sevoflurane, propofol and remifentanil on the tolerance of laryngoscopy. It combines three previous two-drug interaction studies, propofol-remifantanil[10], propofol-sevoflurane[11] and sevoflurane-remifentanil.[7]

Based on the findings in the original three studies (propofol-remifentanil: synergistic interaction, best described by Hierarchical model; propofol-sevoflurane: additive interaction, best described by Greco model; sevoflurane-remifentanil: synergistic interaction, best described by Hierarchical model), the hypothesis was that the triple interaction would be best described by a Hierarchical model between hypnotics (propofol and sevoflurane) and opioids (remifentanil), and an additive model between the two hypnotics:

$$U = \left(\frac{C_{SEVO}}{C50_{SEVO}} + \frac{C_{PROP}}{C50_{PROP}}\right) \times \left(1 + \left(\frac{C_{REMI}}{C50_{REMI}}\right)^{\gamma_o}\right) \quad (1)$$

where U is the combined potency of the drugs, normalized to their respective C50s and γ_o is the slope of the opioid concentration-effect curve. The effect, probability of tolerance of laryngoscopy, or P_{TOL} was calculated as follows:

$$P_{TOL} = \frac{U^{\gamma}}{1 + U^{\gamma}} \quad (2)$$

where, γ is the slope parameter, or steepness of the concentration-effect relationship for the combined drug effect. Because $C50_{REMI}$, γ_o and γ differed in the models between the propofol-remifentanil and sevoflurane-remifentanil interaction, we assumed a priori that this would also differ in the model, where the 'total' $C50_{REMI}$, γ_o and γ would be a combination of the values for propofol and sevoflurane, depending on the propofol:sevoflurane ratio.

In the final triple interaction model, $C50_{REMI}$ and γ for sevoflurane and propofol were not found to be significantly different from each other. Also, γ_o was found not to be significantly different from 1, which means the model can be simplified to a reduced Greco model with an additive interaction between sevoflurane and propofol:

$$U = \left(\frac{C_{SEVO}}{C50_{SEVO}} + \frac{C_{PROP}}{C50_{PROP}}\right) \times \left(1 + \frac{C_{RMI}}{C50_{REMI}}\right) \quad (3)$$

Chapter 6 also reintroduces the Noxious Stimulation Response Index (NSRI), which has previously been published by Luginbühl et al.[12] The NSRI as published by Luginbühl was based on a propofol-remifentanil interaction study by Struys et al.[13] and in our study, we used the triple interaction study as basis for the new NSRI. Contrary to most parameters used in clinical practice for the assessment of anesthesia, NSRI is not a measured but a calculated parameter. It is a transformation of P_{TOL} (Eq. 2):

$$NSRI = \frac{100}{1 + \left(\frac{P_{TOL}}{1 - P_{TOL}}\right)^{s}} \quad (4)$$

where s = 0.63093, so that a P_{TOL} of 0.5 corresponds with an NSRI of 50 and a P_{TOL} of 0.9 results in an NSRI of 20.

The NSRI is scaled from 100 to 0, where at 100 there is no drug effect, and the patient is very likely to be awake (barring other circumstances inducing reduced consciousness), and 0 indicates profound drug effect, with near 0 probability that the patient will respond to laryngoscopy. The NSRI has potential clinical use as an alternative to MAC, which is the minimum alveolar concentration of a volatile anesthetic at which 50% of patients do not move during surgical incision. MAC is, like the NSRI, a calculated parameter derived from population studies, in this case with volatile anesthetics. It has been used in daily clinical practice for decades, and every anesthesiologist is familiar with the concept of MAC. A downside of MAC is that it is only one point on the

concentration-effect relationship, namely C50. Other points have been distinguished in the past, such as MAC95, or the concentration of a volatile anesthetic where 95% of patients tolerate skin incision, but these values are rarely used in clinical practice, and volatile anesthetic delivery devices often only show end-tidal concentrations and end-tidal concentrations relative to MAC. Another issue is that MAC itself does not take any interactions into account. Numerous MAC-reduction studies have been performed, which assess the reduction in MAC due to for instance opioids or nitrous oxide, but like MAC95, they are not used in clinical practice beyond the knowledge of the type of interaction (synergistic, additive).

The NSRI with the triple interaction model provides information about not only one drug, but (currently) up to three drugs, and not only at the level of C50 or 50% probability of tolerance of laryngoscopy, but the full range of effect. An NSRI of 20 indicates a 90% probability of tolerance of laryngoscopy, regardless of whether this NSRI is achieved by sevoflurane alone or any combination of two or even all three drugs. Because the anesthesiologist is already used to working with a population-derived calculated parameter in MAC, the step towards using the NSRI to guide anesthesia should not be a large one, with the additional advantages to guide not only one drug but multiple drugs with changing concentrations as may happen during induction of anesthesia, where anesthesia is induced with propofol and maintained using a volatile anesthetic, combined with opioid administered through bolus doses or continuous infusion.

A limitation of this study is that no patients received all three drugs together in the whole study population, so an additional triple interaction on top of the currently modeled interaction cannot be excluded definitively. A study by Minto et al.[14] on the interaction between midazolam, propofol and alfentanil did not find a triple interaction when all three drugs were combined, on top of the synergistic interactions between the pairs of drugs. Considering the similarly strong synergistic interaction between remifentanil and both hypnotics in our study, and the additive interaction between propofol and sevoflurane, an additional triple interaction on top of this is unlikely.

Finally, as an initial method of validation Chapter 6 investigates the performance of multiple parameters from the three original 2-drug interaction studies (effect-site concentrations of the three drugs, the three hypnotic monitors BIS, SE and RE, and the analgesic monitors CVI and SPI, where available), and the P_{TOL}/NSRI from this study, to predict the probability of tolerance of laryngoscopy, using the prediction probability P_K, as described by Smith et al.[15] A P_K of 1 means there is a perfect correlation; a P_K of 0.5 means 50-50 chance, thus equal to flipping a coin. For the P_{TOL}/NSRI predictions, the dataset was divided into two groups, one for modeling and the second to assess the

performance of the calculated parameters, to ensure the parameter is not based on the same dataset on which it is then tested. Bootstrapping was then used to determine whether there was a significant difference in P_K between two different parameters. In all comparisons, P_{TOL}/NSRI were significantly better predictors compared to any of the other parameters, with a P_K higher than 0.9, with all other parameters having a P_K lower than 0.8. This is a promising initial validation for the use of NSRI as a clinical parameter to help guide anesthesia.

Conclusions and future perspectives

In the first part of this thesis we developed a comprehensive PKPD model for dexmedetomidine. Not only is this the first PKPD model for dexmedetomidine, but there are several rather unique components to this model, like the description of the arousability in BIS, the effect of background noise on MOAA/S, and the biphasic effect of dexmedetomidine on MAP. When used in target-controlled infusion, likely only one part of the model (BIS or probability of a certain MOAA/S score) may be targeted, but the hemodynamic part of the model may facilitate implementation of limitations to the infusion to enhance the safety of dexmedetomidine infusion. Aside from use in TCI, simulations using the model may help to better understand the characteristics of dexmedetomidine on sedation and hemodynamics, and visualization of the model in realtime displays may guide dexmedetomidine sedation and its hemodynamic side effects with or without the use of TCI. However, the model still has to be validated in another population, as only limited internal validation has taken place by use of graphical analysis and out-of-sample validation techniques. The model is also able to describe the initial hypertension after a bolus or rapid infusion. As the infusion rate was limited in the study, this is an extrapolation of the model and also needs to be validated. Also, since the model was developed in a healthy volunteer population, the model will have to be validated in a patient population to evaluate its performance in the presence of possible comorbidities. Future uses of the dexmedetomidine PKPD model are not only in clinical practice as mentioned before, but also in future interaction studies between dexmedetomidine and other anesthetic drugs such as propofol or opioids. A good PK or PKPD model is essential for adequate interaction modeling.

The second part of this thesis describes such interaction modeling studies and techniques on the interaction between sevoflurane and remifentanil, as well as the triple interaction sevoflurane-propofol-remifentanil. The sevoflurane-remifentanil interaction study focusses on the effect on continuous measurements, as well as the effect of noxious stimulation on this interaction. It is mainly descriptive, but clearly demonstrates that while it is known that opioids have a strong effect on clinical

anesthetic endpoints such as tolerance of noxious stimuli, the effect on hypnotic EEG-derived monitors is weak. This enforces the notion that EEG-monitors are poor predictors of anesthetic depth which includes analgesia in the presence of noxious stimulation (the balance between nociception and antinociception). The analgesic monitor CVI can also only describe the antinociceptive effect in the presence of a noxious stimulus, reducing its use to predict beforehand whether a patient will respond, and the poor fit and high variability suggests that it is also not a very strong predictor. The analgesic monitor SPI is unable to describe the interaction between sevoflurane and remifentanil, nor the effect of noxious stimulation. This study therefore shows that there still is not a good monitor that can predict adequacy of anesthesia of both the hypnotic and the analgesic component. Studies like this may be used in the future to investigate whether newer monitors are perhaps better at assessing depth of anesthesia.

The triple interaction study and the use of the triple interaction NSRI may help guide depth of anesthesia in the absence of adequate monitoring. Our study shows that NSRI is a better predictor of tolerance of laryngoscopy than currently used monitors of drug effect and single-drug effect-site concentrations. The NSRI also has to be validated in separate studies and populations, as again only internal validation using cross-evaluations have been performed. But if NSRI proves to be a valuable guide to anesthesia, the possibilities for this parameter may be endless, as other drugs may be included into the calculations after interaction studies with these other drugs have been performed. For instance, if interaction studies with dexmedetomidine and any of the three drugs currently in the NSRI have been performed, dexmedetomidine can be added to the NSRI (limited to the drug combinations with which interaction studies have been performed).

In all, every study in this thesis focusses on reaching the same goal: more accurate drug titration towards what is deemed adequate anesthesia and increasing the safety of anesthesia. In 2003 and again in 2016, Talmage Egan and Steve Shafer coined the process of drug titration towards a point on the E_{max} curve 'surfing the concentration-response curve',[16, 17] or 'surfing the wave'. This is not only the case for single drug titration; it can also be an analogy for drug titration with multiple drugs, where the 'wave' is not a two-dimensional concentration-effect curve, but a three-dimensional response surface model. This thesis therefore provides the means to facilitate surfing the wave in anesthesia practice.

References

1. Avram MJ, Krejcie TC: Using front-end kinetics to optimize target-controlled drug infusions. Anesthesiology 2003; 99: 1078-86

2. Schnider TW, Minto CF, Shafer SL, Gambus PL, Andresen C, Goodale DB, Youngs EJ: The influence of age on propofol pharmacodynamics. Anesthesiology 1999; 90: 1502-16

3. Minto CF, Schnider TW, Egan TD, Youngs E, Lemmens HJ, Gambus PL, Billard V, Hoke JF, Moore KH, Hermann DJ, Muir KT, Mandema JW, Shafer SL: Influence of age and gender on the pharmacokinetics and pharmacodynamics of remifentanil. I. Model development. Anesthesiology 1997; 86: 10-23

4. Bloor BC, Ward DS, Belleville JP, Maze M: Effects of intravenous dexmedetomidine in humans. II. Hemodynamic changes. Anesthesiology 1992; 77: 1134-42

5. Dyck JB, Maze M, Haack C, Vuorilehto L, Shafer SL: The pharmacokinetics and hemodynamic effects of intravenous and intramuscular dexmedetomidine hydrochloride in adult human volunteers. Anesthesiology 1993; 78: 813-20

6. Schoemaker RC, van Gerven JM, Cohen AF: Estimating potency for the Emax-model without attaining maximal effects. J Pharmacokinet Biopharm 1998; 26: 581-93

7. Heyse B, Proost JH, Schumacher PM, Bouillon TW, Vereecke HE, Eleveld DJ, Luginbuhl M, Struys MM: Sevoflurane remifentanil interaction: comparison of different response surface models. Anesthesiology 2012; 116: 311-23

8. Nieuwenhuijs DJ, Olofsen E, Romberg RR, Sarton E, Ward D, Engbers F, Vuyk J, Mooren R, Teppema LJ, Dahan A: Response surface modeling of remifentanil-propofol interaction on cardiorespiratory control and bispectral index. Anesthesiology 2003; 98: 312-22

9. Vanluchene ALG, Struys, M M R F, Heyse BEK, Mortier EP: Spectral entropy measurement of patient responsiveness during propofol and remifentanil. A comparison with the bispectral index. Br J Anaesth 2004; 93: 645-54

10. Bouillon TW, Bruhn J, Radulescu L, Andresen C, Shafer TJ, Cohane C, Shafer SL: Pharmacodynamic interaction between propofol and remifentanil regarding hypnosis, tolerance of laryngoscopy, bispectral index, and electroencephalographic approximate entropy. Anesthesiology 2004; 100: 1353-72

11. Schumacher PM, Dossche J, Mortier EP, Luginbuehl M, Bouillon TW, Struys MM: Response surface modeling of the interaction between propofol and sevoflurane. Anesthesiology 2009; 111: 790-804

12. Luginbuhl M, Schumacher PM, Vuilleumier P, Vereecke H, Heyse B, Bouillon TW, Struys MM: Noxious stimulation response index: a novel anesthetic state index based on hypnotic-opioid interaction. Anesthesiology 2010; 112: 872-80

13. Struys, Michel M R F, Vereecke H, Moerman A, Jensen EW, Verhaeghen D, De Neve N, Dumortier FJE, Mortier EP: Ability of the bispectral index, autoregressive modelling with exogenous input-derived auditory evoked potentials, and predicted propofol concentrations to measure patient responsiveness during anesthesia with propofol and remifentanil. Anesthesiology 2003; 99: 802-12

14. Minto CF, Schnider TW, Short TG, Gregg KM, Gentilini A, Shafer SL: Response surface model for anesthetic drug interactions. Anesthesiology 2000; 92: 1603-16

15. Smith WD, Dutton RC, Smith NT: Measuring the performance of anesthetic depth indicators. Anesthesiology 1996; 84: 38-51

16. Egan TD, Shafer SL: Target-controlled Infusions for Intravenous Anesthetics: Surfing USA Not! Anesthesiology 2003; 99: 1039-41

17. Shafer SL, Egan T: Target-Controlled Infusions: Surfing USA Redux. Anesth Analg 2016; 122: 1-3

Chapter 8: Summary in Dutch/Nederlandse samenvatting

Samenvatting en discussie

Naast de ontwikkeling van nieuwe medicijnen binnen de anesthesiologie, ligt de nadruk in wetenschappelijk onderzoek binnen de anesthetische farmacologie op het nauwkeuriger toedienen en titreren van anesthetische middelen. Dit gebeurt aan de hand van onderzoeken naar de farmacokinetische (PK) en farmacodynamische (PD) kenmerken van de bestaande middelen en het ontwikkelen van zogenoemde PKPD modellen (farmacokinetiek/farmacodynamiek modellen), om de verhouding tussen dosering en het effect beter te begrijpen. Daarnaast omvat het ook onderzoeken naar interacties tussen verschillende middelen en het ontwikkelen van interactiemodellen. Uiteindelijk kan dit in de klinische praktijk toegepast worden door het gebruik van TCI pompen (target-controlled infusion, ofwel titratie op een bepaalde spiegel in het bloed of een bepaalde mate van effect) en door het visualiseren van interacties tijdens een narcose. Zo kan de nauwkeurigheid van de toediening van één of meerdere middelen tegelijk verbeterd worden. Het belangrijkste doel van dit proefschrift is om op meerdere vlakken in deze tak van wetenschap een bijdrage te leveren: het ontwikkelen van PKPD modellen, interactiemodellen tussen meerdere anesthetische middelen, en het uitbreiden van een bestaande interactieparameter welke gebruikt kan worden om een narcose te sturen.

Hoofdstuk 1 geeft een basale weergave over de huidige kennis betreffende farmacokinetiek (hoe een bepaalde dosering resulteert in een bepaalde spiegel in het bloed), farmacodynamiek (hoe een bepaalde spiegel in het bloed of in een orgaan een effect bewerkstelligt), het ontwikkelen van farmacokinetische, farmacodynamische en gecombineerde PKPD modellen, evenals wat er bekend is over interacties en het ontwikkelen van interactiemodellen. Ook geeft het een overzicht over dexmedetomidine, wat één van de middelen is waar in dit proefschrift onderzoek naar is gedaan. Heel kort samengevat wordt PK vaak beschreven door een compartimenteel model: een model met meerdere vaten met een bepaald volume, aan elkaar gekoppeld door leidingen (zie ook figuur 2 in hoofdstuk 1) die een bepaalde klaring leveren tussen de compartimenten, plus een leiding die naar ‘buiten’ loopt (waardoor het middel het lichaam verlaat, in de praktijk meestal door verwerking door de lever of uitscheiding door de nieren). Het centrale compartiment (compartiment 1) komt ruwweg overeen met de bloedcirculatie, en vaak zijn er 1 of 2 perifere compartimenten. De farmacodynamiek wordt vaak beschreven door een zogenaamde ‘effect-site’ aan het centrale compartiment te koppelen, vanwaar het middel naar het orgaan/de receptoren gaat waar het zijn werk uitoefent. Dit zijn overigens allemaal wiskundige modellen die het beschrijven van het tijdsverloop van een spiegel of effect vereenvoudigen, maar de

compartimenten zijn niet rechtstreeks te vergelijken met een anatomisch of fysiologisch substraat.

Hoofdstuk 2 begint met de basis, het ontwikkelen van een PK model. Immers, zonder goed PK model is er geen goed PKPD of interactiemodel te maken. Dexmedetomidine is een middel voor sedatie ('roesje' in de volksmond), dat tevens een angstverminderend en enig pijnstillend effect heeft. Voor dit middel zijn er al een aantal PK modellen, echter deze zijn onderhevig aan een aantal onnauwkeurigheden, wat het gebruik ervan in de klinische praktijk negatief beïnvloedt. Belangrijk voor het ontwikkelen van een goed model is het hebben van goede data. Slechte data kan een model geven dat de data goed beschrijft, maar slecht overeenkomt met de realiteit. Voor het ontwikkelen van ons dexmedetomidine-model hebben we daar zo goed mogelijk geprobeerd rekening mee te houden. Zo hebben we gezonde vrijwilligers onderzocht in plaats van patiënten, waardoor de invloed van ziekten of andere medicatie tot een minimum beperkt is. Daarnaast hebben we vrijwilligers met een brede verdeling van leeftijd, gewicht en lengte onderzocht, om zo te kunnen beoordelen of deze factoren invloed hebben op de farmacokinetiek. Het gebruik van bloedafnames uit de slagader in plaats van een ader kan zo ook fouten in de modellen verminderen, omdat het betere informatie geeft over de spiegels in het bloed dat naar de organen gaat waar het middel zijn werking op uitoefent. Het gebruik van TCI kan ook mogelijk de nauwkeurigheid van het nieuwe model verbeteren, en daarnaast hebben we van tevoren rekenkundige simulaties uitgevoerd om uit te zoeken met welke doseringsschema's en tijdstippen voor bloedafname de meeste informatie over de verschillende parameters van het PK model gehaald konden worden. Bovendien hebben we elke vrijwilliger twee maal onderzocht, waardoor we ook de invloed van factoren als stress en 'angst voor het onbekende' tussen sessie 1 en sessie 2 op de farmacokinetiek van dexmedetomidine, wellicht door veranderingen in de hemodynamiek (= bloedcirculatie, zoals te beschrijven door bloeddruk en hartfrequentie).

We hebben uiteindelijk een zogenoemd drie-compartiment PK model ontwikkeld, waarbij de parameters van de compartimenten (volumes en klaringen), deels indirect, afhankelijk zijn van het gewicht (door middel van allometrische schaling). Leeftijd en lengte hadden geen invloed op het model. Een probleem dat optreedt met compartimentele modellen, is dat het model er vanuit gaat dat een middel direct na toediening gelijk wordt verdeeld over de hele bloedsomloop. Dit komt niet overeen met de werkelijkheid, en kan voor fouten in het model zorgen. Een manier om dit deels te omzeilen is het gebruik van een langzamere toediening van het middel in plaats van een snelle toediening, gecombineerd met een bloedafname die niet te vroeg (het middel is nog niet verdeeld over het bloed) of te laat is (laat in het traject van een snelle daling

van de spiegel, waarmee een te hoog V1 geschat wordt). Ook in onze studie hebben we dit toegepast, met naar het lijkt een betere beschrijving van het volume van compartiment 1.

Een interessante bevinding in hoofdstuk 2 is dat de variabiliteit tussen de twee sessies een grotere invloed had op V1 dan de variabiliteit tussen individuen. Dit verschil was niet systematisch tussen sessie 1 en 2, maar het suggereert wel dat er factoren zijn die met de tijd veranderen die van grotere invloed zijn op V1 dan de verschillen tussen twee personen. Wat deze factoren zijn, is op dit moment nog geheel onduidelijk.

In hoofdstukken 3 en 4 gebruikten we het in hoofdstuk 2 ontwikkelde dexmedetomidine PK model en pasten daarop een PD model toe, om zo een uitgebreid PKPD model te kunnen maken, met de effecten van dexmedetomidine op sedatie (gewenst effect) en hemodynamiek (bijwerkingen). Dit zijn de eerste PKPD modellen die ontwikkeld zijn voor dexmedetomidine.

Hoofdstuk 3 gaat vooral in op de invloed van dexmedetomidine op sedatie: de BIS (bispectral index), een meting die gebaseerd is op het elektro-encefalogram (EEG, 'hersenfilmpje'), en de MOAA/S score, de Modified Observer's Assessment of Alertness/Sedation, een scoresysteem naar de reactie van een persoon op (luid) aanspreken, schudden en/of een pijnprikkel. Dexmedetomidine is een uniek sedatiemiddel in de zin dat een persoon zelfs bij vrij hoge doseringen wekbaar blijft. Dit maakte het ontwikkelen van de modellen ingewikkelder, omdat bij elke prikkel (door het uitvoeren van een MOAA/S score, maar ook andere 'ongeplande' prikkels als ander geluid, dorst of jeuk) de persoon wakkerder wordt, en daarmee de BIS ook stijgt. Dit effect hebben we ook in ons model kunnen implementeren, door een factor toe te voegen die de invloed van zulke stimulatie weergeeft. Indien een stimulatie plaatsvindt, springt het model over naar de 'gestimuleerde toestand', wat effectief betekent dat de C50, of de concentratie die nodig is voor 50% van het maximale effect, met ruim 2,5 keer vermenigvuldigd wordt, ofwel: er is ruim 2,5 keer zo hoge concentratie nodig om 50% van het maximale effect te bewerkstelligen. Wordt de persoon met rust gelaten, dan daalt de factor 'gestimuleerde toestand' langzaam weer naar 'ongestimuleerde toestand'. Door elke vrijwilliger twee keer te onderzoeken, hebben we ook kunnen kijken naar het effect van continu achtergrond geluid op de sedatie (opname van geluid op een operatiekamer). Dit bleek geen effect te hebben op de BIS.

In tegenstelling tot de BIS, vonden we dat stimulatie door plotselinge prikkeling slechts weinig effect had op de MOAA/S score tijdens dexmedetomidine sedatie, en zodanig veel rekenkundige problemen in het model teweegbracht, dat we dit niet in het uiteindelijke model hebben toegevoegd. De continue achtergrondgeluiden hadden

daarentegen wel invloed op de MOAA/S score. Vooraf was de verwachting dat achtergrondgeluid ervoor zou zorgen dat de vrijwilligers minder diep gesedeerd zouden zijn; dat het geluid de patiënten wakkerder zou houden. Echter lijkt het effect omgekeerd te zijn: vrijwilligers met achtergrondgeluid hebben minder dexmedetomidine nodig om gesedeerd te raken. Mogelijk komt dit doordat het verschil in volume bij het aanspreken voor de MOAA/S score gecombineerd met achtergrondgeluid kleiner is dan gecombineerd met stilte, en er daardoor een groter 'schrikeffect' is, en de vrijwilliger vaker zal reageren. Opvallend hierbij is wel dat het effect niet alleen bij het aanspreken was, maar ook wanneer een vrijwilliger niet meer op aanspreken reageerde: er lijkt ook een effect te zijn op schudden of een pijnprikkel. Waar dit door komt, is nog onduidelijk.

Opmerkelijk genoeg, blijkt uit het model de kans op een MOAA/S score van 1 (niet reageren op luid aanspreken en schudden, wel op een pijnprikkel) erg klein te zijn. Dit komt ook overeen met de resultaten uit de studie, namelijk dat maar een klein deel van de reacties een MOAA/S 1 was. Mogelijk is het zo bij dexmedetomidine, dat een persoon zo lang wekbaar blijft, dat wanneer dit effect verdwijnt, iemand al zodanig diep gesedeerd is dat een pijnprikkel ook niet meer tot een reactie zal leiden.

In tegenstelling tot andere anesthetische middelen zoals propofol en remifentanil, bleek er voor dexmedetomidine geen effect te zijn van leeftijd op de sedatie. Door leeftijd gestratificeerd te werk te gaan, en dus een brede verdeling van de leeftijd van de vrijwilligers te includeren, hoopten we een eventueel effect ook te kunnen vinden in ons model. Mogelijk betekent dit dat het effect er in werkelijkheid ook niet is, verklaarbaar door een ander werkingsmechanisme van dexmedetomidine in vergelijking met propofol en remifentanil, maar wellicht is het aantal vrijwilligers te klein geweest om het effect aan te kunnen tonen.

Hoofdstuk 4 is toegespitst op de effecten van dexmedetomidine op de hemodynamiek of bloedcirculatie, met name op de bloeddruk (MAP, mean arterial pressure) en de hartfrequentie (HR, heart rate). Dexmedetomidine heeft als bijzonder effect dat het in lage concentraties een verlaging van de bloeddruk (hypotensie) geeft ten opzichte van de startwaarde (baseline), maar in hoge concentraties juist een belangrijke verhoging van de bloeddruk (hypertensie) tot boven baseline. Dit bifasische effect hebben we in het model kunnen toepassen door het gebruik van twee 'effect-sites', voor hypotensie en voor hypertensie. Dit past ook bij de fysiologie erachter, namelijk dat beide effecten ontstaan op verschillende plaatsen in het lichaam (de hoge bloeddruk met name in de vaatwand, de lage bloeddruk vooral in het centraal zenuwstelsel).

Tevens beschrijft het model de langdurige hypotensie na het stoppen van de toediening. Het model laat zien dat het tot ruim 10 uur kan duren voordat de bloeddruk weer binnen 5% van baseline komt. Echter, aangezien er geen studies zijn met een zodanig lange follow-up, is dit puur extrapolatie, en moet dit nog gevalideerd worden.

Voor het effect van dexmedetomidine op de hartfrequentie was een aanpassing van het model nodig naar een non-lineair model volgens Schoemaker, vanwege beperkte data nabij het maximale effect (in het model: 22,5 slagen per minuut), aangezien de grens van 40 slagen per minuut werd gehandhaafd om uit veiligheidsoverwegingen de toediening van dexmedetomidine te staken.

In hoofdstuk 4 keken we ook naar de gecombineerde effecten van sedatie en hemodynamiek door het gebruik van simulaties. Dit stelt gebruikers in staat om dexmedetomidine dosering te baseren op plasma concentraties, BIS, MOAA/S, bloeddruk en hartfrequentie tegelijk. Zo kan gesimuleerd worden welke doseringsstrategie het snelst tot het beoogde sedatie-effect leidt, met de minste negatieve invloed op de hemodynamiek. Het model is ook in staat om de initiële kortdurende hypertensie te beschrijven die ontstaat na een bolus of snelle toediening van dexmedetomidine. Echter, ook dit betreft een extrapolatie van het model, omdat in de studie alleen 6 of 10 µg/kg/h als maximale toedieningssnelheid is gebruikt. Dit moet in acht genomen worden bij het gebruik van deze simulaties.

In hoofdstuk 5 wordt vervolgens gekeken naar interactie modellen. De studie is een voortzetting van een eerdere sevofluraan-remifentanil interactie studie. In het oorspronkelijke artikel wordt het effect van de interactie op dichotome eindpunten beschreven, namelijk het wel of niet reageren op diverse prikkels, zowel niet-pijnlijke als pijnlijke prikkels. In hoofdstuk 5 ligt de nadruk op het effect van sevofluraan en remifentanil op continue monitoring. Het gaat hier om 3 monitoren die afgeleid zijn van het EEG (‘hersenfilmpje’) en voornamelijk de hypnotische (‘slaap’ inducerende) component van anesthesie beschrijven, namelijk de bispectral index (BIS), state entropy (SE) en response entropy (RE), en 2 monitoren die op de markt worden gebracht als ‘analgetische’ monitoren (effect van pijnstilling): de composite variability index (CVI, gebaseerd op de variaties in de BIS en de spieractiviteit ter hoogte van het voorhoofd) en de surgical pleth index (SPI, gebaseerd op het plethysmogram of golfpatroon gemeten door de saturatiemeter en de variaties in de hartfrequentie).

Er zijn verschillende vormen van interacties: ‘additief’ betekent dat de interactie simpelweg een optelsom is van de effecten van beide middelen, ‘synergistisch’ of ‘supra-additief’ betekent dat het gecombineerde effect van de interactie groter is dan additief en de middelen elkaar dus versterken, en ‘antagonistisch’ of ‘infra-additief’

betekent dat het gecombineerde effect kleiner is dan additief en de middelen elkaar dus tegenwerken. Verschillende mogelijke interactiemodellen zijn hierin te onderzoeken om dit effect te beschrijven. De belangrijkste component van deze modellen is de parameter *U*. *U* is het beste te beschrijven als een 'nieuw' middel, met de karakteristieken van de onderzochte middelen en hun concentraties, genormaliseerd naar hun eigen C50 (concentratie die 50% van het maximale effect bewerkstelligt). *U* kan dan als maat voor concentratie weer gebruikt worden om de concentratie-effect verhouding te beschrijven.

Het effect van sevofluraan en remifentanil blijkt voor BIS, SE en RE additief te zijn. De hoge C50 voor remifentanil toont aan dat remifentanil slechts een klein effect heeft op deze EEG-gebaseerde monitoren. Dit is in tegenstelling tot het bekende synergistische effect van beide middelen op reactie op pijnprikkels, zoals in het originele artikel is beschreven. Zo heeft remifentanil een sterk effect op de reactie op pijnprikkels, en is de interactie met sevofluraan sterk synergistisch. Ook voor andere interacties zoals propofol-remifentanil is deze tweedeling beschreven. Hieruit past ook het klinische beeld dat deze drie hypnotische monitoren geen goede voorspeller zijn of een patiënt wel of niet zal reageren op (pijn)prikkels.

Voor CVI blijkt de interactie matig synergistisch te zijn. Wat hierbij opvalt, is dat er na een pijnlijke stimulus een forse verandering van het model optreedt, waarbij bijna alle parameters veranderen. Dit in tegenstelling tot de 3 hypnotische monitors, waar alleen de C50 voor sevofluraan stijgt met gemiddeld 0,3 vol%. In het geval van CVI, lijkt het erop dat een pijnlijke stimulus nodig is om het analgetische effect goed te kunnen beschrijven. Voor SPI is zowel voor als na een pijnlijke stimulus geen goed model te maken, en lijkt er dus weinig effect van zowel sevofluraan als remifentanil op de SPI te zijn.

Hoofdstuk 6 is gericht op de drievoudige interactie tussen sevofluraan, propofol en remifentanil op het wel of niet tolereren van laryngoscopie, wat een pijnlijke prikkel is. De studie is een combinatie van 3 eerdere studies naar de interactie tussen propofol-remifentanil (synergistische interactie), propofol-sevofluraan (additieve interactie) en sevofluraan-remifentanil (synergistische interactie). Gezien de bevindingen uit de eerdere studies is de hypothese dat de interactie propofol-sevofluraan onderling nog steeds additief zal zijn, en dat beide middelen in verschillende mate een synergistische interactie met remifentanil hebben. Uit hoofdstuk 6 blijkt dat het eerste correct is (de additieve interactie tussen propofol en sevofluraan), en het tweede gedeeltelijk, namelijk dat zowel propofol als sevofluraan een synergistische interactie hebben met

remifentanil, maar de mate is gelijk voor propofol en sevofluraan. Dat wil zeggen: de interactie tussen 1 van beide met remifentanil is niet sterker dan de andere.

In hoofdstuk 6 herintroduceren we ook de term Noxious Stimulation Response Index (NSRI), welke reeds eerder is gepubliceerd op basis van de interactie tussen propofol en remifentanil. NSRI is een berekende parameter, gebaseerd op de P_{TOL} (waarschijnlijkheid van tolereren van laryngoscopie) uit het interactiemodel, geschaald van 100 naar 0, waar 100 betekent dat er geen anesthetische middel is toegediend, en de patiënt normaal gesproken wakker zou zijn, en 0 betekent een zeer sterk anesthetisch effect, met nagenoeg geen kans dat de patiënt reageert op laryngoscopie. In onze studie wordt deze term uitgebreid om ook de drievoudige interactie te beschrijven. In de huidige klinische praktijk wordt voor inhalatie-anesthetica, zoals sevofluraan, de term MAC gebruikt (minimum alveolar concentration). Dit is, net als NSRI, een berekende parameter, alleen in dit geval voor 1 middel (het inhalatie-anestheticum) en beschrijft enkel de dosering waarop er 50% kans is dat de patiënt reageert op een chirurgische prikkel. NSRI beschrijft daarentegen niet alleen 1 middel, maar tot 3 verschillende middelen, voor zover toegediend, en niet alleen op het niveau van 50% kans op wel/geen reactie, maar het hele bereik van klinisch gebruikelijke doseringen. Hierbij is het ook belangrijk dat een anesthesioloog geen genoegen neemt met 50% kans op wel/geen reactie op een bepaalde prikkel, maar liever richting of boven de 95% kans dat de patiënt niet reageert. Het feit dat de MAC reeds in de klinische praktijk gebruikt wordt, maakt dat NSRI, welke op dezelfde basis is gefundeerd en juist meer informatie geeft, mogelijk makkelijker geaccepteerd wordt als maat voor anesthesie.

Tot slot beschrijven we in hoofdstuk 6 in hoeverre verschillende parameters in staat zijn de waarschijnlijkheid van tolereren van laryngoscopie te voorspellen. De verschillende parameters zijn de concentraties van de drie verschillende middelen, de hypnotische monitoren BIS, SE en RE, de analgetische monitoren CVI en SPI, waar beschikbaar uit de oorspronkelijke studies, en de NSRI (en daarmee P_{TOL}) uit deze studie. Uit deze evaluatie blijkt dat NSRI een significant betere voorspeller was dan elke andere parameter. Dit is een hoopgevende eerste validatie voor het gebruik van NSRI als klinisch bruikbare parameter om anesthesie op te sturen.

Conclusie en mogelijkheden voor de toekomst

In het eerste deel van dit proefschrift hebben we een uitgebreid PKPD model voor dexmedetomidine ontwikkeld. Niet alleen is dit het allereerste PKPD model voor dit

middel, er zitten ook een aantal unieke aspecten aan dit model. Zo beschrijft het model de wekbaarheid die kenmerkend is voor dexmedetomidine, en het effect van achtergrondgeluid op reactie op stimuli. Tevens beschrijft het model het bifasisch effect op de bloeddruk. Dit model kan in target-controlled infusion (TCI) gebruikt worden. Hierop kan bijvoorbeeld 1 deel van het model als doel gebruikt worden, zoals de BIS of de waarschijnlijkheid van het behalen van een bepaalde MOAA/S score, terwijl het hemodynamische deel gebruikt kan worden om beperkingen aan de toediening (toedieningssnelheid, piekconcentraties) te implementeren om de veiligheid te verbeteren. Naast het gebruik in TCI kunnen simulaties van het model helpen om de karakteristieken van dexmedetomidine beter te begrijpen op het gebied van sedatie en hemodynamiek. Visualisatie van het model en de simulaties in realtime kunnen helpen met het sturen van dexmedetomidine, met of zonder gebruik van TCI. Hoewel beperkte validatie van het model heeft plaatsgevonden tijdens deze studie, moet het model nog wel gevalideerd worden in een andere populatie, om aan te tonen dat het model ook buiten de onderzochte populatie goede voorspellingen van plasmaspiegels en effect geeft. Het model beschrijft ook de initiële kortdurende hypertensie na een bolus toediening of snelle infusie. Aangezien dit een extrapolatie van het model is waarbij tijdens de studie alleen langzame toediening is toegepast, moet ook dit gevalideerd worden in een studie met verschillende infusiesnelheden. In de toekomst kan het model, naast toepassing in de klinische praktijk, ook gebruikt worden om de interactie tussen dexmedetomidine en andere anesthetische middelen, zoals propofol of remifentanil, te onderzoeken. Een goed PK of PKPD model is hierin essentieel als basis voor interactiemodellen.

Het tweede deel van dit proefschrift beschrijft zulke interactie studies, en de technieken om interacties in een model te kunnen beschrijven. De sevofluraan-remifentanil interactie studie is gericht op continue metingen, evenals de invloed van pijnlijke stimulatie op de interactie. Het hoofdstuk is voornamelijk beschrijvend, maar het laat duidelijk zien dat hoewel opiaten zoals remifentanil een sterk effect hebben op klinische meetpunten zoals het tolereren van pijnlijke stimuli, het effect op hypnotische EEG-afgeleide monitoring slechts zwak is. Dit ondersteunt de gedachte dat EEG-monitoring een slechte voorspeller is van ‘diepte van narcose’, wat naast de hypnotische component ook de pijnstilling in aanwezigheid van pijnlijke stimuli (de zogenoemde balans tussen nociceptie – de pijnprikkel cq. pijngewaarwording – en antinociceptie – pijnstilling cq. het niet gewaarworden van pijn). De analgetische monitor CVI kan het analgetische effect alleen beschrijven in aanwezigheid van een pijnlijke prikkel. Dit beperkt het gebruik van CVI als voorspeller van pijn voordat de prikkel is toegediend, naast dat er heel veel variabiliteit in het CVI model zit. De analgetische monitor SPI is in zijn geheel niet in staat om de interactie tussen sevofluraan en remifentanil, noch het

effect van pijnlijke stimulatie te beschrijven. Deze studie toont derhalve aan dat er nog altijd geen goede monitoring systemen zijn die zowel de hypnotische als analgetische component van anesthesie goed kunnen weergeven, en daarmee de adequaatheid van anesthesie kunnen voorspellen. Studies zoals deze kunnen in de toekomst gebruikt worden om te onderzoeken of nieuwe monitoring systemen beter in staat zijn anesthesie diepte te beoordelen.

De drievoudige interactie tussen sevofluraan, propofol en remifentanil, en de NSRI die uit het interactiemodel voortkomt, kunnen wellicht helpen om de diepte van narcose te beoordelen in afwezigheid van goede monitorsystemen. Onze studie toont aan dat NSRI beter kan voorspellen of iemand wel of niet zal reageren op laryngoscopie dan huidige hypnotische en analgetische monitoren en effect-site concentraties van de individuele middelen. Uiteraard zal ook de NSRI in andere studies en populaties gevalideerd moeten worden. Als NSRI een goede maat voor anesthesie blijkt te zijn uit deze validatiestudies, dan zijn de mogelijkheden voor de NSRI bijna eindeloos, aangezien nieuwe interactiestudies met andere middelen hieraan toegevoegd kunnen worden en de NSRI hiermee uitgebreid kan worden. Als voorbeeld: als er interactie studies zijn gedaan met dezelfde opzet als de huidige interactiestudies met dexmedetomidine en 1 van de 3 middelen die nu in de NSRI zitten, dan kan dexmedetomidine ook aan de NSRI toegevoegd worden (met als limitatie dat alleen de middelen waarmee de onderlinge interactiestudies zijn uitgevoerd worden toegediend).

Alle studies in dit proefschrift zijn gericht op hetzelfde doel: nauwkeurigere toediening van anesthetische middelen, voor de juiste diepte van anesthesie en verbeterde veiligheid van de patiënt onder narcose. In het recente verleden is het titreren van een anestheticum met behulp van PKPD modellen ook wel beschreven als het ‘surfen op een golf’ [Egan, Shafer; Anesthesiology 2003], oftewel: proberen rondom een gewenst punt op de concentratie-effect curve (figuur 3 in hoofdstuk 1) te blijven zitten gedurende de narcose. Niet alleen is dit toepasbaar op titratie van 1 middel, maar ook in het geval van interacties tussen meerdere middelen, waarbij gesurft wordt op een driedimensionale golf in de vorm van een response-surface model (figuur 7 in hoofdstuk 1). Dit proefschrift helpt derhalve met het surfen in de klinische anesthesiologische praktijk.

List of abbreviations

ABP	arterial blood pressure
BIS	bispectral index
BMI	body mass index
C	concentration
C50	concentration resulting in 50% of maximum effect
Ce	effect-site concentration
CL	clearance
CMT	compartment
Cp	plasma concentration
CVI	composite variability index
D50	dose resulting in 50% of maximum effect
E	effect
E0	effect at baseline (no drug present)
ECG	electrocardiograph
EEG	electroencephalograph
E_{max}	maximum effect
HR	heart rate
ICU	intensive care unit
IIV	interindividual variability
IOV	interoccasion variability
IV	intravenous
k_{e0}	equilibration rate constant for the effect-site compartment
k_{ij}	equilibration rate constant between compartment i and compartment j
MAC	minimum alveolar concentration
MAP	mean arterial pressure
MOAA/S	modified observer's assessment of alertness/sedation
NONMEM	non-linear mixed effects modeling
NSRI	noxious stimulation response index
PD	pharmacodynamics
PK	pharmacokinetics
P_K	prediction probability
PKPD	pharmacokinetics/pharmacodynamics
PROP	propofol
P_{TOL}	probability of tolerance of laryngoscopy
RE	response entropy
REMI	remifentanil
SE	state entropy
SEVO	sevoflurane
SPI	surgical pleth index
TCI	target-controlled infusion
U	combined potency of multiple drugs in an interaction model
V	volume
WT	weight
γ	steepness of concentration-effect relationship

List of publications

- Colin P, Hannivoort LN, Eleveld DJ, Reyntjens KMEM, Absalom AR, Vereecke HEM, Struys MMRF. **Dexmedetomidine pharmacokinetic-pharmacodynamic modelling in healthy volunteers: 1. Influence of arousal on bispectral index and sedation.** *Br J Anaesth. 2017 Aug;119(2):200-10.*

- Colin P, Hannivoort LN, Eleveld DJ, Reyntjens KMEM, Absalom AR, Vereecke HEM, Struys MMRF. **Dexmedetomidine pharmacodynamics in healthy volunteers: 2. Haemodynamic profile.** *Br J Anaesth. 2017 Aug;119(2):211-20.*

- Weerink MAS, Struys MMRF, Hannivoort LN, Barends CRM, Absalom AR, Colin P. **Clinical pharmacokinetics and Pharmacodynamics of Dexmedetomidine.** *Clin Pharmacokinet. 2017 Aug;56(8):893-913.*

- Hannivoort LN, Vereecke HEM, Proost JH, Heyse BEK, Eleveld DJ, Bouillon TW, Struys MMRF, Luginbühl M. **Probability to tolerate laryngoscopy and noxious stimulation response index as general indicators of the anaesthetic potency of sevoflurane, propofol, and remifentanil.** *Br J Anaesth. 2016 May;116(5):624-31.*

- Hannivoort LN, Eleveld DJ, Proost JH, Reyntjens KMEM, Absalom AR, Vereecke HEM, Struys MMRF. **Development of an Optimized Pharmacokinetic Model of Dexmedetomidine Using Target-controlled Infusion in Healthy Volunteers.** *Anesthesiology. 2015 Aug;123(2):357-67.*

- Vos JJ, Poterman M, Hannivoort LN, Renardel De Lavalette VW, Struys MMRF, Scheeren TWL, Kalmar AF. **Hemodynamics and tissue oxygenation during balanced anesthesia with a high antinociceptive contribution: an observational study.** *Perioper Med (Lond). 2014 Oct;3:9.*

- Heyse B, Proost JH, Hannivoort LN, Eleveld DJ, Luginbühl M, Struys MMRF, Vereecke HEM. **A response surface model approach for continuous measures of hypnotic and analgesic effect during sevoflurane-remifentanil interaction: quantifying the pharmacodynamic shift evoked by stimulation.** *Anesthesiology. 2014 Jun;120(6):1390-9.*

- Hannivoort LN, Vermeijden JW. **Iatrogenic perforation of a Zenker's diverticulum with a nasogastric tube.** *Neth J Crit Care 2012 Apr;16:52-3.*

Curriculum vitae

Laura Naomi Hannivoort werd op 6 september 1984 geboren, als jongste dochter van Diana en Evertjan Hannivoort. Zij groeide op in Boekelo, samen met oudere zus Rebekka en oudste broer Iskander. Ruim zeventien jaar wonend in een huisartsenpraktijk met apotheek aan huis maakte het moeilijk een andere toekomst te verzinnen dan één in de medische wereld. Na het cum laude behalen van het diploma aan het Gymnasium van het Bonhoeffer College in Enschede in 2002, koos zij dan ook voor de studie geneeskunde in Groningen. In de eerste twee jaar van de studie zat zij in de organisatie van het International Student Congress of Medical Sciences (ISCOMS), waarvan het tweede jaar in het bestuur, als voorzitter van de commissie International Contacts. De wetenschappelijke stage in het laatste jaar van de studie, welke werd uitgevoerd in het Children's Cancer Center van het Royal Children's Hospital in Melbourne, Australië, in combinatie met een keuzecoschap kinderoncologie, deed een carrière in de wetenschap kriebelen.

Eenmaal terug in Nederland, na het behalen van de artsenbul in 2009, startte Laura het werkende leven als arts-assistent op de Intensive Care in het Medisch Spectrum Twente in Enschede. Twee jaar later, in 2011, begon ze aan een promotietraject binnen de farmacologische onderzoekslijn van de afdeling Anesthesiologie in het Universitair Medisch Centrum Groningen, onder de bezielende leiding van Prof. Dr. Michel Struys, Prof. Dr. Tony Absalom en Dr. Hugo Vereecke. In 2013 behaalde zij de tweede plaats in de Best Abstract competitie van Euroanaesthesia, het jaarlijks congres van de European Society of Anaesthesiology.

Inmiddels is Laura sinds 2013 in opleiding tot anesthesioloog onder het opleiderschap van Prof. Dr. Götz Wietasch. Het tweede jaar van de opleiding genoot zij gedeeltelijk in het land van 3 van haar uiteindelijke (co)promotores: België, in Gent om precies te zijn. In dezelfde periode trok de afdeling Dr. Pieter Colin vanuit Gent aan ter aanvulling van het wetenschappelijk team; hij nam eveneens gedeeltelijk de begeleiding van het wetenschappelijk traject van Laura voor zijn rekening. Na nog een korte tussenstop in het tweede opleidingsjaar in de Isala in Zwolle, vervolgt Laura de opleiding weer in het UMCG, inmiddels in het laatste jaar van de opleiding.

Acknowledgments/Dankwoord

Daar ligt ‘ie dan, na ruim 6,5 jaar hard werk, vele uren slaap – in het geval van de patiënten en vrijwilligers – en een lading (virtuele) inkt: het proefschrift. Uiteraard schrijft een proefschrift niet zichzelf, en daarom wil ik iedereen die een steentje, van kiezel tot rots, inhoudelijk of ondersteunend heeft bijgedragen aan de onderzoeken en het uiteindelijke proefschrift, hartelijk bedanken. Promoveren tijdens een fulltime opleiding is niet makkelijk, maar met de juiste mensen om je heen zeker te doen. En dat ik de juiste mensen om mij heen heb, daar ben ik in de afgelopen 6,5 jaar absoluut van overtuigd geraakt.

Allereerst wil ik mijn eerste promotor, Prof. Dr. M.M.R.F. Struys, bedanken. Michel, vanaf dag 1, nee daarvoor al, halverwege mijn sollicitatiegesprek, heb jij me het gevoel gegeven dat je de onderzoeker in me zag, nog voordat ik daar zelf van overtuigd was. Dat je vertrouwen in mijn kunnen had, voordat ik zelf dat vertrouwen had. Binnen de kortste tijd had je door dat het initiële onderzoeksplan onder de omstandigheden van 6,5 jaar geleden niet de juiste kans van slagen had, en dat mijn handigheid met computers en ICT bovendien een weg in een andere richting opende. Het roer ging om, je stuurde me naar de NONMEM-cursus, en ik denk dat dat de beste keuze in mijn wetenschappelijke carrière is geweest. “The rest is history”, maar wel een geschiedenis waarin ik ontzettend veel van jou en de onderzoeksgroep heb kunnen leren, op een onderzoeksgebied waarvan ik nooit had geweten dat het zo interessant was, maar toch perfect bij mijn past. Bedankt dat je de wetenschapper in mij beter kende dan ikzelf, en daar het maximale hebt weten uit te halen.

Vervolgens alle dank aan mijn tweede promotor, Prof. Dr. A.R. Absalom. Tony, voor mij ben je precies wat een goede professor zou moeten zijn voor zijn pupillen: een encyclopedie aan kennis, en altijd bereid om die kennis te delen, met het enthousiasme die alleen iemand kan tonen die met hart voor het vak en voor onderwijs. Je bijdragen aan onderzoeksprotocollen en manuscripten waren daarmee ook uiterst leerzaam voor een beginnend onderzoeker als ik. Naast dat je een onuitputtelijke bron van meer algemene anesthesiologische en farmacologische kennis bent, ben jij ook degene met verreweg de meeste kennis en ervaring met dexmedetomidine in dit ziekenhuis, wellicht zelfs in het hele land. Je bent een belangrijke spil geweest rondom de dexmedetomidine studie, en daarmee een zeer groot deel van mijn promotietraject. Bedankt voor alles wat je me geleerd hebt, en je onuitputtelijke enthousiasme.

Mijn beide copromotores, Hugo Vereecke en Pieter Colin, zonder jullie zou dit proefschrift er zeker niet zijn gekomen. Hugo, jij was degene die mij alle kneepjes van het vak moest leren. Ik, net twee jaar uit de studiebanken, wist nog net dat farmacologie ‘iets met absorptie, distributie, metabolisme en excretie, en zo’ was, en mijn beeld van farmacologie in de klinische praktijk was ‘geef de patiënt een pilletje en kijk een paar weken of maanden later of je het moet ophogen of verlagen’. Natuurlijk is dat in de anesthesiologie anders, en dat heb jij op mij zeer succesvol weten over te brengen en enthousiast voor weten te krijgen. Niet alleen heb je me van alles geleerd over farmacologie in de anesthesiologie, maar ook over onderzoek doen in het algemeen, en je begeleiding hieromtrent, en in het bijzonder het dexmedetomidine onderzoek, is daarbij onmisbaar geweest. Pieter, jij nam het stokje deels over van Hugo na zijn verhuizing naar het

zuiden. Ik heb genoten van onze gedachtewisselingen, met name tijdens de dexmedetomidine PD modeling. Als ik met een idee kwam, dan wist jij dat om te zetten in een model waar ik bij lange na niet op zou zijn gekomen. Ik heb in relatief korte tijd veel van je geleerd, en het besef gekregen dat er nog zo veel meer te leren is op het gebied van modeling.

Leden van de Beoordelingscommissie, members of the Assessment Committee, thank you very much for the time and effort you have invested into reading and assessing my thesis.

Douglas en Hans, vanaf het begin van mijn promotietraject de modeling-guru's. Bedankt voor alles wat jullie me geleerd hebben op het gebied van modeling, en jullie zeer waardevolle bijdrage aan de studies, van planning tot modeling tot publicaties. Als ik weer eens in NONMEM verzandde, wisten jullie me te helpen het beter te begrijpen, of op een andere manier naar de oplossing te zoeken. Ik denk dat jullie niet eens weten hoeveel jullie me geleerd hebben.

Koen, bedankt voor alle hulp tijdens de dexmedetomidine studie. Het maakt het een stuk makkelijker voor alle betrokkenen van zo'n studie om hun werk te doen, wanneer er een anesthesioloog 'aan het hoofd' staat waar je op kan vertrouwen, en die rust behoud en uitstraalt, ook tijdens de meer hectische momenten.

De in wetenschappelijke publicaties vaak onzichtbaar maar o zo waardevolle personen van het onderzoeksbureau. Froukje, partner-in-crime in de dexmedetomidine studie, en 'onderzoekskamergenoot'. Samen waren we de meest constante factor in de Dex-studie. Ik kon altijd op je rekenen dat de onderzoekssessie goed uitgevoerd werd, en we waren elkaars geheugensteun voor het handhaven van het tijdsschema. De gezelligheid op de kamer kon er natuurlijk ook niet aan ontbreken! Ans, bedankt voor de ondersteuning tijdens de dexmedetomidine studie, waar je altijd tijd voor wist te maken ondanks de vele andere studies waar je actief bij betrokken was. Last but not least in het onderzoeksbureau: Rob, bedankt voor – ja, wat eigenlijk niet? – ondersteuning bij het opzetten van protocollen en METc-aanvragen, ICT- en HR-gerelateerde zaken, contacten met QPS, en vast nog genoeg waar ik nu niet op kan komen. Daarnaast ook bedankt voor de ondersteuning bij de dexmedetomidine studie, als manusje-van-alles. Je hielp mee waar handen te kort kwamen, en kon voor zowel Froukje als Ans invallen, en moest dus ongeveer alles aspecten van de studie kennen.

Mijn opleider, Prof. Dr. JKG Wietasch, Götz, dankzij jou heb ik niet alleen de kans gekregen om anesthesioloog te worden, maar je hebt me ook rijkelijk de ruimte gegeven om aan artikelen en het proefschrift te werken. Daarnaast zal ik ook nooit vergeten dat het welzijn van je assistenten voor jou echt van belang is, en de support die ik op dat vlak heb kunnen ontvangen, tijdens mijn eigen 'dip', ben ik je zeer dankbaar voor.

Minke, een vaste pijler in de bijna 7 jaar dat ik al op de afdeling ben. Altijd bereid om een handje te helpen, of de weg te wijzen (letterlijk of figuurlijk), daar waar nodig. Bedankt!

Bedankt aan alle mede-auteurs die ik niet specifiek genoemd heb. Jullie bijdragen aan de artikelen waar dit proefschrift op gestoeld is, zijn onmisbaar.

Aan alle stafleden en AIOS van de afdeling anesthesiologie en zeker niet te vergeten, anesthesiemedewerkers en PACU-verpleegkundigen, bedankt voor het zorgen voor een sfeer op de afdeling waarbij klinisch werk, opleiding en onderzoek vaak goed te combineren zijn, en natuurlijk voor alles wat jullie me op het gebied van anesthesiologie hebben bijgebracht. Bedankt voor de medewerking aan diverse studies in de afgelopen jaren, jullie geduld, en het invullen van eindeloze extra formulieren.
Aan de stafleden, AIOS en verpleegkundigen van de Intensive Care Volwassenen, bedankt voor alles wat jullie hebben bijgeleerd over de zorg van de kritisch zieke patiënt tijdens mijn opleiding. Jaap, bedankt voor de tijd om aan mijn proefschrift te werken.
Mijn dank ook aan de intensivisten en IC-verpleegkundigen van het MST Enschede, van wie ik ontzettend veel heb geleerd, altijd met een overschot aan enthousiasme!
Dit geldt zeker ook voor de afdelingen anesthesiologie in het UZ Gent en de Isala, waar ik mijn tweede jaar heb kunnen genieten van twee nieuwe, uiterst leerzame centra.

Bedankt QPS voor de medewerking aan de dexmedetomidine studie: het screenen van de vrijwilligers en het uitvoeren van de concentratiebepalingen van dexmedetomidine.

Aan alle patiënten en vrijwilligers die hebben meegedaan aan de studies, zonder jullie geen onderzoek, zonder jullie geen proefschrift. Bedankt voor jullie medewerking!

Last but not least: vrienden en familie, in het bijzonder:

Mijn paranimfen, Rebekka en Carlijn. Rebekka, je bent altijd mijn grote voorbeeld geweest. Alles wat jij ging doen, wilde ik ook, zoals kleine zusjes graag doen. Dit gold voor bijna alles, van studie tot sport. Zelfs mijn keuze voor anesthesiologie heb ik voor een belangrijk deel aan jou te danken, al was jij toen nog niet van plan om anesthesioloog te worden. Daarin heb jij mij voor de verandering gevolgd. Je bent altijd een grote steun voor me, ik kan altijd kwijt wat me dwars zit. Je bent de spiegel om voor te oefenen voor een belangrijk praatje, en hoewel ik daar een hekel aan heb, helpt het wel. Bedankt voor alle onvoorwaardelijke support.

Carlijn, ik herinner me nog goed die eerste keer in Café Marleen, maandagavond na een repetitie van Bragi. Sindsdien zijn we geloof ik nooit meer gestopt met kletsen. Over en weer hebben we elkaar gesteund over de jaren. Buiten mijn familie zijn er weinig waar ik zo vrij over alles kan praten, over alle onzekerheden omtrent beslissingen over opleiding en toekomst, of presentaties op congressen, je weet altijd het juiste te zeggen. Bedankt voor alle steun, in het verleden en nu!

Iskander, als grote broer heb je voor mij het voorbeeld gegeven hoe je kan excelleren in wat je echt leuk vindt. Ik heb altijd met bewondering naar je opgekeken hoe je na de middelbare school alles hebt aangegrepen om je droom te volgen, met geweldige studieresultaten, een topbaan, gekroond met een geweldig gezinnetje: je lieve vrouw Moniek, en de schattigste en slimste kinderen, Madison en Tyler. Pap, mam, bedankt voor het creëren van een omgeving waarin ik heb kunnen opgroeien tot wie ik nu ben. Jullie onvoorwaardelijke liefde en steun zijn onbeschrijfelijk belangrijk voor mij geweest. Jullie hebben me de mogelijkheid gegund om mijn grenzen te verleggen, zelfs een klein duwtje richting Australië gegeven. Ik bof maar met ouders zoals jullie!